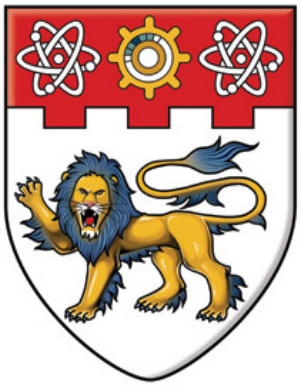

NANYANG TECHNOLOGICAL UNIVERSITY

ADVANCED CONTROL OF WIND POWER SYSTEMS

DANG DINH QUY

SCHOOL OF ELECTRICAL AND ELECTRONIC ENGINEERING

2012

ADVANCED CONTROL OF WIND POWER SYSTEMS

DANG DINH QUY

SCHOOL OF ELECTRICAL AND ELECTRONIC ENGINEERING

A thesis submitted to the Nanyang Technological University

in partial fulfillment of the requirement for the degree of

Doctor of Philosophy

2012

ACKNOWLEDGEMENT

Wind power system control research work was financed and carried out in School of Electrical Electronics Engineering, Nanyang Technological University from January 2008 to January 2012, under supervision and guidance from Professor Wang Youyi; co-supervision from Associate Professor Cai Wenjian. Their constant encouragement and constructive suggestions are greatly acknowledged. I am also heartily thankful for them being so understanding to let me freely to choose my favorite research topic. Most importantly, I would like to express my deepest gratitude to their generosity and forgiveness for my mistakes happening during research progress.

I also express my special thanks to the academic staffs from Electric Power Research Lab, Division of Power Engineering, specifically: Mr. Yeoh Tiow Koon, Ms. Annie Sim, Mr. Lim Kim Peow, Ms. Ng-Tan Siew Hong (Jennifer) and Mr. Lee Ting Yeng. This project will not meet schedules without their unlimited support to use both hardware and software available resources.

I owe enormous debt to my parents, my brother and sisters who show their encouragements and concern throughout my research. Their un-measurable support and care have given me the spiritual strength to continue this higher education.

Not to forget my colleagues at Power Research Lab, I especially send my thanks to Ms. Nirnaya Sarangan and Mr. Mahda J. Jahromi for their valuable time spent on editing and English proofreading. In the very final phase of the project, their kind help is beyond any thankful words.

Last but not least, I would like to thank supervisors at ASM Pacific Technology, Singapore: Dr. Kuang Bo, Dr. Chua Hee Lai and colleagues from R&D Motion for their understanding, helpfulness. Without their supports, I could not finish thesis revision on time.

"Your time is limited, so don't waste it living someone else's life. Don't be trapped by dogma - which is living with the results of other people's thinking…

… And most important, have the courage to follow your heart and intuition"

Steve Jobs, 1955-2001

Table of Contents

SUMMARY

Wind power system control especially for variable speed operation of wind turbine has been carried out in several decades; and the research activities are still on-going with more concern recently. The reason is that a variable speed wind power system produces higher electrical energy and power efficiency than a conventional wind power plant. However, the variance of rotor speed leads to the changes of working conditions in accordance with stochastic wind profiles. The different control objectives for each working condition are also addressed as a problem of controller design. Beyond the multiple operating regions, wind power system control has to deal with the nonlinearity of wind torque and the stochastic behavior of wind. Hence, the control system is further complicated.

The wind power system configuration in this study includes a variable speed wind turbine driving a permanent magnet synchronous generator. The generator is connected to a full-scale back-to-back IGBT converter which is connected to a local grid. This wind turbine configuration is regulated by four individual controllers, which are speed controller of turbine drive-train; generator d-q axis current controllers; dc-bus voltage control of dc-link; and grid side d-q axis currents (also known as grid active and reactive power) control. Among these controllers, the classical PI (proportional integrator) controller has been well applied to d-q axis currents of both generator and grid side from the literature so that it is not a main study in this thesis. The control algorithm for aerodynamics drive-train and dc-link voltage is therefore of the research interest. Through the simulation and experimental results, it is concluded that wind power system control problems are well resolved by proposed algorithms.

There are several methods which are applied for controlling the aerodynamic drive train loop based on model-free, linear to nonlinear models. Model-free fuzzy logic controller (FLC) acts as a human behavior to find appropriate control input based on the knowledge of measurement signals and rules. FLC provides a simple and good optimal power tracking at partial-load region; while the nonlinear PID controller with variable gains gives a simple, stable control scheme for different

operating points. The simplicity of these two methods makes it popular and suitable for small and medium rating wind power systems.

The wide load conditions of wind power system control can be obtained by linear Model Predictive Control (MPC). At partial load working region, a reference tracking quadratic cost function is formulated. Cut-in and full load conditions are considered as lower and upper regions which are integrated as constraints to the partial load condition. The cost function with constraints is then minimized in every sampling time to find optimal control input updates to the plant. Moreover, linearization presentation of nonlinear system always creates mismatch between model and plant hence produces a reference tracking offset. The robust Disturbance Models of Predictive Control (DMPC – modification method from linear MPC) is based on uncertainty linear model which adds a disturbance to the output and an appropriate observer designed for estimation of states to cancel the steady state errors.

Last control algorithm is an extended method of linear MPC, the Nonlinear MPC (NMPC) designs directly from wind power nonlinear model. All the properties of linear MPC are inherited in the nonlinear version with better quality. A real-time process which includes multiple shooting method, partially-reduced sequential quadratic programming and real-time iteration scheme is applied to realize NMPC to wind power application.

The final development in wind power control is equipped with robust DMPC method for a cluster of few wind turbines in connection to the grid. The robust MPC controller for dc-link voltage in cascaded with PI controller of the generator side d-q axis currents is proposed. The result of wind turbine cluster can be extended to a large scale wind farm. Fault-ride through capability of wind farm control is also analyzed.

LIST OF FIGURE S

Chapter 1

Chapter 2

Chapter 3

Chapter 4

Chapter 5

Chapter 6

LIST OF TABLES

LIST OF ABBREVIATIONS

FLC: Fuzzy Logic Control

KKT: Karush-Kuhn-Tucker Condition

LMPC: Linear Model Predictive Control

DMPC: Disturbance Model Predictive Control

NMPC: Nonlinear Model Predictive Control

NLP: Nonlinear Programming

NPID: Nonlinear Proportional Integral Derivative

ODE: Ordinary Differential Equation

PID: Proportional Integral Derivative

QP: Quadratic Programming

GEVSC: Generator Side Voltage Converter

GRVSC: Grid Side Voltage Converter

SQP: Sequential Quadratic Programming

RSQP: Reduced Sequential Quadratic Programming

PRSQP: Partially Reduced Sequential Quadratic Programming

VSWT: Variable Speed Wind Turbine

WECS: Wind Energy Conversion System

LIST OF GREEK SYMBOLS

E, m Kinetic energy, air mass

k_w, C_w Shape coefficient of Weibull distribution

a, z, z_{ref}, σ_w Wind turbine tower radius, tower height, height reference above sea level; surface roughness parameter.

P_a, T_a Aerodynamic power, torque captured from wind

ρ, R, υ, r Air density, turbine blade radius, wind speed and distance from rotor axis

$Cp(\lambda,\beta), Cp(\lambda), Cp_{\max}$ Power coefficient, approximation function, and maximum value of $Cp(\lambda)$

$\beta, \lambda, \theta, \psi$ Blade pitch angle, tip speed ratio, azimuth angle; and constant flux of generator

K_r, K_g, K_t Viscous friction of turbine, viscous friction of generator, and total viscous friction

J_r, J_g, J_t Turbine inertia, generator inertia, and total inertia referring to the low-speed shaft

ω_r, ω_g, η Turbine speed, generator speed, and gear box ratio

T_e, T_g, T_{elec} Electromagnetic torque of generator, generator torque referring to low speed shaft, electrical torque compensation

T_m, ω_m, K_m, J_m Mechanical torque of motor; motor speed, inertia and viscous friction

$\lambda_{opt}, \upsilon_m, \gamma, e(t)$ Optimal tip speed ratio, seasonal wind speed, torque parameter, and white noise

$\Delta\upsilon, \Delta T_a, \Delta T_e$ Turbulence component of wind speed, aerodynamic torque variation, electromagnetic torque variation

$\Delta\omega_r, \Delta\omega_g$ Variation around static value of turbine speed and generator speed

T_w, L_t Time constant of the filter, turbulence length of wind speed

$\omega_g^*, \Delta\omega_g^*, y^*(k)$ Generator speed optimal reference, variation of optimal reference, and general output reference at time k

Q, α Quadratic cost function, weighting factor between output and input cost

N, N_u Digital output prediction horizon, input prediction horizon

$\mu_1, \mu_2, L(x, \mu)$ Lagrange multipliers, Lagrange function

d_k Artificial variable at time k for sub-QP problem

σ, H_k Line search parameter, Hessian matrix

$\Delta\omega_g^{\min}, \Delta\omega_g^{\max}$ Lower and upper bound of the generator speed variations

$\omega_g^{\min}, \omega_g^{\max}$ Lower and upper bound of the generator speed

$\Delta T_e^{\min}, \Delta T_e^{\max}$ Lower and upper bound of the electromagnetic torque variations

$T_e^{\min}, T_e^{\max}$ Lower and upper bound of the generator speed

u_d, i_d, u_q, i_q Voltages and currents in d-q rotational frame

E_d, E_q: Back EMF voltages in d-q frame

ω_s, p, R_s, L Electrical synchronous speed, number of pole pairs, stator resistance, and inductance respectively

Ψ, K_t: Magnetic flux, generator torque constant

T, δ: Sampling time of NPC, piecewise interval of multiple-shooting method

Q_{npc}, Q_{wecs}, Q: General cost function of NPC, cost function applied for WECS, weighting matrix

x_i, u_i, s_i, v_i: Piecewise state, control, artificial state, and system parameter

$g_1(w), g_2(w), H_k$: Function contain linear equality and non-linear equality, Hessian matrix

∇, ∇^2: Gradient operator, and second order derivative operator

ω_{gr} Grid electrical speed

J_{eq}, B_{eq}: Equivalent inertia of aggregated turbine, total equal viscous friction

$u_d^s, i_d^s, u_q^s, i_q^s$: Voltages and currents in d-q rotational frame from generator side

u_d^g ,i_d^g , u_q^g , i_q^g : Voltages and currents in d-q rotational frame from grid side

E_d^s , E_q^s ; E_d^g , E_q^g : Back EMF voltages in d-q frame; grid voltage in d-q frame

R_g , L_g , U_g : Grid resistance, grid inductance, grid rated voltage

C_link ,U_{dc},U_{dc_ref} : DC link capacitor, DC link voltage, DC voltage reference

T_p : Prediction horizontal

CHAPTER 1

INTRODUCTION TO WIND POWER SYSTEM CONTROL

1.1. Introduction

Wind is a natural phenomenon being exploited from ancient time in agriculture like windmill to our modern life in the power generation industry. Energy for daily consumption such as heating and manufacturing has been always a basically vital demand for human life. While the other natural resources such as oils and fossils are now becoming exhausted, wind energy and other renewable energy resources like solar, fuel cell and hydro generations are drawing much more attentions from R&D researchers and governmental policy makers. Among these renewable energy recourses, wind energy is becoming the fastest growing electrical generation worldwide. Since the oil crisis in the 1970s, commercial wind turbines have gradually become an important industry with an annual turnover in the 1990s of more than a billion US dollars per year. With an addition of 38 GWs in 2010, which sums up the total installed capacity of 197 GWs, wind power registers an increase of more than 30.0% during last few years [1, 2]. It is expected that wind power continues the fast growing trend in the future due to the priority from government policy. The U.S department of energy has dropped a scenario in which wind power is a major electricity source, with a 12% market share in 2020 and 20% in 2030 [3]. To meet 20% of that demand, U.S wind power capacity would have to reach about 300 GWs in contrast with no wind growth level in 2006. In Denmark, wind power penetration in the total of electricity supply currently takes 20% and it will increase to 50% by 2025 from mostly offshore power plants. In some Asian countries, wind power gradually takes its role in electricity generation. The People's Republic of China is the strongest market, followed by India standing at second place. At the end of 2010, wind power in the People's Republic of China accounted for 41.8 GWs and it could meet all of their electricity demands from wind power by 2030 [4].

Wind turbine is a mechanical device specifically designed to convert part of the kinetic energy from wind into useful mechanical energy then to electrical energy. In

the history, the most successful vertical-axis wind turbine is the Darrieus rotor which is able to capture the wind from any direction without the need to yaw. However, this type of wind turbine requires complex maintenance; it usually requires rotor removal and fewer life cycles. In the beginning of wind power development in the early 1980s, fixed-speed wind turbine schemes with the electric generator directly connected to grid predominated for a long time. The rotational speed is imposed by the grid frequency. Although reliable and low-cost, these fixed-speed configurations are too rigid to adapt to the wind speed variations. Thus the maximum power captured of wind turbine is achieved at single speed and produces mechanical stresses at other wind speed outside designed speed region.

The next generation of wind turbine, fixed-speed pitch-controlled scheme prevailed early in medium to high power wind turbines that are able to control the captured aerodynamic power by pitch angle adjustment. Although maximum power is not obtained by this method, the energy production can be maintained at required amount and this type of wind turbine reduces the fatigue load to the mechanical components. Nowadays, to gain better use of the turbine capacity as well as the alleviation of aerodynamic and mechanical loads that reduce the useful life of the system installation, and to cope with the intermittent variability of the wind, the variable speed wind turbine, with or without the pitch angle controlled, is introduced. The obvious advantage of variable speed wind turbine over the classical turbine is the ability to follow the non-stationary optimal power curve since generator speed can be controlled through a full-scaled back-to-back converter. Hence, the new turbine technology gains better use of the system capability. The more electrical power is harnessed, the less cost in per kilo-watts of production; hence, wind power is more competitive than the other renewable power sources.

Permanent Magnet Synchronous Machine (PMSM), which consists of magnets on rotor, has some advantages such as an external excitation not required, light weight, small size, high reliability… etc [5-9]. This type of generator is widely used in the wind industry from small to large scale [10-14]. In the offshore wind farm, mega-watt class multi-pole PMSGs have been introduced and are widely used. Their advantages include the use of smaller gearboxes or even gearless turbines, no

requirement for an excitation system, and simple fault ride-through by blocking the PWM signals to the generator side converter [15]. With the ability of full range speed control in the active stall scheme, the variable speed wind turbine driving PMSG has settled new trends in wind power system. Despite the fact that doubly-fed induction generators (DFIG) are widely employed in modern large scale wind power industry; however, in this research, the control algorithms are in concern much rather than the wind power system configuration and specification. From control engineer standpoint, once algorithm is well performed for PMSG-based structure could be applied to DFIG-based wind power system with minor modification. Hence, PMSG wind power system was chosen intensively to illustrate the proposed control algorithms.

The typical structure of a single PSMG-typed wind power system in connection with the grid is shown Figure 1.1 [1]. The horizontal 3 blade- wind turbine with or without pitch angle mechanism drives the generator via a gear box or directly coupled to a multi-poles PMSG. The generator itself is connected to a full scale bidirectional rectifier which enables full torque control strategy. An inverter and transformer act as intermediate devices to connect wind power system to electrical grid.

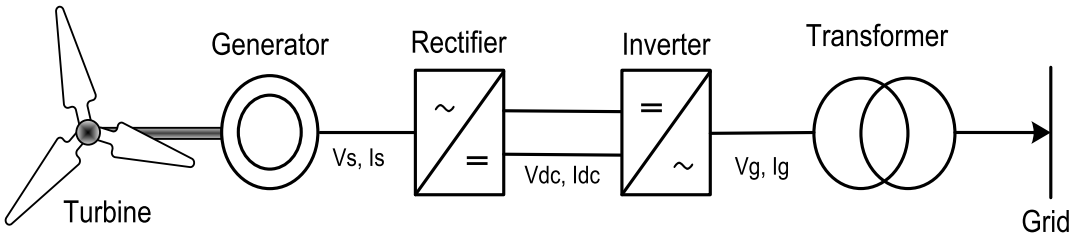

Figure 1.1. Typical single wind power system [1]

The traditional fixed speed wind turbine requires simple controller for pitch angle mechanism or even no controllers if the turbine speed is imposed by grid frequency [16, 17]. In contrast, more complex working conditions are observed for modern wind turbine. The control objectives and system modelling are changed accordingly to wind velocity. The typical power curve of a wind turbine is illustrated in Figure 1.2 which divides working conditions of turbine into three sub-regions [1]. When

wind speed is too small, which is known as cut-in wind velocity, wind power system is not operating due to very small power produced. If wind speed is under rated condition, this is so called partial load condition, is the main working region of wind turbine. In this region, the maximum power capture is the main target of controller. The turbine speed is regulated to track optimal reference at which power coefficient gets maximum value under presence of wind variations. It also reduces the alleviation of aerodynamic and mechanical loads which decrease the useful life of the installation. The third region is known as full load condition where wind power system reaches its upper limitation of electrical production. The power coefficient is now reduced to lower value and power captured is set to constant.

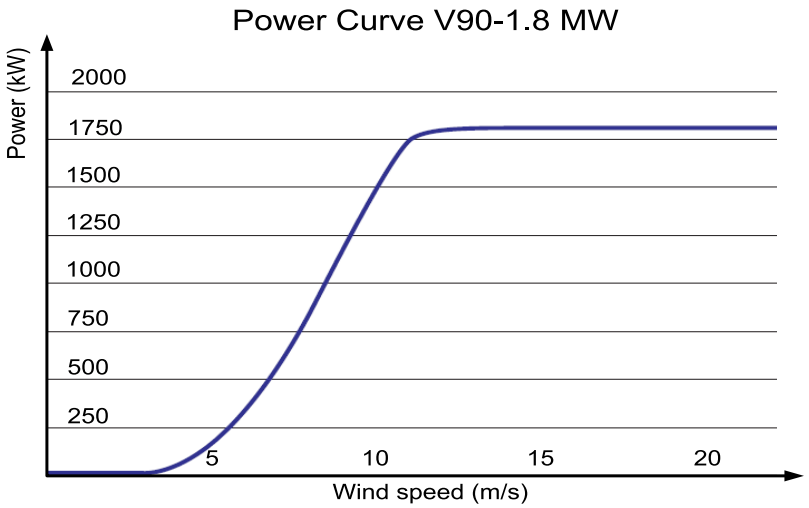

Figure 1.2. Power curve of VESTAS V90-1.8 wind turbine [1]

In the next section, a number of control algorithms are reviewed and summarised. It is not a complete and detailed review; however, it provides general approaches which have been applied to a long-history wind power control.

1.2. Reviews of Control Algorithms for Wind Power System

Wind energy conversion is a sophisticated process that involves a complex combination of aerodynamics, electrical phenomena and the autonomous action of winds [18]. Different working regimes in terms of wind speed, rapid wind fluctuations, and the limitations of mechanical- electrical systems make wind

turbine control design more challenging [19]. A lot of research has been carried out in wind turbine control. In the following section, the most commonly used algorithms in literature will be presented. These controllers consider the plant to be controlled by as signal-processing devices that transform certain input signals into the desire outputs. In other words, this is so called signal-processing-based controller. The other type of controller, the energy-based control which deals with nature of wind power system as an energy transformation plant, is found in the literature. This control idea was firstly originated from [20] and was successfully applied to DFIG-based wind power system control [21]. It is an interesting control approach and worthy to further study.

Maximum power point tracking (MPPT)

This method is very efficient since only speed and power of generator are measured whereas power characteristic of the turbine rotor is completely unknown. The purpose of this method is to operate the wind turbine around the maximum power using information from the static power characteristic and a minimum of information from the system [19]. This method is employed in a hill-climbing-like method of power curve. By computing the gradient and sign of power in term of rotational shaft speed $\partial P_a / \partial \omega_g$ at operating point, controller calculates speed to be controlled of generator. Because of the simplicity, MPPT has been a popular method for wind power system as well as other renewable energy systems such as solar power [22-28]. The gradient and sign of $\partial P_a / \partial \omega_g$ are determined as following Table 1 and are illustrated descriptively in Figure 1.3

Table 1. Gradient determination of MMPT algorithm

$\partial P_a / \partial t$ / $\partial \omega_g / \partial t$	< 0	> 0
< 0	Increase ω_g (case I)	Decrease ω_g (case II)
> 0	Decrease ω_g (case III)	Increase ω_g (case IV)

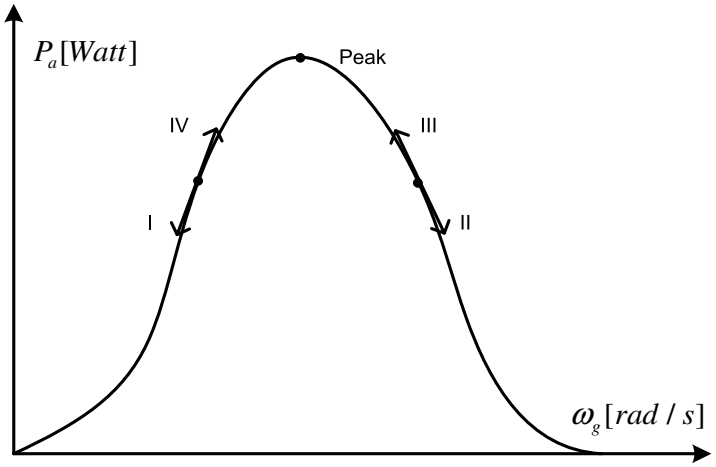

Figure 1.3. Hill-climbed MPPT searching

Basically, MPPT algorithm is illustrated as following:

1. Measure rotational speed $\omega_k \approx \omega_g$, electrical power $P_k \approx P_r$ and the wind speed $\upsilon_k \approx \upsilon$.
2. Depending on the instant value of wind speed, set the rotational speed variation step (equivalent to the searching speed) $\Delta\omega_0$.
3. Estimate the power and speed gradients and deduce their signs: A = sign ($(P_k - P_{k-1})/(t_k - t_{k-1})$) and B = sign $((\omega_k - \omega_{k-1})/(t_k - t_{k-1}))$
4. Deduce the rotational speed variation sign as logic follows: $sign(C)$ = NOT of EXOR(A,B) and obtain the speed variation value at step k: $\Delta\omega_k = sign(C)\Delta\omega_0 \frac{1}{2}$
5. Obtain the control input by integration, as $\omega^*_k \approx \omega_k + \Delta\omega_k$
6. Repeat for $k = k+1$.

In this control algorithm, the rotational speed ω_g is controlled in the sense of approaching the maximum power available based on the operating point position on the power characteristic. The searching procedure of the maximum point, together with the wind speed variations and high turbine inertia, beside its simple controller,

have some drawbacks in significant estimation errors and important high frequency power fluctuations with negative influence on the system overall reliability and less accuracy. MPPT is simple controller algorithm applicable to where has limited resource of sensor measurement; hence, it is widespread in the industry especially in small wind power system [24, 26, 27].

Classical PID Controller

The classical PID control, owing to its key features like simple design, less feedback information required and easy implementation, is widely used in industry applications. It is also a popular choice for wind power system control. PI controller is mostly applied to pitch angle regulated wind turbine in servo control loop to control blades angle [29] and a more complex design PI controllers is for generator and drive train [16, 30, 31]. At partial load condition, PI controller gets the maximum energy capture available from the wind by maintaining the turbine rotor operates on the optimal region where the tip speed ratio must be made to equal the optimal value. In other words, PI controller regulates the rotor shaft speed to follow the optimal speed as presented in a control strategy through speed control loops [16].

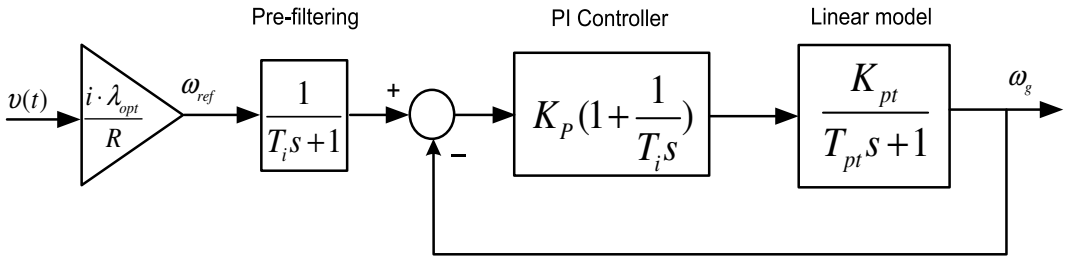

Figure 1.4. PI speed control loop for wind turbine

Speed controller is based on linearization model where the steady state point corresponds to maximum energy efficiency for the wind speed in the long term wind speed component and control structure generally shown in Figure 1.4. To tune parameters of PI controller, we can apply pole placement procedure which will exhibit a two pole one zero dynamic.

Linear Quadratic Gaussian (LQG) Controller

Linear Quadratic Gaussian (LQG) algorithm is probably the most fundamental optimal control problem. It concerns uncertain linear system disturbed by addition white Gaussian noise and quadratic costs. Moreover, the solution is unique and constitutes a linear dynamic feedback control law that is easily computed and implemented. Moreover, the LQG controller is also fundamental to the optimal perturbation control of non-linear systems. The LQG controller is simply the combination of a KALMAN filter i.e. a Linear-Quadratic Estimator (LQE) with a Linear Quadratic Regulator (LQR). LQG control applies to both linear time-invariant systems as well as linear time-varying systems [32-34]. The application to linear time-invariant systems is well-known. The application to linear time-varying systems enables the design of linear feedback controllers for non-linear uncertain systems [19, 34]. In the other approach, uncertainty, wind turbine is model as varying matrices in state space model then multiple model approach is used for controller synthesis [33].

Controller evaluation shows that LQG optimal control is particularly well suited for wind turbine controller synthesis. Indeed, for a linear system, LQG synthesis guarantees an optimal behavior for selected criteria depending on several control objectives. Moreover, LQG synthesis takes into account stochastic properties of the system disturbances, and thus in our case, stochastic properties of turbulent part of wind speed. Static state feedback is calculated in order to minimize a quadratic function depending on control objectives, which are dependent on operating zone.

Fuzzy Logic Controller

Control systems for variable speed wind turbines should continue to evolve towards more and more effective and innovative solutions, also based on soft-computing methodologies, such as fuzzy systems and artificial neural networks. The MPPT tracking control method can be replaced by the sensor-less maximum power point tracking fuzzy system for variable speed wind generators. Fuzzy inference allows to approximate non-linear functions with finite fuzzy rules and the main advantage of

a rule-based system over the neural network is to capture cause and effect in the inference process. Proposed Takagi-Sugeno-Kang (TSK) fuzzy system, by acquiring and processing at each sample instant the inputs, is able to calculate the maximum power that may be generated by the generator. The generator speed will be controlled in order to reach the speed allowing the extraction of the maximum power from the turbine with knowledge from previous operating point; therefore, represents a sensor-less approach since it is not necessary to measure the wind velocity [32]. A simplified illustration of TSK fuzzy system for wind power system is presented in Figure 1.5.

FLC is widely used in combination with other methods which operate in synchronism with each other [22, 35-41]. At below-rated wind speed, the inner loop adopts adaptive fuzzy control based on variable universe for generator torque regulation to realize maximum wind energy capture [22, 35-41]. At above-rated wind speed, a controller based on least square support vector machine is proposed to adjust pitch angle and keep rated output power.

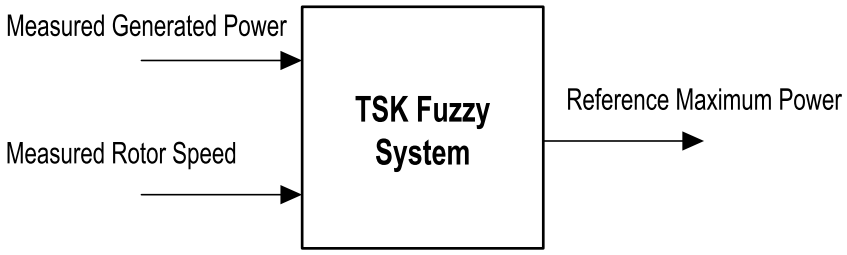

Figure 1.5. TSK Fuzzy control

Linear Parameter Time-varying Control

LPV was first introduced in the early 1990s, are generally obtained by reformulating a nonlinear or time varying system as a linear system whose dynamics depend on a vector of time varying parameters. Natural design method for linearized controllers along some chosen operating trajectories firstly carried out, and then to interconnect them in an appropriate way to get a control formulation for the entire operating region. This method is known as gain scheduling method which is lack of stability and performance guarantees for the nonlinear or time varying

closed loop system since controller parameters for one point cannot be applied to another point even in the same class. Gain scheduling method will work well if the scheduling variables capture the nonlinearities and vary slowly. As an improved version of gain scheduling techniques, LPV model will be represented by a linear model at all operating conditions and a controller with similar parameter dependency is synthesized to guarantee a certain performance specification for all possible parameter values within a specified set. This improvement makes it possible to take into account that the scheduling parameters can vary in time. Linear Parameter Varying controller performs well suited control method for wind energy conversion system and exploited in industry now [16, 32, 42].

Robust Control based on LMIs

Even though gain scheduling techniques are common in wind turbine control, robust controller accounts better for turbine model uncertainties as well as error in measuring the wind speed. Wind power system is a high nonlinearity complex mechanical system leading to significant variations in the dynamic behavior of the system over its operating range.

In literatures, there is a number of work presented robust control for pitch angle control in certain working regions of windmill. A linear model of the wind turbine is first derived from a nonlinear aero-elastic model. Control objectives that associate H_2 and H_1 are formulated in LMI form, which is known to offer powerful tools to mixed criterion optimization to present multi channel-method that provides an efficient way to handle a multi-objective synthesis in variable speed wind turbine control [43]. Nonlinear robust control to maximize energy capture in a variable speed wind turbine with strategy simultaneously controls the blade pitch and tip speed ratio, via the rotor angular speed, to an optimum point at which the efficiency constant (or power coefficient) is maximum. The control method allows for aerodynamic rotor power maximization without the restrictions of exact wind turbine model knowledge [44]. Robust control strategy is developed to regulate the blade pitch angle and rotor speed of a variable speed wind turbine system. The control objective is to maximize the energy captured by the wind turbine in low to

medium wind speeds by tracking a desired pitch angle and rotor speed, with the wind turbine system nonlinearities structurally uncertain. Additionally, the maximization of the energy captured is achieved without the knowledge of the relationship that governs the power capture efficiency of the wind turbine. Instead, an optimization algorithm is developed to seek the unknown optimal blade pitch angle and rotor speed that maximize the energy captured (via the aerodynamic rotor power) while ensuring that the resulting trajectories are sufficiently differentiable.

Wind energy is not constant and windmill output is proportional to the cube of wind speed, which causes fluctuating power of wind turbine generator (WTG). In order to reduce the fluctuating power of WTG, [45] presents an output power leveling technique of WTG by pitch angle control using H_∞ control, and the control input of WTG linear model is separated from the disturbance. The proposed controller is designed using H_∞ control by the Linear Matrix Inequality (LMI) approach.

Grid connection of wind power and control

An increased number of medium and large wind farms connected to national transmission systems, especially offshore plants, are being built. Economies of large scale wind farm deliver more significant savings; thus, there are many wind farm developments involving a large number of machines. Wind power plants now play a more important role as an active generation source in electrical networks. In other words, wind farms must have the capability to support the electric grid when required. A wind power plant controller design is highly necessary for engineers and scientists to find new, smart control algorithms to meet new complex grid codes requirements [26, 28, 30, 46, 47].

1.3. Motivations

Last decade has witnessed a strong attention in wind power from government policies all over the world, so does Singapore government and our NanYang Technological University (NTU). Not standing outside the global trends in the renewable energy, the local government has provisioned for clean energy since the last decade. As a result, more and more research projects related to clean energy are

being run by NTU, in the school of EEE. This research project is one of the educational targets under granted by NTU.

Controllers for wind power have to cope with stochastic behavior of the wind. In order to harvest optimal wind power, the variable speed wind turbine is controlled to track the optimal regime which depends on wind profiles. The natural wind is intermittent and high turbulence phenomenon; hence, the optimal regime is a non-stationary and highly fluctuation reference. Moreover, different working conditions, with corresponding control objectives, accordingly to the variation of wind profiles are another challenging factor for wind power controller design.

Aerodynamics torque produced by a wind turbine is a highly nonlinear function in term of its rotational speed. The wind power system control faces the issue with classical linear control technique even though industrial application of wind power system has gained benefit from PI controller. In literature, there exist a lot of control techniques waiting for field testing. A newly advanced control algorithm applicable to real-world implementation of wind power is in high demand.

Beside the basic goal of maximum power captured from wind, wind power system control also has other requirements such as reducing the fatigue load of mechanical structure opening multi-criterion global control approach. At wind farm level, new grid code requirements for wind farm plants are also intensive for research developments in grid interface control and power control. All these challenging issues are motivations for the author to propose newly designed controllers applicable to wind power system.

1.4. Objectives

The primary objective of this research is to design high-performance controllers for aerodynamic drive-train loop of variable speed wind turbine that will meet the following objectives:

- It should be a controller which provides an excellent optimal power regime tracking to ensure maximum power capture from wind.
- It should be a controller which sufficiently solves the nonlinearity of wind turbine dynamic.

- It should be a robust controller which actively adapts to the changes of stochastic wind profiles.
- It should be a global controller for all operating conditions of wind turbine which smoothly switch between partial load and full load conditions.
- It should be a multi-objectives controller for not only maximizing power but also increasing life-cycle of wind power system.
- The study controller must be possible to apply in real-world application in wind power industry. It secures fast sampling time at higher the turbine dynamic frequency.

Wind turbine is now being larger in size and capacity with few MWs rated power wind turbine having been introduced and implemented. Moreover, there is an increasing number of wind farms are being built and wind power plants are playing a more important role in the national grid system. New grid code standards for wind farm are hence introduced. It is essential to have a new control algorithm to improve the role of wind farm in the grid system. So, wind farm control for new grid connection codes is also a target of this thesis.

The developed control algorithms in this research are Nonlinear PID, Disturbance Models of Predictive Control and Nonlinear Model Predictive Control. Some major development on these control schemes are listed in the next section.

1.5. Major contributions of the Thesis

There are several contributions to scientific research made during the process of finding new control algorithms for wind power system.

Firstly, a comprehensive study of existing controllers reported in the literature is carried out and summarized. The advantages and disadvantages of these controllers are acknowledged as a supporting base to recommend new controllers, linear predictive, nonlinear PID and nonlinear predictive control, for wind power system.
Traditional controllers separate working conditions of wind turbine in some different modes then a single control strategy is designed for each working

condition. In the proposed controller design approaches, a new concept is proposed. Different working regions are considered and combined in only one continuous region with lower and upper bounds.

Another contribution is the solution to cope with intermittence behavior of wind profiles. Wind speed is high frequency fluctuated; hence, a fast online optimal controller is necessary to adjust control input adaptively with changing wind speed.

The new control technique, the Disturbance Models of Predictive Control (DMPC), is a successful solution to the nonlinearity problem of wind aerodynamics. DMPC uses the linear presentation at one specific working point plus the uncertainty. Output disturbance signal and appropriate observer design guarantee offset-free tracking due to linear and plant miss-matches.

Another proposed control technique for wind power system is nonlinear model predictive control (NMPC) which design directly from nonlinear model of wind aerodynamics. NMPC is originally developed to control slow processes in the process control. It is now improved with real-time capability to suitably apply for wind power system control.

The simulation programs as well as the laboratory test rig system are developed to validate the effectiveness of the proposed controllers. From the experimental results with the linear predictive control, it is concluded that these controllers are highly suitable for real-world application.

Real-time evaluation of nonlinear predictive control is also discussed by the means of a C++ program which is complied to run in a real-time Linux computer workstation. This simulation study does not represent all implemental practice issues; however, it provides a tool to examine the capability of nonlinear predictive control in real-time application.

In wind farm control, new application of DMPC controller promises attractive solution to replace conventional control scheme such as PID to fulfill new grid-code requirements. High-performance and stability are properties drawn from simulation results for a wind farm.

A proper sequence of designing controller is to get detailed modeling of wind power system and results validation. The sequence of designing procedure is summarized in the next section.

1.6. Organization of the Thesis

Chapter 2 presents the wind and wind power system characteristics. The behavior of wind and its effects to wind turbine are studied. A multi-criterion objective, aerodynamic power from wind, and system modeling appropriate for controller designs are also presented in this chapter. In the last section, the wind power system test-rig for testing controller at laboratory scale and the simplified setup for speed controller testing are illustrated.

In Chapter 3, a numerous number of control algorithms theory for wind power system are reviewed and summarized. The first control method, Fuzzy Logic Controller (FLC), considers complex wind power system as a black box. The next, linear controller designs are based on linear presentation of the nonlinear modeling at some specific points. The extended PID, linear model predictive control (MPC) and the disturbance model predictive control (DMPC) are studied. Finally, fundamental nonlinear version of MPC which directly designs from nonlinear modeling will be presented.

Chapter 4 presents the application of control methods reported in Chapter 3 for speed loop control of variable speed wind turbine. At first, conventional PID controller for speed loop and current loops of permanent magnet generator are presented. Then, in the next section, different control algorithms for controlling speed loop are replaced the PI speed loop while PI current loops are still unchanged. Simulation and experiment results are presented to demonstrate the performance of these methods for wind power control.

In Chapter 5, the basic of nonlinear predictive controller and real time algorithm, for wind power system, are introduced then designing of this controller is presented. The complex procedure of how to obtain a fast calculation of nonlinear predictive control and practically oriented simulation results are mentioned.

Chapter 6 presents the strategy and control of wind farm connected to the national grid system. In small capacity, wind turbine is considered as a passive distributed generation, which means that the technical requirements to connect generation source are determined by the public electricity system. In contrast to a large capacity turbine (at farm level), wind turbine system has more active capability to assist the power system by supplying the ancillary services such as voltage control and fault ride-through by DMPC controller.

The design process of control schemes for wind power system is better understandable with the background of the system. In the next chapter, therefore, wind and wind power system characteristics are studied in details from wind behaviours and wind effects by wind turbine; wind generation system modelling; control objective and emulator system for better understanding of wind power system control in context of proposed control schemes.

CHAPTER 2

WIND AND WIND POWER SYSTEM CHARACTERISTICS

This chapter presents the basic of wind turbine system driving a permanent magnet synchronous generator. In the first section, the wind, wind speed characteristics and power from wind are studied to understand fundamentals of wind aerodynamics. A complete detail of wind power system modeling, which includes aerodynamics, generator and converter, is presented in the following section. The objective of wind power system control is studied with concern to economic aspects as well as technical consideration. The last section illustrates the emulator test-rig system for testing controller at laboratory scale.

2.1. Wind and Wind Speed Characteristics

Wind is the movements of air masses in the atmosphere on the earth's surface. The movement of air is mainly caused by the effects of the temperature differences between tropics and earth's poles. In addition to uneven heating, the Coriolis forces associated with the spin of the Earth around its axis less than 30^0 latitude also cause the air to move. Wind carries energy so called aerodynamic energy which is exploited from ancient time to ease labors to the modern life in electrical generation. The kinetic energy contained in the wind is [1]:

$$E = \frac{1}{2} m v^2 \tag{2.1}$$

where m is air mass and v is wind speed. The mass is defined as mass contained in the volume of the air that flows to the rotor. However, for the convenience reason, mass per second is often used. The energy per second is the same as power. Hence, the aerodynamic power from wind flowing through a rotor disc is given in (2.2)

$$\begin{aligned} P_a &= \dot{E} = \frac{1}{2} \dot{m} v^2 = \frac{1}{2} \rho \pi R^2 v^3 \\ \dot{m} &= \rho \pi R^2 v \end{aligned} \tag{2.2}$$

Wind speed is a stochastic quantity due to the surface of the earth is not homogeneous and amount of energy varies both in space and time. Wind is changing from time to time and between locations with different terrain conditions. Wind speed is commonly considered to be composed of a seasonal wind plus turbulence component [1, 16, 19, 48].

$$\upsilon = \upsilon_m + \Delta\upsilon \tag{2.3}$$

In practice, the mean speed is usually represented by statistical distribution of the wind. The most common density function used to represent the real distribution of winds is Weibull function as following [1, 16, 19, 48]

$$Weibull = \frac{k_w}{C_w}\left(\frac{\upsilon}{C_w}\right)^{k_w-1} e^{-(\upsilon/C_w)^{k_w}} \tag{2.4}$$

where k_w and C_w are the shape and scale coefficients. Figure 2.1 shows the distribution curve of the case with $k_w = 2$ and $C_w = 7$. The Weibull probability function reveals that high wind speed with small distribution value rarely occurs. The moderate wind speed which is around 5 m/s to 8 m/s happens more frequently. This is crucial information to determine the economical viability of the wind power project.

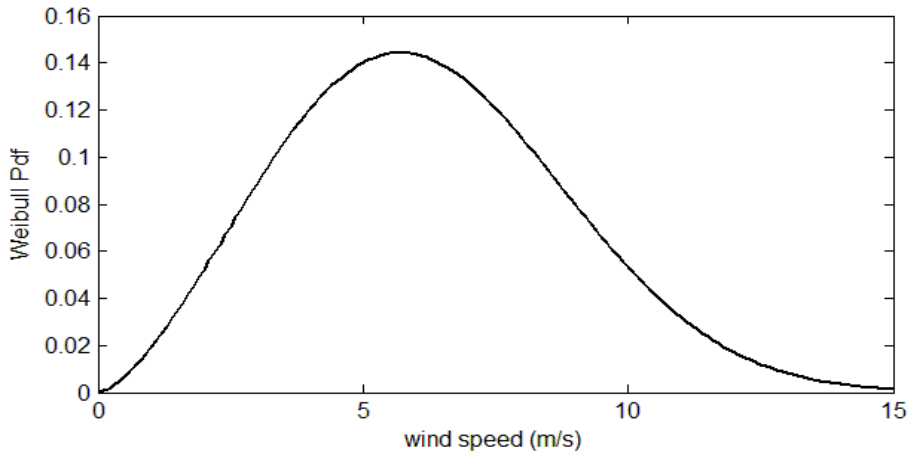

Figure 2.1. Weibull probability distribution of wind speed

Mean of wind speed also changes in accordance with the height by a function known as wind shear. At lower layer near earth surface, obstacles such as plants and

houses produce friction forces that reduce wind speed. At higher level, reduced friction produces higher wind velocity. This phenomenon can be represented by mathematical equation as follows [1, 19]

$$v_m^z = v_m^{zref} \left(\frac{z}{z_{ref}}\right)^{\sigma_w} \tag{2.5}$$

The surface roughness exponent σ_w depends on type of terrain. It is obtainable by experiment for some certain type of surfaces.

Turbulence term of wind speed includes all high frequency components which fluctuate around seasonal term. In general, wind turbulence has small effect on the annual energy production, which is mainly determined by seasonal winds. However, high frequency components have considerable impact on power quality and aerodynamic load. Hence, effects of this term should be considered in controller design process in order to attain good control algorithms.

2.2. Wind speed simulation for testing controller at laboratory scale

2.2.1. Fixed-point wind speed model

Wind model is crucial to obtain realistic simulation that gives fundamental information for determining dynamic power available from wind, especially for testing controller at laboratory scale. A detail presentation of large band simulation of wind speed for a single turbine study is first presented in [48] and being adapted later in [16, 49]. For wind speed simulation at wind farm level and interconnection between farms, an extensive huge work is presented in [18]. Wind model combining both seasonal term and stochastic component in [48] is also adopted in this section for the controller testing study. In the context of [48], one of the best known references in large band wind speed modeling for seasonal wind speed is the Van der Hoven's model which has harmonic power spectrum in the range from 0.0007 to 9000 cycles/h. This frequency range contains the spectral domain for both medium to long term variations and turbulence component. For every discrete

angular frequency $\omega_i, i = \overline{1,..N+1}$ having power spectral density of $S_{vv}(\omega_i)$ then the harmonic at frequency ω_i has amplitude A_i [48].

$$A_i = (2/\pi)\sqrt{0.5[S_{vv}(\omega_i) + S_{vv}(\omega_{i+1})][\omega_i - \omega_{i+1}]} \tag{2.6}$$

Wind speed as function of time takes the formula [48].

$$\upsilon_m = \sum_{i=0}^{N} A_i \cos(\omega_i t + \varphi_i) \tag{2.7}$$

The results of Van der Hoven's model has the same magnitude regardless of the mean wind speed and this model cannot be used for a complete description of the wind speed over a time scale of seconds, minutes and hours because this model has a significant drawback: the turbulence component is treated as a stationary random process.

Turbulence component known as fast wind speed variations typically occurs within 10 minutes. The mathematical description of the turbulence dynamic can be obtained by using Von Karman's spectra which has the form [19, 48]

$$S_{vv}(\omega) = \frac{0.475\sigma^2 \dfrac{L_t}{\upsilon_m}}{[1 + \dfrac{\omega L_t}{\upsilon_m}]^{5/3}} \tag{2.8}$$

To present turbulence component, a suitable shaping filter with a white noise is usually synthesized. The shaping filter adapted in [48] has transfer function based on experimental identifying process.

$$H_t(j\omega) = \frac{K_F}{(1 + j\omega T_F)^{5/6}} \tag{2.9}$$

where parameters K_F, T_F, which depend on the low-frequency wind speed, are obtained with a white noise having one-unit variance. The non-stationary wind speed, computed by this procedure, can be seen from Figure 2.2. The simulated wind speed has turbulence length of $L_t = 150$; turbulence density of 20% around seasonal speed of 7 m/s; in 80 seconds. Most importantly, simulation of wind speed resembles to the actual wind realizing controller design testing at laboratory scale.

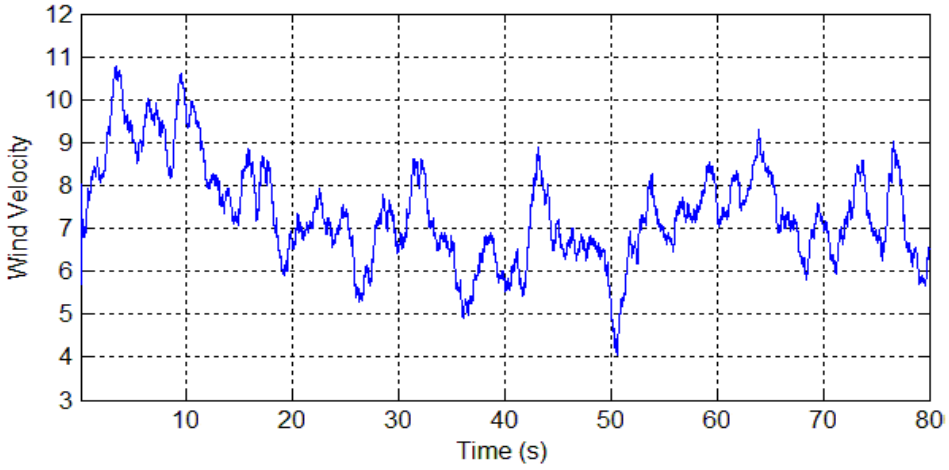

Figure 2.2. Wind speed simulation in a range of 80 seconds

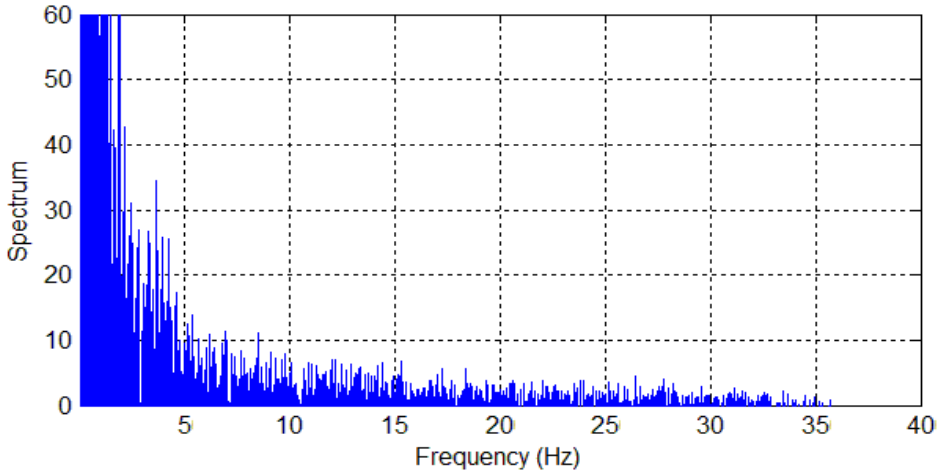

Figure 2.3. Spectral in frequency domain of simulated wind speed

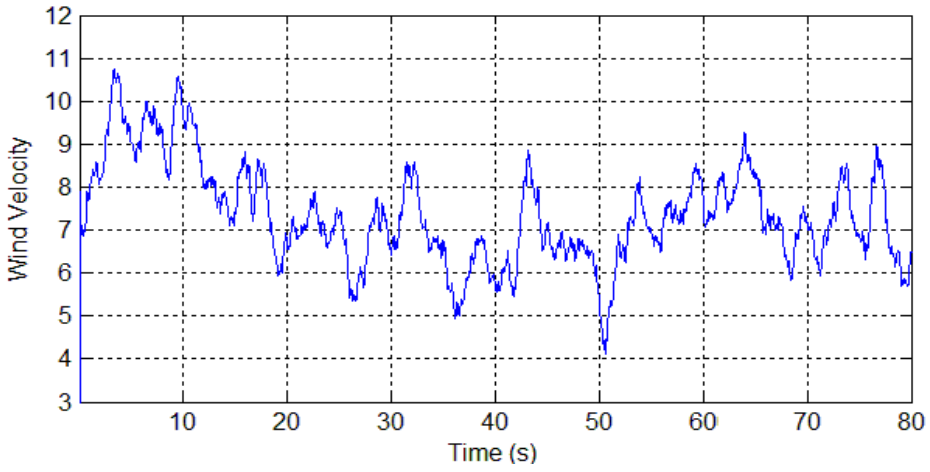

Figure 2.4. Filtered wind speed simulation

Figure 2.3 shows simulated wind speed spectrum in the frequency domain. More power spectral density distributes at frequency below 5 Hz where high turbulence wind has spectrum around 25 Hz. However, very high frequency wind speed does not affect the power production of a wind turbine since the turbine itself acts as a low-pass filter. Hence, the very high turbulence term of the wind speed is filtered out in this study of controller designing and testing. The remaining component, which mainly contributes to aerodynamic power, has a frequency of less than 10 Hz. This means that the wind speed can be assumed constant during the time interval of 100 milliseconds. The filtered wind speed can be seen in Figure 2.4. This interval is really meaningful for practical oriented controller testing in comparison to standard requirement of wind speed measurement. In IEC 61400-21, it is stated that the minimum 200 ms average power must be measured as a part of power quality test of wind turbine [18].

2.2.2. Wind speed experienced by turbine rotor

The single point wind speed model presented in Section 2.2.1 represents only the initial information for determining the wind speed experienced across the turbine's blades. However, wind speed experienced by rotor motion is affected by a series of aerodynamic actions. The two typical effects are known as wind shear and tower shadow [18, 19, 50]. These two cumulative effects yield periodic wind torque variations with a frequency which is an integer multiple of the blades' rotational speed and they are significant, especially for large wind turbines.

Wind shear

For large scale wind turbine system which has long blades and tall tower, there will be differences of wind speed at their tip blades. Wind shear is known as the effect of increase with height by wind speed. The blade pointing downward will encounter lower speed that pointing upward then torque will oscillate three times (3p effect) as shaft speed because of each blades passing though minimum and maximum point. The periodic variation in wind speed produces periodic wind torque variations. Wind shear model in term of radial distance from rotor axis r and azimuth angle θ in the polar coordinate is presented in [51] and is adapted in this study.

$$V(r,\theta) = V_{H_b}(\frac{r\cos(\theta)+H_b}{H_b})^{\delta} = V_{H_b}[1+V_s(r,\theta)] \tag{2.10}$$

where V_H is wind speed at hub height, δ is empirical wind shear exponential which depends on terrain of wind farm. H_b is the hub height and $V_s(r,\theta)$ is wind shear shape function; α_w is empirical wind shear exponent. The third order approximation for $V_s(r,\theta)$ should be as follows.

$$V_s(r,\theta) = \delta(\frac{r}{H_b})\cos\theta + \frac{\delta(\alpha_w-1)}{2}(\frac{r}{H_b})^2\cos^2\theta$$
$$+ \frac{\delta(\delta-1)(\delta-2)}{6}(\frac{r}{H_b})^3\cos^3\theta \tag{2.11}$$

Tower shadow

Horizontal-axis wind turbines always have tower to support nacelle, turbine and generator, which affects to the airflow. It is resulting to wind speed is redirected thereby reduces the torque as each time a blade passing to tower. The torque pulsation of tower effect has more contribution compared to that of wind shear at about 5%. The 3p oscillations caused by tower effect is an addition of turbulence term to the hub height wind speed using reference frame and parameters illustrated in Figure 2.5 [51].

$$V(x,y) = V_H + v_{tower}(x,y) \tag{2.12}$$

$$v_{tower}(x,y) = V_0 a^2 \frac{y^2-x^2}{(y^2+x^2)^2} \tag{2.13}$$

$$V_0 = V_H[\frac{1+\alpha(\alpha-1)R^2}{8H_b^2}] = mV_H \tag{2.14}$$

Now we can compute the spatially total wind field model:

$$v(t,r,\theta) = V_H(t)[1+\delta(\frac{r}{H_b})\cos\theta + \frac{\delta(\delta-1)}{2}(\frac{r}{H_b})^2\cos^2\theta$$
$$+\frac{\delta(\delta-1)(\delta-2)}{6}(\frac{r}{H_b})^3\cos^3\theta + \frac{ma^2(r^2\sin^2\theta-x^2)}{(r^2\sin^2\theta+x^2)^2}] \tag{2.15}$$

This total wind speed formulation provides observation of wind at any point of rotor disk area in term of turbine parameters. The question now is how to obtain the equivalent total wind speed giving the same aerodynamic torque. By extracting into each terms of contribution, we get [51]:

$$\upsilon_{eq}(t,\theta) = \upsilon_{eq0} + \upsilon_{eqws} + \upsilon_{eqts} \tag{2.16}$$

where: $\upsilon_{eq0} = V_H$

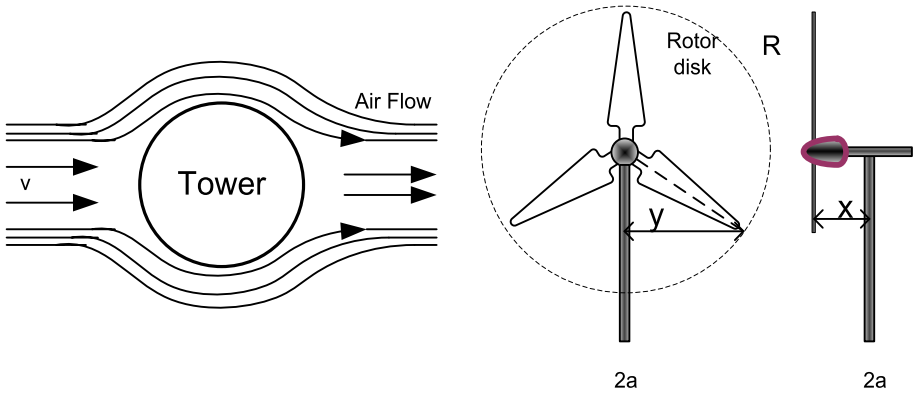

Figure 2.5. Dimensions used in shadow formulas

$$v_{eqws} = V_H[\frac{\delta(\delta-1)}{8}(\frac{R}{H_b})^2 + \frac{\delta(\delta-1)(\delta-2)}{60}(\frac{R}{H_b})^3\cos 3\theta] \tag{2.17}$$

$$v_{eqts} = \frac{mV_H}{3R^2}\sum_{b=1}^{3}[\frac{a^2}{\sin^2\theta_b}\ln(\frac{R^2\sin^2\theta_b}{x^2}+1) - \frac{2a^2R^2}{R^2\sin^2\theta_b + x^2}] \tag{2.18}$$

This total equivalent wind speed in (2.16) has three components. The last two is the modifications due to wind shear and tower shadow effects to the single point wind speed simulation presented in Section 2.2.1. This total wind speed from now on can be used to calculate aerodynamic torque, optimal trajectory in later sections. For the limited research condition, this thesis only studied the 3p effects of tower shadow and wind shear. For a completely comprehensive model of wind speed experienced by rotor, a 3p of turbulence components should be added to wind speed model which was described in [18]. Those 3p components are significant for wind power aerodynamics study. However, the effect of turbulence component could be reduced since wind turbine acts as a low pass filter in control engineering approach [52].

2.3. Wind Energy Conversion System Modeling

A typical single VSWT system includes a wind turbine driving generator. In this study, a permanent magnet type is used, fed by a full-scaled IGBT converter and loads as in Figure 2.6. The flow of wind stream onto the wind turbine blades generates an aerodynamic torque to rotate the wind turbine at a low shaft speed. The speed of the lower shaft is increased to a higher shaft speed by a gear box in order to feed the rotation of the generator. The converter is configured as a 3-phase 2-level structure and is controlled by space-vector pulse width modulation (SV-PWM) which allows a bidirectional power flow.

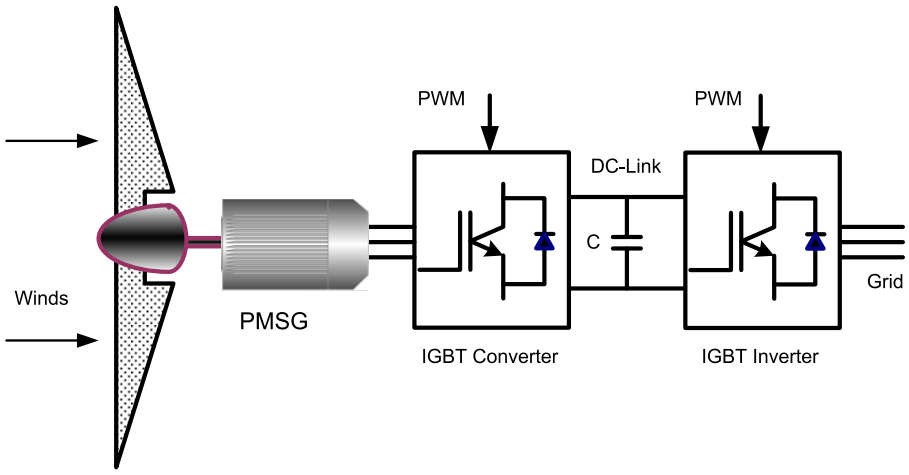

Figure 2.6. General single wind power system structure

System modeling is crucial point before applying control methods for wind power system. To get model of wind turbine, two approaches are usually used. The first considers wind turbine as black box then the order and parameters of the model which meets the WECS dynamics at each operating condition through identification. Since the operating points are determined by the wind speed, which is a non-controllable input variable, it is necessary to conduct measurement during long periods. The data collected during intervals of stationary wind speed are therefore used to identify a linear model. Thus, a family of linear models is obtained. In contrast, the other approach relies on a lumped representation of the mechanical system. The drive train and structure are modeled as a series of rigid bodies linked to each other by flexible joints and excited by aerodynamic torque. Within this work, we adopted the later method to get model of wind turbine.

2.3.1. Aerodynamic wind power model

The turbine aerodynamics describes the forces developed when wind turbine rotor interacts with the wind stream. Actuator disc theory (in Figure 2.7) based on the momentum theory is commonly used to illustrated aerodynamics [16, 19]. The turbine is considered as an actuator disc, which is a generic device that extracts energy from the wind. The actuator disc is immersed in an airflow round rotor in the atmosphere. With the condition that air is incompressible; the mass flow rate must be the same everywhere within the tube. Since the actuator disc extracts part of the kinetic energy of the wind, the upstream wind speed υ_1 is necessarily greater than the downstream speed υ_2. Consequently, for the stream tube just enclosing the disc, the upstream cross-sectional area A_1 is smaller than the disc area A_d, which in turn is smaller than the downstream cross-sectional area A_2.

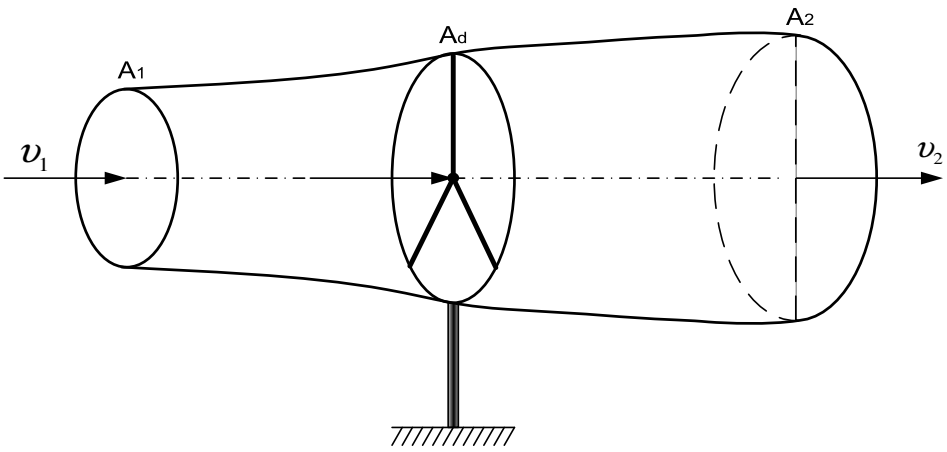

Figure 2.7. Actuator disc theory illustrated aerodynamics

By definition, wind turbine rotor only subtracts energy from the wind speed; air mass flow rate is equal at every where round the tube.

$$\rho A_1 \upsilon_1 = \rho A_d \upsilon_d = \rho A_2 \upsilon_2 \tag{2.19}$$

The air that passes through the disc undergoes a speed drop by a factor a which is defined as the axial flow interference.

$$\upsilon_d = (1-a)\upsilon_1 \text{ where } 0 \le a \le 1 \tag{2.20}$$

The force F_d which is originated by the pressure drop introduced by the actuator disc on the incident airflow is the total speed drop multiplying the mass flow rate

$$F_d = (\upsilon_1 - \upsilon_2)\rho\upsilon_d A_d = (\upsilon_1 - \upsilon_2)\rho A_d \upsilon_1(1-a) = (p^+_d - p^-_d)A_d \tag{2.21}$$

where p^+_d and p^-_d are the air pressure immediate before and after the disc.

Using Bernoulli's equation, the pressure difference is

$$p^+_d - p^-_d = \frac{1}{2}\rho(\upsilon_1^2 - \upsilon_2^2) \tag{2.22}$$

Replacing (2.22) into equation (2.21), we get

$$\upsilon_d = \frac{1}{2}(\upsilon_1 + \upsilon_2) => (\upsilon_2 - \upsilon_1) = 2(\upsilon_1 - \upsilon_d) \tag{2.23}$$

The kinetic energy of an air mass travelling at the speed υ is in (2.1), the power extracted by the disc is:

$$P_a = E_1 - E_2 = \frac{1}{2}\rho A\upsilon_d(\upsilon^2_1 - \upsilon^2_2) = \frac{1}{2}\rho A\upsilon_1^3 4a(1-a^2) \tag{2.24}$$

A conventional way of characterizing the ability of a wind turbine to capture wind energy is the power coefficient:

$$C_p = 4a(1-a)^2 \tag{2.25}$$

Then aerodynamics power captured by wind turbine is expressed

$$P_a = \frac{1}{2}\rho A\upsilon_1^3 C_p = P_{wind}C_p \tag{2.26}$$

where P_{wind} is the power available from wind power. Equation (2.26) shows that the power captured is less than actual wind power by a fraction C_p. The maximum value of power coefficient is 16/27=0.593, known as Betz limit theorem, and occurs at a =1/3. In the pitch angle controlled wind turbine, C_p is the function of pitch angle and tip speed ratio which is discussed in details in the next section.

2.3.2. Drive Train Dynamics

The aerodynamic torque generated by flows of wind speed into turbine blades is known as

$$T_a = 0.5\rho\pi R^3 v^2 C_q(\lambda,\beta) \tag{2.27}$$

where the tip-speed ratio λ is defined as the ratio between the linear blade tip speed and wind speed

$$\lambda = \omega_r R / v \tag{2.28}$$

The torque coefficient $C_q(\lambda,\beta)$ is commonly approximated by a polynomial nonlinear function. In this manuscript, the authors adopted the approximation function $C_q(\lambda)$ as a case-study when $\beta = 0$ for the case of a fixed-pitch angle wind turbine [19].

$$\begin{aligned} C_q(\lambda) = {} & 0.0061 - 0.0013\lambda + 0.0081\lambda^2 - 9.7477\cdot 10^{-4}\lambda^3 - 6.5416\cdot 10^{-5}\lambda^4 \\ & + 1.3027\cdot 10^{-5}\lambda^5 - 4.54\cdot 10^{-7}\lambda^6 \end{aligned} \tag{2.29}$$

The power coefficient is then defined by (2.28). The power coefficient function reaches its maximum value of $Cp_{\max} = 0.47$ when the tip-speed ratio is at its optimal value $\lambda_{opt} = 7$; the curves of C_p, C_q are illustrated in Figure 2.8.

$$C_p(\lambda) = C_q(\lambda)\lambda \tag{2.30}$$

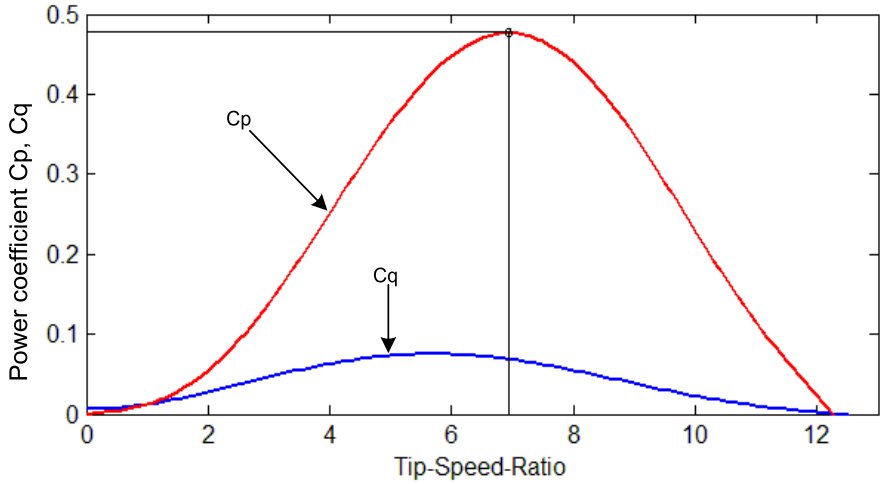

Figure 2.8. Power coefficient approximation curve

The aerodynamic torque polynomial curves in terms of turbine speed with different wind speeds are illustrated in Figure 2.9.

Aerodynamic torque can also be re-written in other form of shaft angular speed,

$$T_a = \frac{1}{2}\rho\pi R^2 Cq(\lambda,\beta)\frac{R^3}{\lambda^2}\omega^2 \tag{2.31}$$

The equation (2.27) presents the aerodynamic torque available by wind energy in term of wind speed. However, wind speed is not always trusted measurement due to disturbance and anonymous changes of wind so the equation (2.31) is used for shaft speed representation instead of wind speed.

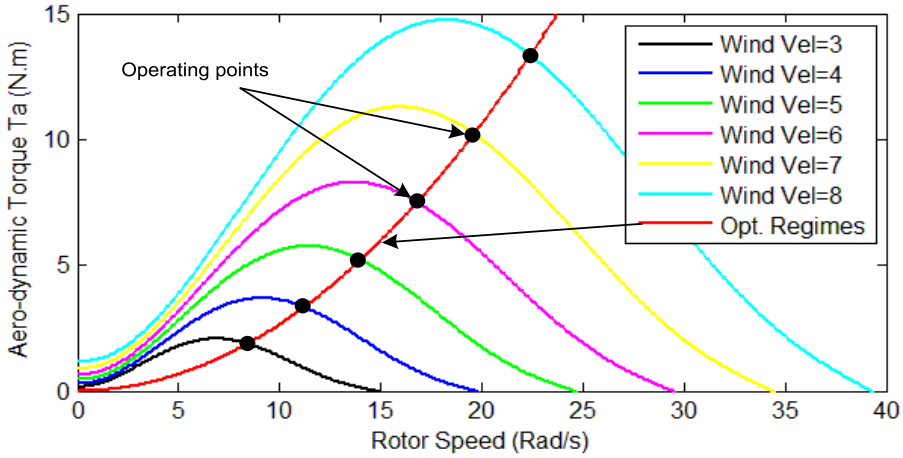

Figure 2.9. Aerodynamic torque curve in term of rotor speed

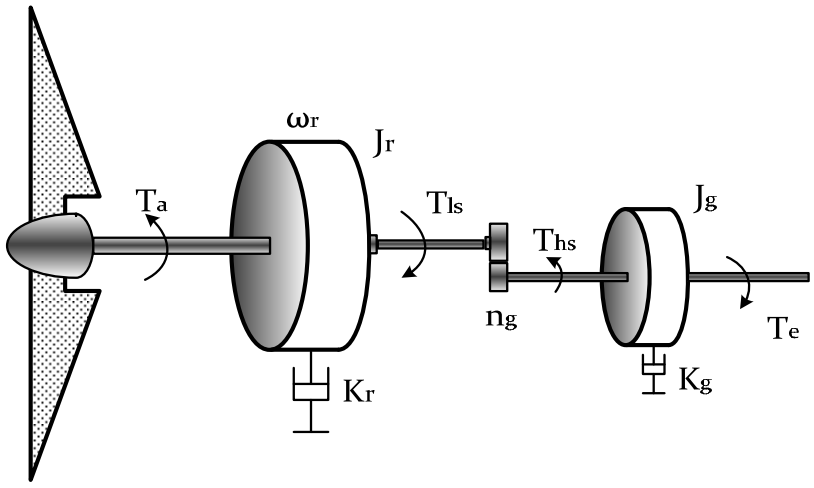

Figure 2.10. Two-mass model of wind turbine

Wind power captured will generate drive train subsystem that is modeled as two-mass model (Figure 2.10). The first mass includes turbine blades and drive-train while the second mass is generator rotor. Two mass bodies are coupled each other through gear box.

The dynamic response of the rotor driven by aerodynamic torque T_a is derived as

$$J_r \dot{\omega}_r = T_a - T_{ls} - K_r \omega_r \tag{2.32}$$

Mechanical dynamic equation of the gear box considered about torsion and friction:

$$T_{ls} = B_{ls}(\theta_r - \theta_{ls}) + K_{ls}(\omega_r - \omega_{ls}) \tag{2.33}$$

The generator is driven by high speed torque and is brake by T_e, the dynamic equation mechanical aspect of generator:

$$J_g \dot{\omega}_g = T_{hs} - K_g \omega_g - T_e \tag{2.34}$$

Assuming the ideal gear box give transmission ratio n_g we have:

$$\eta = \frac{T_{ls}}{T_{hs}} = \frac{\omega_g}{\omega_{ls}} \tag{2.35}$$

Substitute into equation (2.32) and (2.34), the generator mechanical dynamics:

$$J_t \dot{\omega}_r = T_a - K_t \omega_r - T_g \tag{2.36}$$

where: $J_t = J_r + \eta^2 J_g$, $K_t = K_r + \eta^2 K_g$, $T_g = \eta T_e$

In general, there is flexibility (or stiffness) in the connection between the first mass (wind turbine blades and drive-train) and the second mass (generator) through gear box. The gear box ratio in (2.35) is not always perfectly obtainable; however, this flexibility is not a significant hence it is ignored in this thesis study. Two-mass body system is simplified in to one mass body system. Equation (2.36) presents drive-train dynamic of wind turbine as one rigid body which includes turbine blades, drive-train and generator rotor (Figure 2.11).

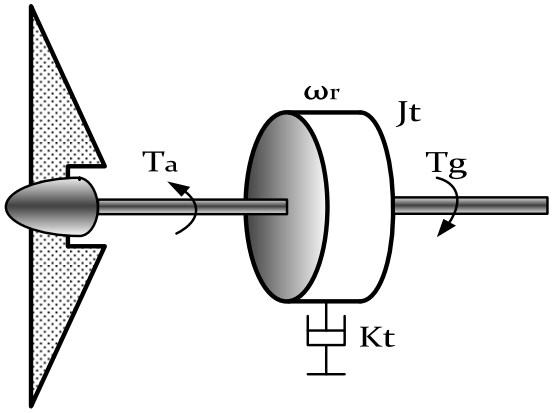

Figure 2.11. One-mass model equivalent of wind turbine

2.3.3. Linear Presentation of Drive train Modeling

Wind turbine aerodynamic torque T_a is known as nonlinear and stochastic system seen from equations (2.29–2.31). T_a is nonlinear function in term of two variables such as rotor speed and wind speed. Figure 2.12 illustrates the curves of aerodynamics torque as nonlinear function of rotor speed with different wind speeds from 5-8 m/s. To obtain a linear presentation of the nonlinear dynamic in (2.36), Taylor series expansion of nonlinear function gives

$$\Delta T_a(\omega_r, \upsilon) = \Delta\omega_r \frac{\partial T_a}{\partial \omega_r}\bigg|_{(\omega_r^0, \upsilon^0)} + \Delta\upsilon \frac{\partial T_a}{\partial \upsilon}\bigg|_{(\omega_r^0, \upsilon^0)} \tag{2.37}$$

where $\Delta T_a, \Delta\omega_r, \Delta\upsilon$ are variation of torque, speed and wind speed around the operating point (ω_r^0, υ^0)

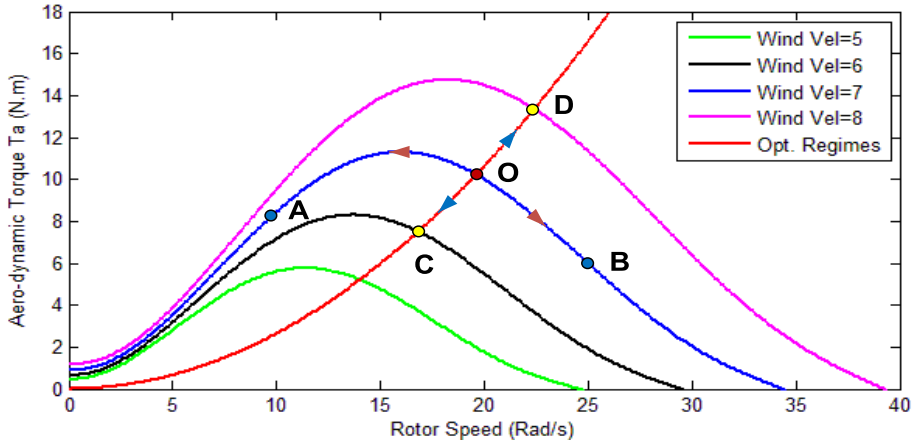

Figure 2.12. Step responses of linear models VSWT

In general, linearization of the aerodynamic torque is performed at the optimal point which lies on the optimal regimes (red colour in Figure 2.12). The optimal point i.e. the linearization point, is where $Cp(\lambda)$ gets the highest value of $Cp_{max}=0.47$ when the tip-speed-ratio is at its optimal value, $\lambda_{opt}=7$. More specifically, at wind speed of 7 m/s, operating point of wind turbine is O in Figure 2.12; this point will move to point C or D when wind speed decreases or increases respectively. Other possibility, if the wind turbine is not well controlled to track optimal regime closely, lower power coefficient at point A and B with smaller/bigger tip-speed-ratio than optimal value could be the operating point.

The process of linearization becomes difficult since one linear model for all the large range of nonlinear functions is not possible. Some different linear models at different working points are represented for nonlinear wind turbine aerodynamics. The snap shot linear analysis function of MATLAB for a horizontal axis fixed pitch angle wind turbine, which was introduced in [19], gives linear transfer functions.

$$G_O(s)=\frac{\omega_r}{T_g}=\frac{-1.944}{s+1.75} \qquad \text{at operating point O} \qquad (2.38)$$

$$G_A(s)=\frac{\omega_r}{T_g}=\frac{-1.944}{s+1.292} \qquad \text{at operating point A} \qquad (2.39)$$

2.3.4. PMSG Modeling

Electrical generator is the main device converting wind energy into electric power. The most popular and largely used is induction generator (IG) and doubly-fed induction generator (DFIG) systems which offer more advantages in for exchanging of active and reactive power with the grid as well as the capability of fulfillment with grid codes. However, permanent magnet machines are today manufactured for high capacity up to a rated power of about 6 (MWs), which settles a new trend in wind power generation. It delivers more efficiently than the conventional synchronous machine since there is no exciter needed. In this project, the PMSG associated with IGBT converter is therefore investigated.

The stator of the PMSG and the wound rotor synchronous motor (SM) are similar. In addition, there is no difference between the back EMF produced by a permanent magnet and that produced by an excited coil. Hence the mathematical model of a PMSG is similar to that of the wound rotor synchronous machine. The stator d-q equations in the rotor reference frame of the PMSG are [19]:

$$\begin{aligned} u_d &= R_s i_d + \omega_s L_q i_q + \frac{dL_d i_d}{dt} \\ u_q &= R_s i_q - \omega_s (L_d i_d + \psi) + \frac{dL_d i_d}{dt} \end{aligned} \tag{2.40}$$

$$J_g \frac{d\omega_r}{dt} = T_{hs} - K_g \omega_g - T_e \tag{2.41}$$

$$\frac{d\theta}{dt} = \omega_g \tag{2.42}$$

ψ is the constant flux that is due to the permanent magnets. The electromagnetic torque is:

$$T_e = \frac{3}{2} p((L_q i_q + \psi) - L_d i_q i_d) \tag{2.43}$$

$$\begin{bmatrix} u_d \\ u_q \\ u_0 \end{bmatrix} = \frac{2}{3} \begin{bmatrix} \cos(\theta) & \cos(\theta - 2\pi/3) & \cos(\theta + 2\pi/3) \\ \sin(\theta) & \sin(\theta - 2\pi/3) & \sin(\theta + 2\pi/3) \\ 1/2 & 1/2 & 1/2 \end{bmatrix} \begin{bmatrix} u_a \\ u_b \\ u_c \end{bmatrix} \tag{2.44}$$

where p is pole pairs. In a magnet surface mount machine with coils in slots and $L_d = L_q = L_s$ and the inductances are not functions of time. The equations are simplified to:

$$u_q = R_s i_q + \omega_s (L i_d + \psi) + L_s \frac{di_q}{dt} \tag{2.45}$$

$$u_d = R_s i_d - \omega_s L i_q + L_s \frac{di_d}{dt} \tag{2.46}$$

$$T_e = \frac{3}{2} p \psi i_q = K_e i_q \tag{2.47}$$

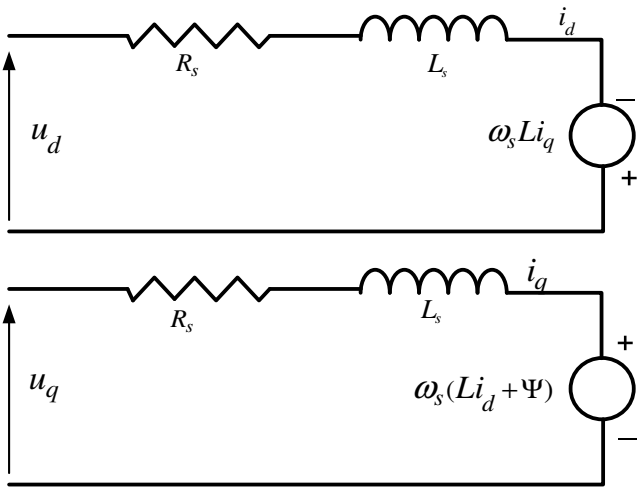

Figure 2.13. Equivalent circuit for PMSM

The stator frequency ω_s is proportional to the shaft rotational speed, $\omega_s = p\omega_g$ which depends on how the electrical generator interacts mechanically. K_e is known as torque constant in the DC machine. As can be seen from modelling details, WECS is a strongly nonlinear system. Firstly, the aerodynamic torque from (2.27) is second order in terms of turbine speed and the main nonlinearity contribution from the torque coefficient, which is a sixth order polynomial nonlinear function in terms of turbine speed in (2.29). Secondly, the electrical modelling of PMSG also has the cross-coupling term in the d-q current. Moreover, the high frequency of change in wind speed results in the WECS and has strong time varied parameters.

2.3.5. Power Converter

The power converter has important roles in the wind turbine variable-speed operation as interfacing between generator and the electrical grid. It functions as a decoupling device between the two above elements and allows the power flow control effectively. The interest in this thesis study will be focused on one of the most popular converter structures, namely the back-to-back converter [53], employing two PWM controlled voltage-source inverters (VSI), as shown in Figure 2.6.

The back-to-back configuration consists of a 3-phase converter (rectifier) connected to the PMSG, which will be further denoted as generator-side converter; and a

converter connected to the mains, called in the following as grid-side converter. The two power electronics converters are connected through the so-called DC-link, which represents a direct current circuit having a smoothing filter, *e.g.*, a capacitor. Therefore, the general control objectives associated with variable-speed wind turbine are divided in two independences, namely in generator speed control and electrical power transfer control respectively. The first objective is implemented within the generator-side converter connected to the turbine-generator to aim directly controlling the captured power by variable-speed operation. The system subjected to control is therefore composed of the wind aerodynamics, mechanical transmission, electrical machine and the turbine-side converter. The second control scope is associated with the interaction between the grid side inverter and the grid, focusing on the active and reactive power control. Here, the system subjected to control is composed of the electrical grid, the grid-side converter and the DC-link.

Converter model can be considered as continuous function due to the PWM switching frequency is much higher than the fundamental frequency of electrical machine and inductance devices has the property to smooth the electrical current. With the switching states of converter are determined by the state of PWM signals sent to pin G of IGBT gates as follows:

$$s_a = \begin{cases} 1, & \text{if } S_1 \quad on \quad ; \quad S_2 \text{ off} \\ 0, & \text{if } S_1 \quad \text{off} \quad ; \quad S_2 \; on \end{cases} \tag{2.48}$$

$$s_b = \begin{cases} 1, & \text{if } S_3 \quad on \quad ; \quad S_4 \text{ off} \\ 0, & \text{if } S_3 \quad \text{off} \quad ; \quad S_4 \; on \end{cases} \tag{2.49}$$

$$s_c = \begin{cases} 1, & \text{if } S_5 \quad on \quad ; \quad S_6 \text{ off} \\ 0, & \text{if } S_5 \quad \text{off} \quad ; \quad S_6 \; on \end{cases} \tag{2.50}$$

Then the phase voltages are expressed in the relations with the leg state of converter

$$\begin{bmatrix} u_a \\ u_b \\ u_c \end{bmatrix} = \frac{u_{dc-link}}{3} . \begin{bmatrix} 2 & -1 & -1 \\ -1 & 2 & -1 \\ -1 & -1 & 2 \end{bmatrix} . \begin{bmatrix} s_a \\ s_b \\ s_c \end{bmatrix} \tag{2.51}$$

Phase voltage then transformed to magnitude-phase reference frame:

$$\begin{bmatrix} u_\alpha \\ u_\beta \end{bmatrix} = \sqrt{\frac{2}{3}} \cdot \begin{bmatrix} 1 & -\frac{1}{2} & -\frac{1}{2} \\ 0 & \frac{\sqrt{3}}{2} & -\frac{\sqrt{3}}{2} \end{bmatrix} \cdot \begin{bmatrix} u_a \\ u_b \\ u_c \end{bmatrix} \tag{2.52}$$

Finally, the voltage in the d-q rotor flux reference frame can be expressed as a function of converter leg state using (2.48-2.50) and Park's transformation (2.44) with θ_g is measured angle by using incremental encoder. However, converter model is not included in controller design since the SV-PWM will select appropriate leg configurations for IGBTs with reference d-q voltage calculated from generator controller

$$\begin{bmatrix} u_d \\ u_q \end{bmatrix} = \begin{bmatrix} \cos(\theta_g) & \sin(\theta_g) \\ -\sin(\theta_g) & \cos(\theta_g) \end{bmatrix} \cdot \begin{bmatrix} u_\alpha \\ u_\beta \end{bmatrix} \tag{2.53}$$

In the generator vector control, the time constants introduced by the generator side converter can easily be neglected in relation to the others in the WECS; also, the power loss can be ignored. Furthermore, the switching frequency of the power converters is high enough to be filtered by the inductances involved in their circuits. The influences of the high order harmonics can be neglected for a global WECS modeling. This observation together with expression (2.51-2.53) leading to the conclusion that power converter can be expressed as gain in controller design.

2.4. Multi-criterion objectives of wind power system control

The controller is apparently needed due to the origins of wind turbines. The main control goals are increase of power efficiency in low wind speed and limitation of power and speed below some specified values to prevent the turbine from unsafe operation under high wind conditions. Former wind turbine, which is constant speed and pitch, includes primitive mechanical devices to attain these objectives. As wind turbines augments in size and power, control specifications become more demanding and regulation mechanisms are more sophisticated. Increase control systems have been expected not merely to keep the turbine within its safe operating region but also to improve efficiency and quality of power conversion and power quality produced. They gradually evolve in consequence until playing a decisive

role in modern wind turbines. A wind turbine is essentially a device that captures part of the wind energy and converts it into useful work. In particular, a wind turbine connected to electric power networks must be designed to minimize the cost of supplied energy in order to ensure safe operation as well as acoustic emission and power quality standards.

The minimization of the energy cost involves a series of partial objectives. These objectives are actually closely related and sometimes conflicting. Therefore, they should not be pursued separately. Conversely, the question is to find a well balanced compromise among them. These partial goals can be arranged in the following topics [16]:

- *Energy capture:* Maximization of energy capture taking account of safe operation restrictions such as rated power, rated speed and cut-out wind speed,
- *Mechanical loads:* Preventing the WECS from excessive dynamic mechanical loads. This general goal encompasses transient loads alleviation, high frequency loads mitigation and resonance avoidance.
- *Power quality:* Conditioning the generated power to comply with grid interconnection standards.

2.4.1. Variable-speed Fixed-pitch with Active Stall Regulation

The variable-speed alternative to fixed-speed has become popular in commercial wind turbines, particularly for operation in low wind speeds. The benefits commonly ascribed to variable-speed operation are larger energy capture, dynamic loads alleviation and power quality enhancement. With wind energy currently reaching large penetration factors, the demands for power quality improvement give a decisive impetus to the use of variable-speed schemes.

Active stall control strategy that actively controls rotor speed in different wind speed by using more complex algorithm but it reduces the drawbacks of passive stall controlled method. WECS undergoes energy capture and higher stresses that potentially increase the fatigue damage. Aerodynamic power and torque of the wind turbine with this concept are limited by reducing the rotor speed at wind speed

above rated. The rotor speed is controlled by regulating the generator torque. Therefore the turbine with this concept can be operated at any desired tip speed ratio within the design limits of the generator and rotor blades. The rotor speed is accelerated by decreasing the generator torque below the aerodynamic torque. The rotor speed is decelerated by increasing the generator torque over the aerodynamic torque. However, it is a disadvantage of this concept that the generator must reduce the rotor speed even if the wind speed increases in order to force the rotor blades into stall. This means that the maximum torque of generator must be larger than the torque produced at rated power. To produce large torque, over dimensioning of the generator system is required. The wind turbine with the active stall control concept can be operated with various control methods to reduce the rotor speed. Therefore, there are a number of possible ways to control the wind turbine.

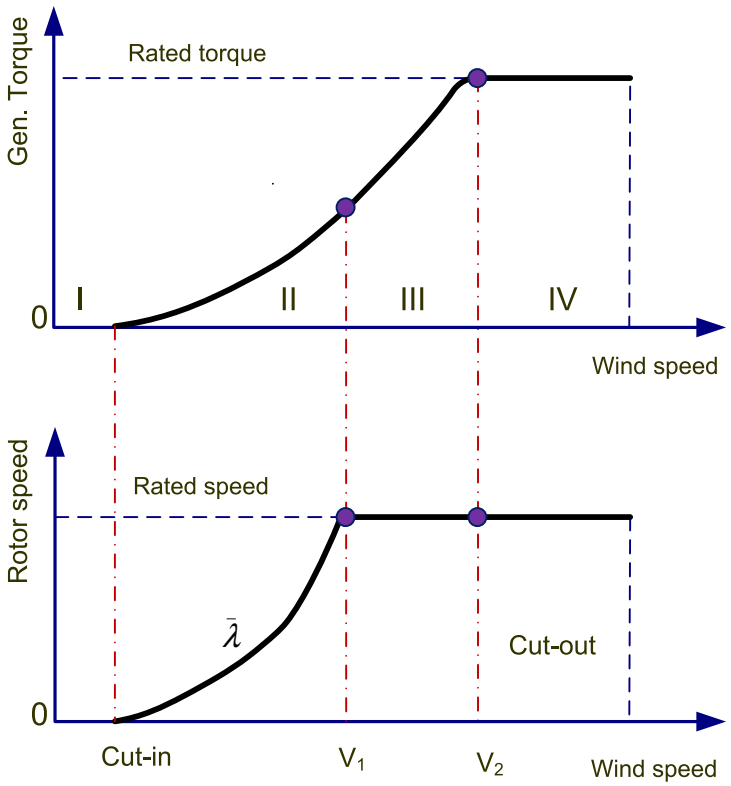

Figure 2.14. Power curve in active stall control

The control strategy adopts an active stall strategy which is described in more detail in [54] for a fixed-pitch angle wind turbine. Generator torque is considered as a control input to regulate generator speed at overall range of wind speeds, both

below and above rated. The strategy eliminates the pitch angle mechanism, thus reducing the production cost of the wind turbine. The strategy divides the working conditions of the wind power system into four regions as shown in Figure 2.14 as follows.

If the wind speed is below the cut-in speed, the controllers do nothing since the power from the wind is too small to be harvested (Region I).

At region II, when the wind speed is below the rated speed, maximum efficiency conversion, which is achieved at $\beta = 0$; $\lambda = \lambda_{opt}$, is the main target of controller. Therefore, to maximize energy capture below rated power, both the pitch angle and the tip-speed-ratio must be kept constant at these values. In particular, the condition $\lambda = \lambda_{opt}$ means that the rotor speed must change proportionally to wind speed, i.e.

$$\omega_g^* = \frac{\eta \lambda_{opt} \upsilon}{R} \tag{2.54}$$

As it is known, variable-speed operation requires decoupling the rotational speed from the line frequency. A suitable control of the underlying electronic converters produces parallel displacements of the generator torque characteristic towards higher or lower speeds. Thus, the turbine can be controlled to operate at different points, for instance to track the non-stationary optimum speed (2.54) as wind speed fluctuates.

When the wind speed increases to above rated level (Region III), the optimal speed reference ω_g^* is higher than the rated speed. However, the actual generator speed ω_g doesn't go higher than the rated value because of limitations in the electrical and mechanical design of the wind turbine. Therefore, in this case, the generator torque is controlled to increase higher than the aerodynamic torque resulting in deceleration of the actual generator speed to rated values. If the wind speed maintains its increase, generator torque also increases accordingly; however, rotor speed is always maintained at its maximum value, i.e. rated value. This means the generator speed will be reduced from optimal levels, with the wind turbine subsequently running at a lower power coefficient point or stall mode (generator speed is stalled by the rated value). Finally, when the generator speed reaches its

rated value, the generator torque continues to increase, with stronger wind speeds to the torque rated level. The fourth scheme is known as power limitation (Region IV). In this scheme, when the wind turbine reaches its power limitation level, the controller pushes the system into cut-out or shut-down mode by activating the brake system in order to avoid damage.

2.4.2. Mixed Criterion Control Strategy

In the purpose of guaranteeing good performance of wind energy system, the idea of balancing the trade-off between energy efficiency and increasing the service lifetime of wind power system by alleviating fatigue loads is continuously being paid special attention. With the aim of keeping the operating point at the maximum power coefficient locus, a control requiring a drastic fulfillment of the performance criteria will induce significant stress due to important torque variations. In contrast, reasonably diminishing control performance may result in reducing the torque variations without altering the energy performance. However, this approach does not allow a rigorous control design in order to perform a fine tuning of the trade-off between the energy performance and the reliability demands. Therefore, two-term performance criterion will be considered in most wind energy control applications [19]:

- Energy performance versus reliability performance, where the wind power system operates on the optimal regime (red color in Figure 2.12).
- Accuracy in ensuring the imposed values of the system parameters (rotational speed, torque or active power) versus reliability performance, where the system works either in partial load, but with speed/torque limitation, or in full load.

Unlike the case of small- and medium-power wind generation system, the control objectives of megawatt power system are more diversified. At this level of rated power, the tower dynamics need to be taken into account because they may decisively influence the global dynamic properties. The modes induced by the blade dynamics and by the drive train must also be included in the global mathematical model. The tower, the turbine, the drive train and the electrical generator compose an interaction chain exhibiting complex dynamic behavior, both in relation with its

internal variables (rotational speed, power factor, mechanical loads, etc.) and with the grid. Under these circumstances, the control demands should be reconsidered. Some of the wind power control functions can be summarized as [1]:

- Basic functions: active power limitation at the rated value in full load, along with shaft rotational speed and sometimes torque limitation.
- Energy conversion optimization in partial load.
- Mixed-criterion optimization, expressing a trade-off between optimal regime tracking and alleviation of electromagnetic torque variations.

In general, the requirements listed above do not cover all the technical and economical demands imposed by the exploitation practice; especially in the case of high capacity wind power. A "good control" should comply with a larger number of demands, either generic or depending on each particular system.

2.5. Laboratory Wind Power System Simulator

Wind turbine system simulator is on high demand in research and development of wind power system for testing controller design without reliance on wind profiles. It provides a fast and safe prototype method at any wind speed regions since wind speed is synthesized in computer software inspiring a number of researches in wind turbine simulators (WTS) with different system configurations and equipments. Authors in [55] used induction machine driven by torque controlled inverter for fixed pitch variable speed wind turbine. Wind speed model by Van der Hoven power spectrum with tower effect to the torque was in consideration. A single phase half-controlled converter for dc motor is found on [56]. Wind shear and tower shadow were mentioned for a fixed pitch angle for both static and dynamic simulator. In large scale wind turbine, blade inertia and rotor inertia, act as mechanical energy storage which creates delays in dynamic control, are compensated [55, 56]. Classical wind power system is normally fixed pitch and constant speed which have less power efficient and high dynamic loads. That results in decrease in life cycle of system. In order to minimize this disadvantage, the introduction of new generation of variable speed wind turbine in [57], is promised to be future wind turbine for variety of control algorithm.

In our emulation system, wind speed and blades of real wind turbine are replaced by simulation and mathematical expression then being computed by computer software. Computer sends torque command to controller of brushless dc motor. Now the output torque of the motor T_m needs to be generated and it is exactly equal to aerodynamic torque T_a generated by wind power referring to high speed shaft (Figure 2.15).

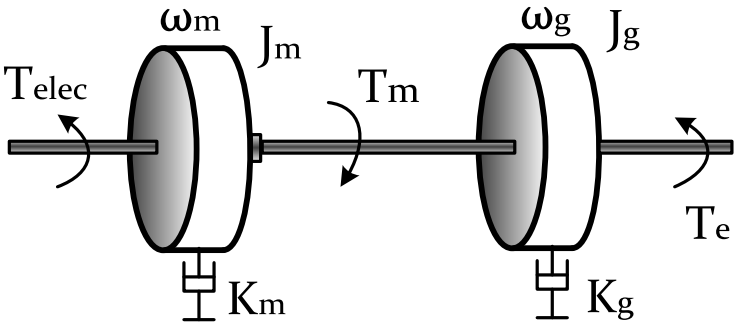

Figure 2.15. Two-mass model equivalent using motor driving wind turbine emulator

The dynamic response of the rotor driven by aerodynamic torque T_{elec} is derived:

$$J_r \dot{\omega}_m = T_{elec} - T_m - K_m \omega_m \tag{2.55}$$

Balancing equation (2.32) and equation (2.55) with the note that: $T_{hs} = T_m$; $\omega_m = \omega_g$; we get:

$$T_{elec} = (J_m - \frac{J_r}{n_g^2})\dot{\omega}_g + \frac{T_a}{n_g} + (K_g - \frac{K_r}{n_g^2})\omega_g \tag{2.56}$$

where, T_{elec} is electrical reference torque applied to motor controller. The first element of (2.56) shows inertia compensation for large scale wind turbine.

Hardware experiment

Figure 2.16 shows a schematic of the test-bed system. The main idea of building the test rig system is to produce the mechanical torque generated by the brushless DC motor driven generator in a similar way to the aerodynamic torque generated by the

wind speed. A DSP controller for a BLDC motor working under analog torque command mode receives a control signal from an I/O board. The utilized dSPACE 1103 not only acts as an I/O interface, but also as a controller for the drive train loop and generator current control loops. The aerodynamic torque of the wind turbine is used as a torque command reference signal sent to the motor drive.

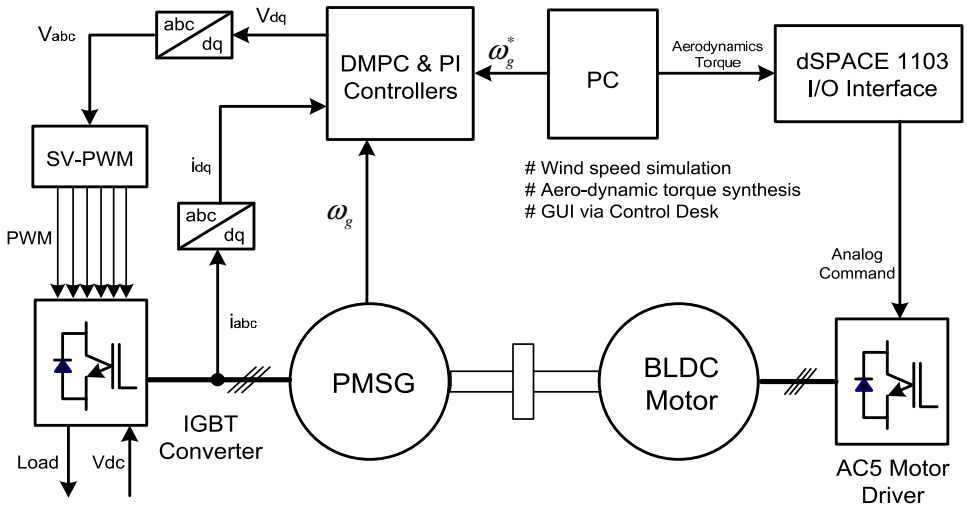

Figure 2.16. Hardware structure for experiment

Figure 2.17 illustrates the experimental set-up which was composed of a 750 watt BLDC motor (see Appendix 4) and its motor driver. Motor operating under an analog torque control scheme receives the analog aerodynamic torque command from the DAC port of dSPACE 1103, and then produces a signal corresponding to the exact value of the output electrical torque. This BLDC motor is directly coupled to the shaft of a 600 watt PMSG (see Appendix 4). The three output terminals of the generator are connected to a SEMIKRON 6-IGBT gates SKM50Gb 123D converter. The DC-bus is connected to the DC voltage source, which guarantees a 48V DC-bus voltage, and a parallel resistive load consuming the output power from the generator. Current measurements as feedback signals for the PMSG PI controllers are obtained through LEM LA-25 current transducers connected to three ADC ports of the controller card. The generator speed is measured through an incremental encoder as a feedback signal for the DMPC speed controller. The outputs of controllers are d-q voltages that are used as the control signals for the

space vector modulation (SVM) operating IGBT converter. The controller board is a 1 GHz dSPACE processor, which has 6 incremental encoders, analog-to-digital (ADC) and digital-to-analog (DAC) ports (see Appendix for specifications). The 32 bit encoder port measures the position and angular velocity of the generator for controller feedback. A Control Desk provides the graphical human machine interface and data logger, which can be interpreted by MATLAB.

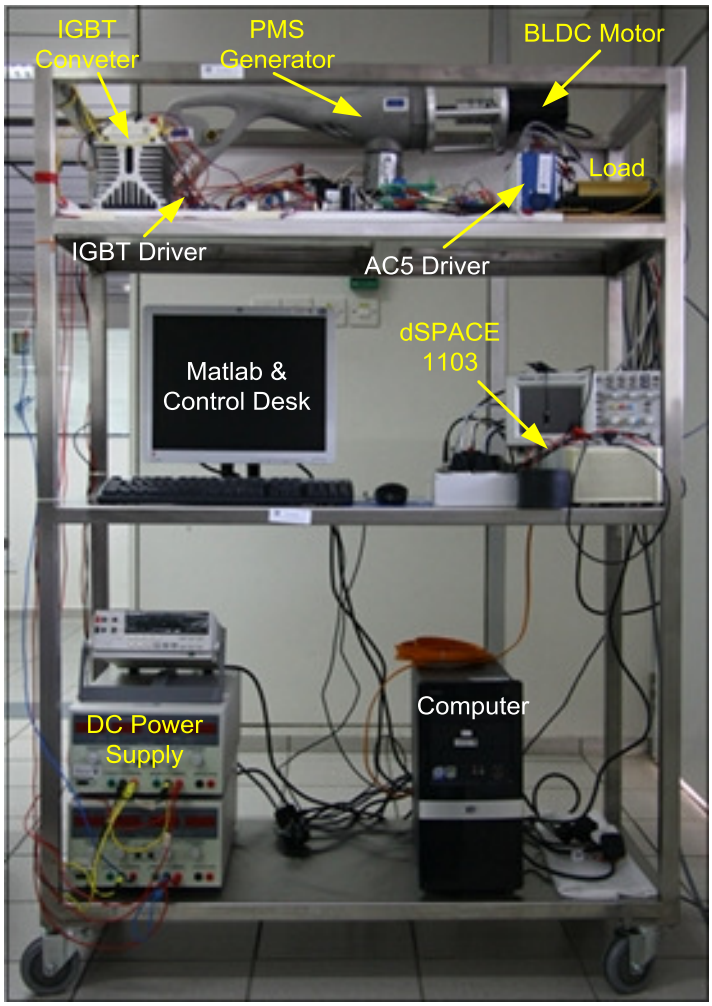

Figure 2.17. Hardware experiment kit

2.6. Simplified emulator setup

Section 2.5 presents a conventional test-rig system which uses two machines; the first one is as a prime mover which produces mechanical torque in a similar way of wind torque while the second one is for electrical generation. Wind aerodynamic

torque is synthesized by software then being sent to motor controller card which works in the torque controlled scheme. The output mechanical torque of the motor operates in a similar way as the torque from wind. The shafts of the two machines are directly coupled by a high accurate mechanical coupling device. However, the oscillation problem of speed may occur when there are no machine shafts which are well aligned. This external unknown disturbance affects seriously the testing system.

This section presents a simple setup which omits the mover in the conventional system. Aerodynamic torque from wind is purely computed from software program and is not being sent to driving motor. Instead of sending aero-dynamics torque and electromagnetic torque command separately to the mover and generator, an aggregate torque command is being sent to the PMSM. The total torque signal has the same effect in speed control loop as the two individual torques. As the results, emulator system is simplified while speed controller testing is easily achieved. The details emulator setup process in laboratory environment including wind profiles modeling and drive train modeling with inertia compensator are presented in the next section. The traditional PI controller for speed loop and generator current loops are also mentioned. All these components are analytically modeled then simulated in Matlab/Simulink interfaced to dSPACE control card working as data acquisition device for quick prototype hard hardware in loop simulation. Real-time card dSPACE 1103 is not only the interface I/O but also is controller for generator side implementation.

Drive train of wind turbine can be modeled as two-mass model structure. The first mass is the turbine blades and their inertia; the second mass is generator inertia as follows:

The (2.32) is re-written in the other form

$$T_{hs} = \frac{T_a}{\eta} - \frac{K_r}{\eta}\omega_r - \frac{J_r}{\eta^2}\dot{\omega}_r \qquad (2.57)$$

With our proposed system, the motor as prime mover and gear box are eliminated so only total torque $T_{hs} - T_g$ is being sent to generator controller. From the observation, it is shown that the running mode of electrical machine (motoring or

generation) only depends on the sign of T_g signal despite of its wave form. In our test-rig system, the permanent magnet synchronous machine is always running at motor mode which absorbs power from power source. However, it is therefore to define new clue as the following:

If $T_{hs} - T_g \geq 0$ and $T_g \geq 0$, the machine runs at positive speed which is equivalent to generation mode of generator in conventional method.

If $T_{hs} - T_g \leq 0$ or $T_g \leq 0$ machine runs at negative speed which is considered to be motoring mode.

By defining this new clue, the mechanical simulated aerodynamic torque which is generated by BLDC motor in Figure 2.15 is now fully replaced by mathematical signal which is then computed by software program.

Various control loop elements are for individual sub-systems of wind power system based on the knowledge of modeling details from wind speed, turbine aerodynamics; drive train, generator and converter are presented in this chapter. The control objective of wind power system employed the active stall control also studied as primary goal for controller design. The next chapter will be about the fundamentals of studied control algorithms applicable for controlling wind power system. These control algorithms performance will be validated by an experiment set-up which was presented in the last section of this chapter.

Chapter 3

LINEAR AND NONLINEAR CONTROL ALGORITHMS

This chapter presents the fundamental of control algorithms which will be applied to wind power system. The first control method, Fuzzy Logic Controller (FLC), considers complex wind power system as a black box. The system modeling is not required for operation of FLC control scheme; only measurements of inputs are used to find control input by using "fuzzy" behaviors. The next, linear controller designs are based on linear presentation of the nonlinear modeling at some specific points. The extended PID, linear model predictive control (MPC) and the disturbance model predictive control (DMPC) are studied. Finally, theoretical aspect of nonlinear version of MPC which directly designs from nonlinear modeling is presented.

3.1. Fuzzy Logic Controller (FLC)

Fuzzy Logic Control (FLC) was pioneered by Mamdani research and motivated by Zadeh's using linguistic approach and system analysis based on theory of fuzzy set. Fuzzy set theory is methods which mimic human thinking and reacting by using a multivalent fuzzy logic and elements of artificial intelligence [58]. There are a lot of situations which are based on estimation or experiences of human thinking in a way the degree of ambiguity, hence, fuzzy logic control is known as an effective means of capturing the approximate, inexact nature of the world. It is viewed as a step toward the rapprochement between precise mathematical control and human-like decision making. However, no systematic procedure for the design of an FLC is found in literature [59]. The basic theory of fuzzy controller lies on fuzzy sets, linguistic variables, fuzzy rules, fuzzification interference and defuzzification.

Fuzzy Sets

Let U_{FZ} be a collection of objects denoted generically by $\{u_{FZ}\}$. U_{FZ} is called the universe of discourse and u presents the generic element of U_{FZ}. Fuzzy set definition is presented in [59] as follows: A fuzzy set F_{FZ} in a universe of

discourse U_{FZ} is characterized by a membership function μ_{FZ} which takes the values in the interval $[0,1]$ namely, $\mu_{FZ}: U_{FZ} \to [0,1]$. A fuzzy set is viewed as a generalization of the concept of an ordinary set whose membership function only takes two values $\{0,1\}$. Thus a fuzzy set F_{FZ} in U_{FZ} in generic element u_{FZ} and its grade of membership function: $F_{FZ} = \{(u, \mu_{FZ}(u_{FZ})) \mid u_{FZ} \in U_{FZ}\}$. When U_{FZ} is continuous, a fuzzy set F_{FZ} can be written concisely as $F_{FZ} = \int_{U_{FZ}} \mu_{FZ}(u_{FZ}) / u_{FZ}$.

The membership function is the range of possible quantitative values set for fuzzy set members. The universe of discourse in the fuzzy logic can be continuous or discrete. Therefore, these membership functions usually attain different forms, e.g. Trapezoidal, Triangular, Gaussian… etc.

Triangular:

$$\mu F(x) = \begin{cases} 0, for\ x < a \\ \frac{x-a}{b-a}, for\ a \le x < b \\ \frac{c-x}{c-b}, for\ b \le x \le c \\ 0, for\ x > c \end{cases}$$

Trapezoidal:

$$\mu F(x) = \begin{cases} 0, for\ x < a \\ \frac{x-a}{b-a}, \quad for\ a \le x < b \\ 1, for\ b \le x < c \\ \frac{d-x}{d-c}, for\ c \le x \le d \\ 0, for\ x > d \end{cases}$$

Gaussian:

$$\mu F(x) = e^{-(x-c_F)^2/w}$$

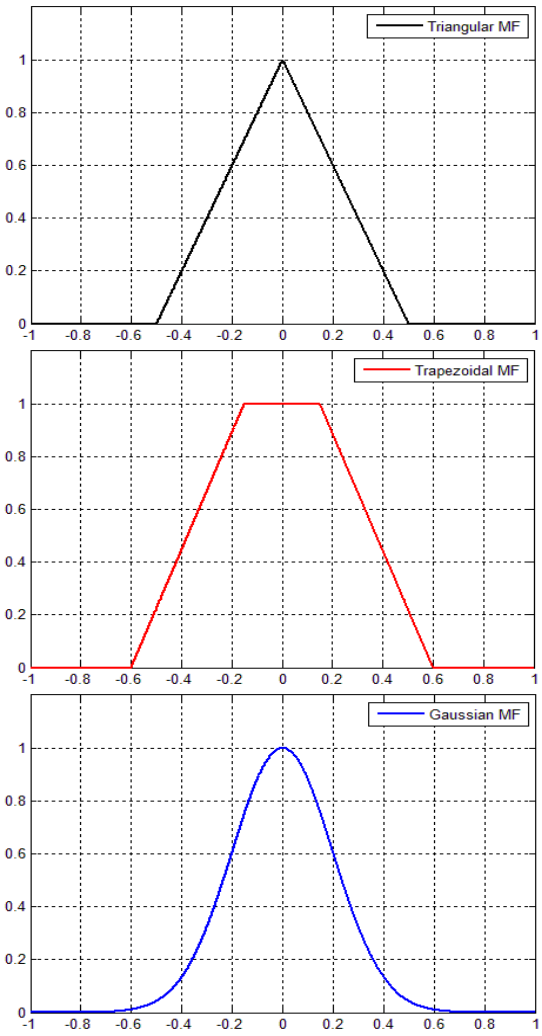

Figure 3.1. Different forms of membership functions

Linguistic Variables

In fuzzy logic, variables are determined with words or sentences rather than numbers. These variables are known as linguistic variables. The linguistic variables are used in determining the fuzzy sets. For examples, variable weather temperature can be very low, low, medium, high or very high and these variables are meant for different ranges of temperature assigned by the user. We can interprets "very low" as "a temperature below about minus 20 Celsius degree", "medium" as "a temperature about 30 Celsius degree"; and "very high" as "a temperature below above 50 Celsius degree".

Fuzzy Rules

Fuzzy rules in fuzzy controllers are used to make humanlike decisions with the use of knowledge to control a system. The combination of these rules is known as fuzzy rule base. In the fuzzy rule, IF-THEN pattern is used and it can be divided as antecedent parts and consequent parts. The IF (antecedent part) relates the fuzzy sets of the controller depending on the relation between the different inputs while THEN gives the action needed to be taken from relation . The organization of the fuzzy rule base is the most crucial part as it determined the process of the outcome result.

Rules 1: IF x is A THEN z is B

The fuzzy set associated with linguistic variables represents fuzzy proposition and it is denoted as, for example, P_m^x, where x is the linguistic variables. For the antecedent part, the multiple fuzzy propositions are put into relation and normally denoted as R_{pq} , p and q denotes the linguistic variables of the fuzzy. If multiple rules are implanted in the fuzzy rule base, it can be written as

Rules i : IF x is R_{pq} THEN z is P_m^x

The number of input and output variables and it's relation to each other determine the number of fuzzy rules and the number of fuzzy rules decide the size of the fuzzy rule base. An example of fuzzy rule base is shown below.

Table 2. Fuzzy Rule Base

	Negative	Zero	Positive
Negative	NB	NM	ZE
Zero	NM	ZE	PM
Positive	ZE	PM	PB

Fuzzification and Defuzzification

Fuzzification can be determined as the process of converting the numerical value into a corresponding linguistic value by associating a membership degree. To do so, a procedure of three steps includes: i) measures the values of input variables; ii) performs a scale mapping that transfers the range of values of input variables into corresponding universe of discourse; iii) performs the function of fuzzification that converts input data into suitable linguistic values which may be viewed as labels of fussy sets.

The fuzzy output set resulted from the fuzzy inference needed to be converted into crisp output value. This process is known as defuzzification. The defuzzification interfaces performs the following functions: i) a scale mapping, which converts the range of values of output variables into corresponding universe of discourse; ii) defuzzification which yields a non-fuzzy control action from an inferred fuzzy control action.

3.2. Extended Nonlinear PID (NPID)

Despite of there are a lot of control algorithms developed in the control engineering, it is undoubtedly that PID controller has been most widely used in the industry during last 60 years. The same conclusion can be made for the popularity of PID controller in the wind power system. The widespread use of PID is attributed primarily to its simple in design but well performance characteristic. Therefore, classical controller employing proportional and integral gains for wind power is studied in this chapter.

However, the conventional linear PID is adequate for controlling the nominal processes with Linear Time Invariant (LTI) parameters. The requirements of high-performance control for nonlinear systems which have changing operating points such as wind power system are not obtained by using traditional PID controller. For instance, a well tuning PID controller for transfer function at optimal operating point of wind power gives large overshot during transient period, and vice versa another PID tuned well for transient period delivers large off-set tracking at steady-state [60]. These problems can be avoided by employing an extension of linear PID to a nonlinear PID controller. The similar approaches for other industrial processes are found in [60-63] while a self-tuning PID based on Lyapunov approach for wind energy conversion system is presented in [64]. The combination of fuzzy and PID for a wide range of wind speed is popular and it is found in the [65-67]. In this section, rather than using fuzzy PID controller, polynomial nonlinear PID controller with variable gains accordingly to different operating points of wind power system is presented. The proportional, integral and derivative gains are nonlinear functions which adaptively adjust to the change of mechanical angular speed.

The proposed controller has the general transfer function as (3.1) which has PID gains are a continuous nonlinear function

$$G_{npi} = f_p(e) + \frac{f_i(e)}{s} + sf_d(e) \tag{3.1}$$

The nonlinear functions $f_p(e), f_i(e), f_d(e)$ are polynomial functions of variable $e = y_r(t) - y(t)$ which is error in reference and actual output. The controller structure is the same as the classical PID controller. The only difference is that fixed gains PID are replaced by nonlinear gains PID controller.

3.3. Linear Model Predictive Control (LMPC)

Model Predictive Control (MPC) is one of the most well-known and successful control algorithms in the process industry because it easily handles multi-variables and constraints. The future values of the output are predicted by using a state space model to formulate the tracking cost function. Optimization of a least squares tracking function is generally re-written in the form of a QP problem, which is finalized in order to determine the optimal feedback control input signal to the plant. The first element of control input prediction is applied to the plant as a control input at current time; then new optimization is shifted to the next sampling time and so on. QP problem is solvable online in real-time so that predictive control has been successful in fast-sampling time applications. Linear predictive control with application to electrical drive is presented in [9, 68, 69]; while some others refer PC as a powerful method to control the power converter [70, 71]. These references show that predictive controller is an advanced algorithm for electrical and power electronics application.

There exist similar works that have applied the linear model predictive control to wind turbine control; they are showed in [72-74]. In [72], different optimization cost functions were synthesized for different modes of controller according to the input wind speed. Reference [73] presented a multi-model predictive control at different working points. A number of single predictive controllers were designed and then synthesized to obtain global multi-model controller. A maximum power strategy of wind power system is attained by predictive control in [74]; however, it requires the information from wind profiles such as turbulence length and time constant for linear modeling of wind power aerodynamics. This is not always available in practice. All of these works provide only simulation results without experimental validation. Disturbance and nonlinear version of model predictive control, within my knowledge, have not been applied to wind power system in literature. A complete picture of model predictive control family, from linear to nonlinear, inspires me to study within this research project. The fundamental start should be with foundation of linear model predictive control in this section then its variations following consequently.

In general, the state space presentation of a linear plant has the form as follows.

$$\begin{aligned} x(k+1) &= Ax(k) + Bu(k) \\ y(k) &= Cx(k) \end{aligned} \tag{3.2}$$

The main concept of predictive control is to use a model of the plant to predict the future evolution of the system. By iterating substitution the first element of model (3.2), the state prediction is obtained in (3.3); where $\bar{x}(k+i\,|\,k)$ and $\bar{u}(k+i\,|\,k)$ are predicted state and control inputs at time i respectively; N_p is the state prediction horizon; and $\bar{x}(k\,|\,k)$ is the current measurement state.

$$\begin{aligned} \bar{x}(k+1\,|\,k) &= Ax(k) + B\bar{u}(k\,|\,k) \\ \bar{x}(k+2\,|\,k) &= A^2x(k) + AB\bar{u}(k\,|\,k) + B\bar{u}(k+1\,|\,k) \end{aligned} \tag{3.3}$$

And so on till the time $k = N_p$:

$$\bar{x}(k+N_p\,|\,k) = A^{N_p}x(k) + A^{N_p-1}B\bar{u}(k\,|\,k) + \ldots + B\bar{u}(k+N_p-1\,|\,k) \tag{3.4}$$

Similarly, the control predictions are obtained as (3.5)

$$\begin{aligned} \bar{u}(k\,|\,k) &= \Delta\bar{u}(k\,|\,k) + u(k-1) \\ \bar{u}(k+1\,|\,k) &= \Delta\bar{u}(k+1\,|\,k) + \Delta\bar{u}(k\,|\,k) + u(k-1) \\ &\vdots \\ \bar{u}(k+N_u-1\,|\,k) &= \Delta\bar{u}(k+N_u-1\,|\,k) \\ &\quad + \ldots + \Delta\bar{u}(k\,|\,k) + u(k-1) \end{aligned} \tag{3.5}$$

where N_u is the input prediction horizon. By substituting (3.5) into (3.4), for time prediction $i = 0 \ldots N_u$, we get

$$\begin{aligned} \bar{x}(k+i\,|\,k) &= A^ix(k) + (A^{i-1} + .. + A + I)B\Delta\bar{u}(k\,|\,k) \\ &\quad + B\Delta\bar{u}(k+i-1\,|\,k) + (A^{i-1} + .. + A + I)Bu(k-1) \end{aligned} \tag{3.6}$$

Additionally, for $i = (N_u+1) \ldots N_p$,

$$\begin{aligned} &\bar{x}(k+i\,|\,k) = A^ix(k) + (A^{i-1} + .. + A + I)B\Delta\bar{u}(k\,|\,k) \\ &+(A^{N_p-i} + .. + A + I)B\Delta\bar{u}(k+N_u-1\,|\,k) + (A^{i-1} + .. + A + I)Bu(k-1) \end{aligned} \tag{3.7}$$

With the observation that $\bar{y}(k+i|k)=C\bar{x}(k+i|k)$, it is easy to get the prediction evolution of the output variables from (3.6) and (3.7).

$$\begin{bmatrix} \bar{y}(k+1|k) \\ \vdots \\ \bar{y}(k+N_u|k) \\ \bar{y}(k+N_u+1|k) \\ \vdots \\ \bar{y}(k+N_p|k) \end{bmatrix} = \begin{bmatrix} CA \\ \vdots \\ CA^{N_u} \\ CA^{N_u+1} \\ \vdots \\ CA^{N_p} \end{bmatrix} x(k) + \begin{bmatrix} CB \\ \vdots \\ \sum_{i=0}^{N_u-1} CA^iB \\ \sum_{i=0}^{N_u} CA^iB \\ \vdots \\ \sum_{i=0}^{N_p-1} CA^iB \end{bmatrix} u(k-1) + \begin{bmatrix} CB & .. & 0 \\ \vdots & .. & 0 \\ \sum_{i=0}^{N_u-1} CA^iB & .. & CB \\ \sum_{i=0}^{N_u} CA^iB & .. & CAB+CB \\ \vdots & \vdots & \vdots \\ \sum_{i=0}^{N_p-1} CA^iB & & \sum_{i=0}^{N_p-N_u} CA^iB \end{bmatrix} \begin{bmatrix} \Delta\bar{u}(k|k) \\ \vdots \\ \Delta\bar{u}(k+N_u-1|k) \end{bmatrix} \tag{3.8}$$

The (3.8) can be re-written in a short form of matrix as (3.9)

$$Y(k)=\Psi x(k)+\Upsilon u(k-1)+\Theta\Delta U(k) \tag{3.9}$$

In this equation, the true measurements of state variables $x(k)$ are used to predict the outputs. However, in the real application, most of the time, the measurements of whole state vectors are not provided and/or some measurements are very noisy. In such cases, the standard observer based on model (3.2) is always introduced [75].

$$\hat{x}(k+1|k)=(A-LC)\hat{x}(k|k)+Bu(k)+Ly(k) \tag{3.10}$$

where $\hat{x}(k+1|k)$ is the estimated state base on current the measurement output $y(k)$; and the gain matrix L is used to correct the estimate $\hat{x}(k|k)$. If the state and output of the plant are assumed to be subjected to white noise, then the observer is known as the Kalman filter. With an observer, it is noticed that all the gain matrices involved in (3.9) are exactly the same as the normal case. The only difference is that the observer is in use, this means that the state estimate $\hat{x}(k|k)$ is used to replace the measured state $x(k)$

The equation (3.9) is re-written as

$$Y_s(k) = \Psi \hat{x}(k \mid k) + \Upsilon u(k-1) + \Theta \Delta U(k) \tag{3.11}$$

where $Y_s(k)$ with small "s" is used to show that the prediction is based on the standard observation from (3.10).

In predictive control, a quadratic criterion function of errors between the prediction outputs and the references over the prediction horizons is defined as [75].

$$V(k) = \sum_{i=1}^{N_p} \| \bar{y}(k+i \mid k) - y^*(k+i) \|_{Q_i}^2 + \sum_{i=0}^{N_u-1} \| \Delta \bar{u}(k+i \mid k) \|_{R_i}^2 \tag{3.12}$$

where Q_i, R_i are weighting matrices which determine the balance of tracking errors with rates of change in control input. This cost function can be re-written in matrix form (3.13)

$$V_s(k) = \| Y_s(k) - Y^*(k) \|_{Q_i}^2 + \| \Delta U(k) \|_{R_i}^2 \tag{3.13}$$

Defining $$\Lambda(k) = Y^*(k) - \Psi \hat{x}(k) - \Upsilon u(k-1) \tag{3.14}$$

Now we can write

$$\begin{aligned} V_s(k) = & \| \Theta \Delta U(k) - \Lambda(k) \|_{Q_i}^2 + \| \Delta U(k) \|_{R_i}^2 = \Lambda(k)^t Q_i \Lambda(k) \\ & -2\Delta U(k)^t \Theta^t Q_i \Lambda(k) + \Delta U(k)^t [\Theta^t Q_i \Theta + R_i] \Delta U(k) \end{aligned} \tag{3.15}$$

The first term of (3.15) is not related to the control input, hence it is a constant value, by defining the prediction control input $\Delta U(k)$ as variable, the cost function $V(k)$ is re-written as follows

$$V_s(k) = Const - \Delta U(k)^t G + \Delta U(k)^t H \Delta U(k) \tag{3.16}$$

where $G = 2\Theta^t Q_i \Lambda(k)$, $H = [\Theta^t Q_i \Theta + R_i]$. The constraint in general is re-written in terms of control variable $\Delta U(k)$ which has the general form

$$W \Delta U(k) \le w \tag{3.17}$$

The cost function (3.16) and constraint (3.17) are then formulated as a Quadratic Problem to determine the control input matrix $\Delta U(k)$. The QP is typical and

solvable in state-of-the-art of QP programming (interior-point method and active-set method). The first element of $\Delta U(k)$ is applied to the plant as a control input at time k then the new optimization is shifted to the next time at $k+1$ and so on.

QP Programming Tutorial

To get more understanding of quadratic programming and its application to MPC algorithm, this section studies two examples. The first one is a simple QP problem with two variables subject to inequalities constraints as following.

$$Min \quad \frac{1}{2}x_1^2 + 3x_2^2 - 4x_1x_2 - 5x_1 - 2x_2 \tag{3.18}$$

$$\text{s.t.} \quad \begin{aligned} & x_1 + 2x_2 \le 3 \\ & -2x_1 + 5x_2 \le 7 \\ & 3x_1 + 2x_2 \le 6 \\ & 0 \le x_1; 0 \le x_2 \end{aligned} \tag{3.19}$$

This optimal problem can be written as a QP problem of the form

$$Min \quad \frac{1}{2}x^t Hx + G^t x \tag{3.20}$$

$$\text{s.t.} \quad \begin{aligned} & Ax \le b \\ & lb \le x \le ub \end{aligned} \tag{3.21}$$

Some scripts in the MATLAB are written as

```
H = [1 -4; -4 6]; % Enter these coefficient matrices.
f = [-5; -2];
A = [1 2; -2 5; 3 2];
b = [3; 7; 6];
lb = zeros(2,1);

 % Next, invoke a quadratic programming routine.

[x,fval,exitflag,output,lambda] = quadprog(H,f,A,b,[],[],lb)
```

This command generates the solutions

```
x = [1.5472;    0.6792]; % is the optimal solution

fval = -10.7170; % optimal value of cost function

Number of iterations: 2
```

QP Programming application to MPC algorithm

The second example is to illustrate a simple MPC algorithm for a linear system has the state space modeling of the form

$$\begin{bmatrix} \dot{x} \\ \Delta \dot{x} \end{bmatrix} = \begin{bmatrix} 0.7 & 2 \\ 0 & 0 \end{bmatrix} \begin{bmatrix} x \\ \Delta x \end{bmatrix} + \begin{bmatrix} 2 \\ 1 \end{bmatrix} u \tag{3.22}$$

Input prediction $N_u = 2; N_p = 5$, weighting factor $\alpha = 0.5$. A MATLAB commands for MPC algorithm to track a constant reference $w = 1$ are presented in the Appendix 1. Controller design follows a finite number steps

i) at time $t = 0$, set samples $k = 0$

ii) Calculate the matrices G, H based on system modeling (3.8) until prediction horizons are reached.

iii) Formulate QP problem as (3.16-3.17) and applying QP solution method (in the example, the QUADPROG function is applied) to find optimal control input u

iv) Applying calculated to the plant, and increase samples $k = k + 1$.

v) Stop simulation if samples $k = 20$

Figure 3.2 and 3.3 show the output response of tracking constant trajectory and corresponding control input of simulation results with all initial condition are set to 0. Output response follows to reference after few samples with 5 control input movements.

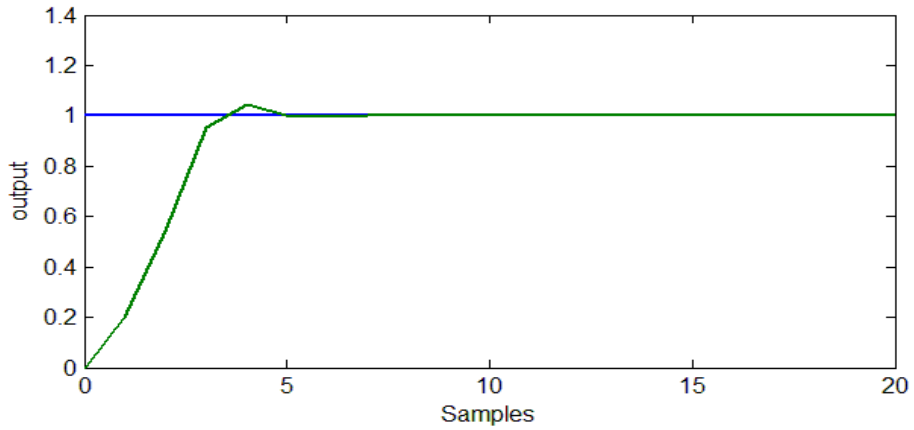

.

Figure 3.2. Output response of MPC controller for tutorial problem

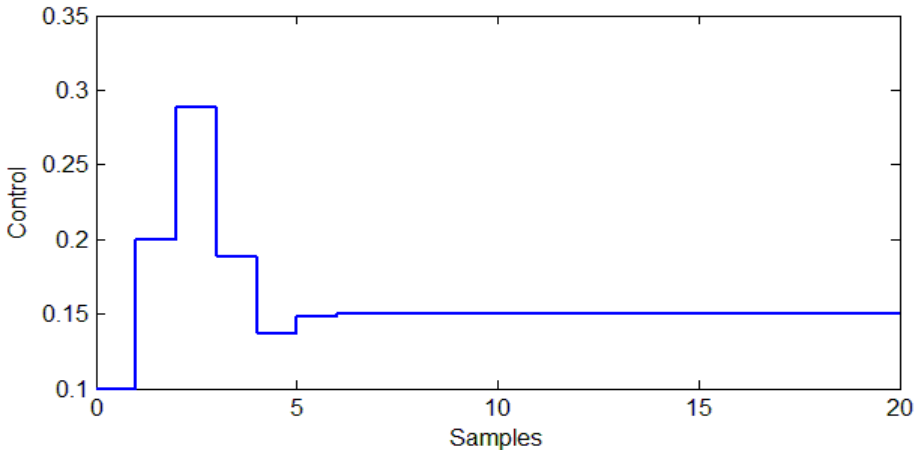

Figure 3.3. Control input of MPC controller for tutorial problem

3.4. Output Disturbance Model Predictive Control (DMPC)

Ideally, the linear model (3.2) matches the nonlinear plant; the predictive controller provides excellence tracking results. However, in many systems there are always model-plant mismatches. More specifically, the linear model of nonlinear wind turbine aerodynamics at a specific operating point produces a mismatch between plant and model, which is the main reason for reference tracking errors. The proposed DMPC control scheme attempts to add additional disturbance signals to the linear model of wind turbines to lump the plant-model mismatches and/or un-modeled disturbances. The linear model (3.2) is augmented with a constant disturbance signal $d(k)$. Disturbance models of predictive control (DMPC) are now formulated as follows

$$\begin{aligned} \begin{bmatrix} x(k+1) \\ d(k+1) \end{bmatrix} &= \begin{bmatrix} A & 0 \\ 0 & I \end{bmatrix} \begin{bmatrix} x(k) \\ d(k) \end{bmatrix} + \begin{bmatrix} B \\ 0 \end{bmatrix} u(k) \\ y(k) &= \begin{bmatrix} C & I \end{bmatrix} \begin{bmatrix} x(k) \\ d(k) \end{bmatrix} \end{aligned} \tag{3.23}$$

The first row in (3.23) is the same as that of model (3.2); only modifications to the two last rows are made. The output of the plant is augmented by a constant disturbance $d(k)$.

The observer concept is also applied to the disturbance models of the predictive controller; hence, the state and disturbance estimator is designed based on the

augmented model (3.23) with the observer gain has one more element L_d from the disturbance signal

$$\begin{bmatrix}\hat{x}(k+1)\\ \hat{d}(k+1)\end{bmatrix}=\left(\begin{bmatrix}A & 0\\ 0 & I\end{bmatrix}-\begin{bmatrix}L\\ L_d\end{bmatrix}\begin{bmatrix}C & I\end{bmatrix}\right)\begin{bmatrix}\hat{x}(k\,|\,k)\\ \hat{d}(k\,|\,k)\end{bmatrix}+\begin{bmatrix}B\\ 0\end{bmatrix}u(k)+\begin{bmatrix}L\\ L_d\end{bmatrix}y(k) \qquad (3.24)$$

where L, L_d are tuned so that the estimator is stable. The first row of (3.23) gives

$$\hat{x}(k+1|k)=(A-LC)\hat{x}(k\,|\,k)+Bu(k)+Ly(k)-L\hat{d}(k) \qquad (3.25)$$

The DMPC with the new observer in (3.24) has the prediction matrix (3.9) which is re-written as (3.26). $Y_d(k)$ has a small notation "d" to show that this is the prediction matrix obtained by the disturbance model (3.23). With the note that $\hat{x}(k\,|\,k)$ now is the estimated variable from (3.24)

$$Y_d(k)=\Psi\hat{x}(k\,|\,k)+\Upsilon u(k-1)+\Theta\Delta U(k) \qquad (3.26)$$

The DMPC algorithm for the augmented model is now formulated as

$$Min \quad V_d(k)=\|Y_d(k)-Y^*(k)\|^2_{Q_i}+\|\Delta U(k)\|^2_{R_i} \qquad (3.27)$$

$$\text{subject to} \qquad W\Delta U(k)\le w$$

Now we have to prove that the solution to (3.27) will find control inputs which provide zero offset tracking of the non-linear plant.

Proof:

The proof of the offset-free model predictive control for a general case is found in [76]. However, this thesis presents a simpler and more intuitive method which is applicable for VSWT application. We assume that the solution of the standard QP in (3.16-3.17) achieves its optimal value. In the steady state we will have:

$$\Delta u^s_\infty=0;\ \bar{y}_\infty=y^s_\infty;\ y^s_\infty=y^*_\infty+\varepsilon \qquad (3.28)$$

where Δu^s_∞ is the first element of the control input matrix which is the solution of QP programming (3.16,3.17); $\bar{y}_\infty$ is the prediction of output using (3.11); y^s_∞ is the

measured output from the plant with standard predictive controller using model (3.2); y_∞^* is the output reference at steady state; ε is the tracking error due to the plant-model mismatch.

On the other hand, taking (3.11) and subtracting (3.26), and with the note that $y_\infty = Cx_\infty$, we have:

$$\bar{y}_\infty - \hat{y}_\infty = CL\hat{d}_\infty \tag{3.29}$$

With the same assumption that the QP problem in (3.27) obtains its optimal value, gives

$$\Delta u_\infty^d = 0\,;\ \hat{y}_\infty = y_\infty^d \tag{3.30}$$

where $\hat{y}_\infty$ is output prediction using (3.26); y_∞^d is the measured output using DMPC. Making observations on (3.29), it is seen that L is a tuning matrix and $\hat{d}_\infty = d_k$ is an arbitrarily chosen disturbance signal. Without loss of generality, we can find L, d_k such that (3.30) holds.

$$CLd_k = \varepsilon \tag{3.31}$$

So from (3.28-3.31) we have

$$y_\infty^d = y_\infty^s - \varepsilon\ ;\ y_\infty^d = y_\infty^* \tag{3.32}$$

Equation (3.32) shows that the output of the plant which uses the DMPC controller as in (3.27), provides offset-free tracking. The process of finding the observer gain and disturbance signal L, d_k ,with which (4.31) holds, can be followed by a simultaneous design. The procedure and criterion to obtain the combination of these parameters is presented in details in [77].

3.5. Nonlinear Model Predictive Control (NMPC)

By using a system model, future plant output is predicted within a finite step ahead based on current measurements. Open loop online optimization solutions then provide the calculated control inputs to the plant. Optimization is subsequently

repeated on the next sampling occasion to obtain a new control inputs. Based on measurement and/or observation of plant output, open loop optimization actually acts as a closed loop control. More specifically, the nonlinear plant model in can be expressed in the general form ($f(.)$ and $h(.)$ as nonlinear functions); with $x(k)$ as state variable, $u(k)$ as control input, $v(k)$ as system parameter, and $y(k)$ as output variable.

$$\begin{aligned} x(k+1) &= f(x(k),u(k),v(k)) \\ y(k) &= h(x(k)) \end{aligned} \tag{3.33}$$

The predicted outputs are obtained from the nonlinear model (3.33). Successive iterations of the model equations yield

$$\begin{aligned} \bar{y}(k+1|k) &= h(x(k+1|k)) = h(f(x(k|k),u(k|k),v(k|k))) \\ &= g_1(x(k|k),u(k|k),v(k|k)) \end{aligned} \tag{3.34}$$

$$\begin{aligned} \bar{y}(k+2|k) &= g_1(x(k+1|k)) = g_1(f(x(k|k),u(k|k)),u(k+1|k),v(k+1|k)) \\ &= g_2(x(k|k),u(k|k),u(k+1|k),v(k+1|k)) \end{aligned} \tag{3.35}$$

$$\text{Finally,} \quad \bar{y}(k+j|k) = g_j(x(k|k),u(k|k),u(k+j-1|k),..,v(k+j-1|k)) \tag{3.36}$$

where $x(k|k)$ is a vector of the current state variable, $x(k+j|k)$ is predicted state variable at time j. The same notation is used for output $\bar{y}(k+j|k)$, input $u(k+j|k)$ and independent variable $v(k+j|k)$. Based on the prediction (3.36), the optimization function for the NMPC is formulated same as the linear MPC quadratic function in (3.12). The only difference is that the predicted output is now a non-linear function with order equal to j times the order of function $f(.)$. In a similar way, the limitation of generator speed and torque can be incorporated to the quadratic function by forming output and input constraints which have the general form:

$$\begin{aligned} u_{\min} \le u(k) \le u_{\max} \\ y_{\min} \le y(k) \le y_{\max} \end{aligned} \tag{3.37}$$

These constraints can be generally re-written as one contour constraint

$$r(x(k),u(k),v(k)) \le 0 \tag{3.38}$$

The calculated control input of NMPC is the solution of the nonlinear programming (NLP) problem which is formulated from the constraints (3.38) together with cost function (3.12) and nonlinear model (3.33), as follows.

$$\text{Min: } Q = \sum_{i=0}^{N} [\bar{y}(k+i\,|\,k) - y^*(k+i\,|\,k)]^2 + \alpha \sum_{i=0}^{N_u} [u(k+i\,|\,k) - u(k+i-1\,|\,k)]^2 \qquad (3.39)$$

subject to

$$\begin{aligned} x(k+1) &= f(x(k), u(k), v(k)) \\ y(k) &= h(x(k)) \\ r(x(k), u(k), v(k)) &\leq 0 \end{aligned} \qquad (3.40)$$

Taking note that the quadratic function Q in the (3.39) contains the current measurement of state and output variables $y(k\,|\,k), x(k\,|\,k)$ and unknown future control inputs $u(k+i\,|\,k)$ for $1 \leq i \leq N_u$. The solution of NLP (3.39-3.40) will find the optimal value $u^*(k+i\,|\,k)$ of input $u(k+i\,|\,k)$ for $1 \leq i \leq N_u$. Then, only the first term of optimal solution $u^*(k\,|\,k)$ is applied to the plant.

To solve this complex NLP, the general aim is to transform a difficult problem into an easier sub-problem that can then be solved and used as the basis of an iteration process. Both necessary and sufficient to obtain a global solution for NLP, Karush-Kuhn-Tucker (KKT) equations are used which can be stated to have a Lagrange function (3.41). The function $L(x, \mu)$ is formulated in every controller sampling time. In the next sequence, the new function is re-formulated for the incoming of measured parameters.

$$\begin{aligned} L(x, \mu) = Q(u^*) + \mu_1 f(u^*) + \mu_2 r(u^*) &= 0 \\ \mu_1 f(u^*) &= 0 \\ \mu_2 r(u^*) &\leq 0 \\ \mu_1 = 0; \mu_2 &\geq 0 \end{aligned} \qquad (3.41)$$

where $\mu = (\mu_1, \mu_2)^t$ is Lagrange multipliers. The process of finding the vector (u^*, μ^*), which is true solution of (3.41), can be done though an iteration procedure of the form.

$$u_{k+1} = u_k + \sigma_k \bar{d}_k \tag{3.42}$$

where $\sigma_k \in [0,1]$ is the line search parameter; u_k is initial value of control input which actually is current value generated from previous sampling time; $\bar{d}_k$ is intended to be an estimate of the step from the current iterate u_k to a local solution u^*. The search direction $\bar{d}_k$ is obtained by another iteration process (3.43) with initial guess of d_0

$$d_{k+1} = d_k + \Delta d_k \tag{3.43}$$

where Δd_k is the solution of the new QP problem approach.

$$\text{Min } P_k: \quad \frac{1}{2}\Delta d^t H_k \Delta d + Q(x_k)^t \Delta d \tag{3.44}$$

$$\text{subject to:} \quad \begin{cases} \nabla f(u_k)^t \Delta d + f(u_k) = 0 \\ \nabla r(u_k)^t \Delta d + r(u_k) \le 0 \end{cases} \tag{3.45}$$

where Δd is artificial variable introduced in new QP problem. The Hessian matrix $H_k \approx \nabla_k^2 L(u_k, \mu_k)$ provides an approximation of the second order derivative of the Lagrangian formulation in the above NLP.

It should be noted that the transformation of the NLP (3.39- 3.40) to the QP sub-problem in (3.44-3.45) requires a calculation Hessian matrix H_k on every sampling occasion. This is the most expensive resource dedicated to the optimization problem. To avoid process of re-calculation H_k, an updated Hessian matrix via the Broyden–Fletcher–Goldfarb–Shanno (BFGS) method is usually used [78].

$$H_{k+1} = H_k + \frac{q_k q_k^T}{q_k^T s_k} - \frac{H_k^T s_k^T H_k s_k}{s_k^T H_k s_k} \tag{3.46}$$

where: $$s_{k+1} = u_{k+1} - u_k \tag{3.47}$$

$$q_k = \nabla Q(u_{k+1}) + \mu_1 \nabla f(u_{k+1}) + \mu_2 \nabla r(u_{k+1}) - \nabla Q(u_k) + \mu_1 \nabla f(u_k) + \mu_2 \nabla r(u_k) \tag{3.48}$$

Each time the Hessian matrix is updated, a new QP problem stated in Section 3.3 is formulated as shown in (3.44-3.45), which follows the standard procedures to obtain solutions. This involves two phases: the first consisting of the calculation of a feasible point; the second the generation of an iterative sequence of feasible points that converge to the solution. The solution of (3.44-3.45) does not only provide search direction $\overline{d}_k$ of the original NLP problem (3.39-3.40) but also gives solution of Lagrange multipliers solution μ^*. The solution of Lagrange multipliers of the new QP problem μ^{QP} is also the solution of the original problem, such that $\mu^{QP} = \mu^*$ [79].

Remarks: 1) By converting the NLP (3.39-3.40) problem to the sub-problem QP (3.44-3.45), the NMPC has a root back to a LMPC.

2) One SQP-iteration (3.42) requires few QP iterations (3.43) so that SQP is more time consumed process than QP problem. The most time consuming in SQP is the process of updating the Hessian matrix H_k, this process plus more calculation time of SQP.

3) To get true solution of NLP (3.39-3.40), few SQP iterations is required. It means that one sampling time of NMPC controller requires multiple SQP iterations.

3.6. Alternative NMPC formulation

The formulation of NMPC as in Section 3.6 is for discrete time domain. However, system modelling basically is in analogue by a continuous function. For a conventional NMPC design, the continuous formulation of NMPC is also usually used [80]. The optimal control problem in Ordinary Differential Equation (ODE) is as (3.49) below. T_p is a so-called prediction horizon which may change for a moving horizon optimization problem.

$$Min \quad Q_{npc} = \int_0^{T_p} L(x(t), u(t), v(t))dt \tag{3.49}$$

subject to an Ordinary Differential Equation (ODE) function and all the terminal as well as contour constraints.

$$\begin{aligned} dx(t)/dt &= f(x(t),u(t),v(t)) \\ x(0) &= x_0 \\ u(0) &= u_0 \\ 0 &= g(x(t),u(t),v(t)) \\ 0 &\le h(x(t),u(t),v(t)) \end{aligned} \tag{3.50}$$

where $x(t)$ is the state variable, $u(t)$ is the control input, and $v(t)$ is the system variable. The standard procedure to solve this continuous optimal control problem is presented in Chapter 5.

Nonlinear Problem Tutorial

For illustration of nonlinear control problem, the following tutorial example is used, with only one state and one control variable. The example is a second order nonlinear system.

$$Min \quad \int_0^2 (x-5)^2 dt \tag{3.51}$$

$$\begin{aligned} \text{s.t.} \quad & dx/dt = -x^2 + 5x + u^2 \\ & x_0 = 1 \\ & 0.1 \le u \le 1.0 \end{aligned} \tag{3.52}$$

MATLAB codes can be written using the ACADO toolbox and are shown in Appendix 4. Simulation results in Figure 3.4 and 3.5 show the state variable and control signal.

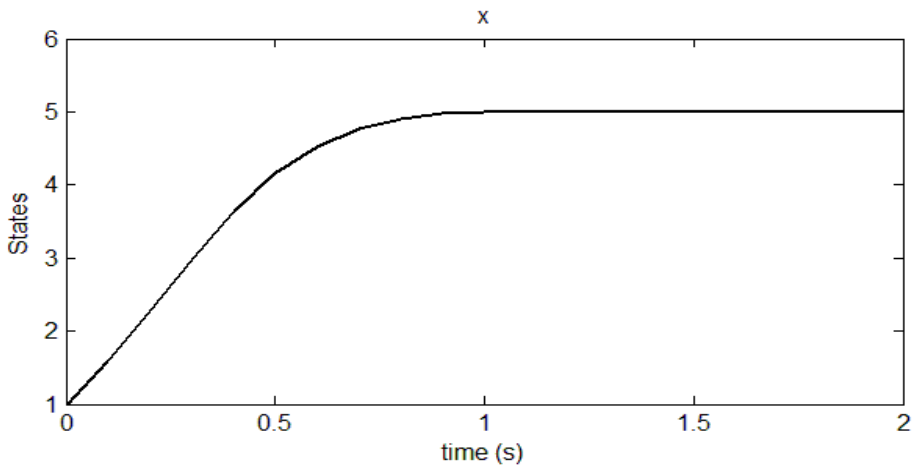

Figure 3.4. State variable of NMPC tutorial problem

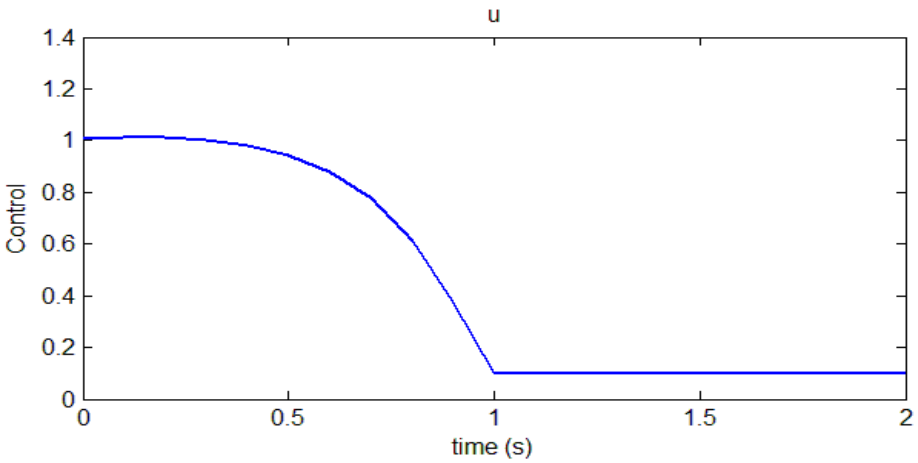

Figure 3.5. Control input of NMPC tutorial problem

3.7. Conclusions

Although there are many control methods in control engineering, by all means, could be applied to wind power system; however, within the resource limitation of this research project, these particular methods were chosen intensively for some particular study purposes. This chapter presents fundamental of linear and nonlinear control techniques which uses no modeling required (FLC) to nonlinear mathematic algorithms (NMPC). General theory and example to support basic idea of control methods were studied. The next chapter in consequence is about the application of these control algorithms to wind power application. Controller designs as well as validation results to show performance of proposed method are presented.

CHAPTER 4

APPLICATION OF CONTROL ALGORITHMS FOR VARIABLE SPEED WIND TURBINE

This chapter presents the application of control methods in Chapter 3 for speed loop of variable speed wind turbine. At first, conventional PI controller for speed loop as well as current loop of permanent magnet generator is revised. Then, in the next section, different control algorithms for controlling speed loop to replace the PI speed loop while PI current loops are kept unchanged. The simulation program with comparison results among these controllers select the best suitable algorithm. The two good algorithms are then undergoing a further experimental test to validate implemental suitability for industrial application.

4.1. Conventional PID

The linear PID controller reviewed in Chapter 1 and being revised in this section has only proportional and integral term since the derivation component is not necessary. The transfer function of PI controller takes the form.

$$G_{pi}(s) = K_p + \frac{K_i}{s} \tag{4.1}$$

The closed loop transfer function in a control structure as mentioned in Figure 1.3 for a linearized drive-train model (2.38-2.39) in Section 2.3.3 is obtained from

$$G_c(s) = \frac{(K_p + \frac{K_i}{s})G(s)}{1 + (K_p + \frac{K_i}{s})G(s)} \tag{4.2}$$

This closed loop transfer function has standard damping and oscillation frequency ξ, ω_n of a second order function

$$G(s) = \frac{\omega_n^2}{s^2 + 2\xi\omega_n s + \omega_n^2} \tag{4.3}$$

The tuning process determines the controller gain as $K_p = -5;\ K_i = -10$ for the transfer function obtained at point O while $K_p = -2;\ K_i = -10$ for that of point A in Figure 2.12.

The second objective of the wind turbine controller is to determine the generator unity power factor; all mechanical power from the turbine is converted into active power in the generator. This goal can be obtained by regulating the d-axis current from the generator side control at zero, i.e. the generator is fully exited by the permanent magnet while the q-axis current is used for regulating torque. As can be seen from Chapter 2, the generator torque is proportional to the q-axis current by a constant gain (2.47). Therefore, generator torque is directly manipulated though the q-axis current. With the assumption that d-q currents are well controlled at a steady state, the nonlinearity of the electrical model of the PMSG can be avoided by the de-coupling method with the introduction of new control inputs.

$$\begin{aligned} u_{ds}^{'} &= u_d + \omega_s L_s i_q \\ u_{qs}^{'} &= u_q - \omega_s L_s i_d - \phi\omega_s \end{aligned} \tag{4.4}$$

Generator electric current equations in (2.45-2.46) are now re-written in the Laplace domain as following:

$$(R_s + sL) i_d = u_d + \omega_s L_s i_q \tag{4.5}$$

$$(R_s + sL) i_q = u_q - \omega_s (L_s i_d + \psi) \tag{4.6}$$

From (4.4-4.6), the transfer function of the current loop is obtained as (4.7), and then the PI controller designs for the two current loops are similar to the speed loop.

$$G_i(s) = \frac{i_d}{u_d^{'}} = \frac{1}{sL_s + R_s} \tag{4.7}$$

The PI controllers for d-q current loops of PMSG are typical and have been widely applied in the industry. This is not a main study of the thesis work. Hence, in the rest of this document, the main concern is addressed for speed control loop. The controller structure is shown in Figure 4.1.

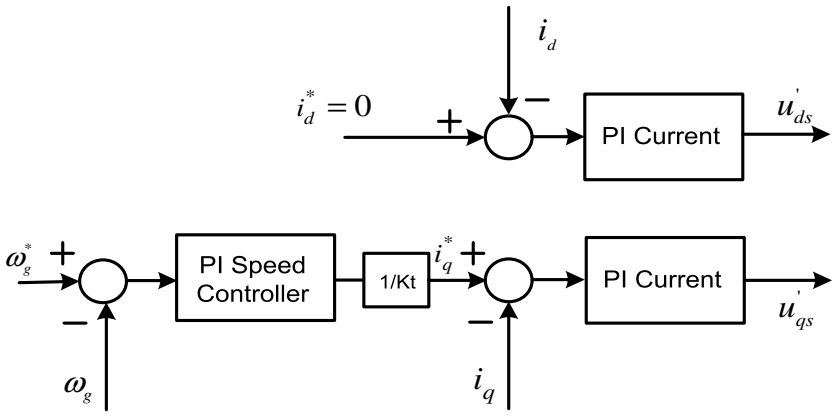

Figure 4.1. Conventional PI controller structure

4.2. Fuzzy Logic Controller (FLC)

In classical control such as PID controller aforementioned in Section 4.1, controller design requires a modelling of the system. However, an accurate model of a nonlinear plant such as wind power system is not always obtainable. This problem can be avoided by exploited the artificial intelligence techniques of fuzzy logic which is recently showing a lot of promise in wide area of applications. Based on observation of signal feedback, fuzzy controller acts as humanity behavior to adjust control signal appropriately without the knowledge of modelling details. Wind turbines system is considered as a black box with inputs and outputs. More specifically, fuzzy controller for wind power system has two inputs and one output. The first one is error of actual speed and the reference while the second one is rate of change seen from the first component. The output of fuzzy controller is the generator torque. The nature of fuzzy actions can be illustrated as following: when the error between reference and actual output is large, it is required to increase the control input to larger value to accelerate turbine speed until reaching the set point. On the other hand, when the error is small, an accordingly small value of control input should be maintained. The reference is the optimal trajectory which is obtained in (2.54) while the actual speed can be measured by encoder. Lastly, when the error is around zero, the rate of change in turbine speed should be considered. If the rate of change is zero, it is likely that turbine speed will remain at the set point without lost of tracking. If the rate of change is positive, the turbine speed tends to

go further beyond the desired value. Hence, even the speed error is zero; a negative change of control input should be applied. Vice versa, if a negative rate of change in turbine speed is observed, a positive change in control input is introduced. The more details in fuzzy logic rules are shown in Table 3.

Table 3. Fuzzy rules for wind power system control

RES / ES		NB	NM	ZE	PM	PB
PB	PB					
PM	PM					
PS	PS					
ZE		PM	PS	ZE	NS	NM
NS	NS					
NM	NM					
NB	NB					

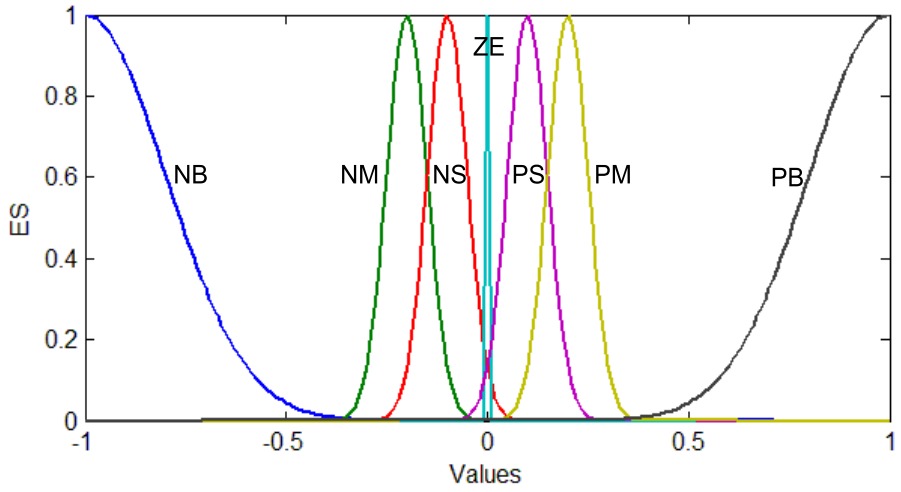

Figure 4.2. Membership functions of reference tracking error

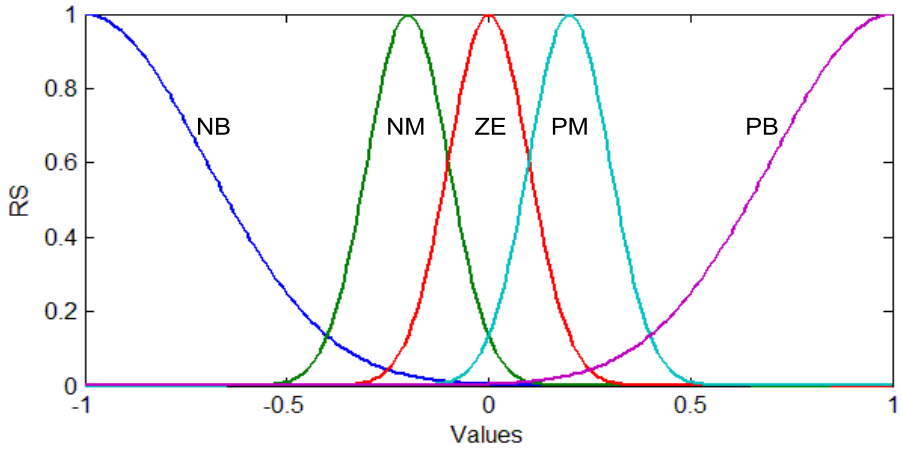

Figure 4.3. Membership functions of rate of speed

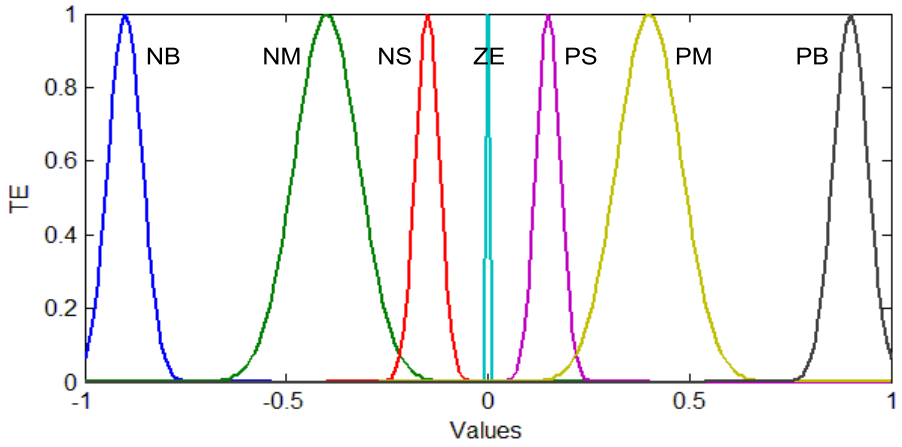

Figure 4.4. Membership functions of control input

From Table 3, there are 7 linguistic values are defined for wind power control application. They are: NB-negative big, NM-negative medium, NS-negative small, ZE-zero, PS-positive small, PM-positive medium, PB-positive big. The typical fuzzy rules can be read as: IF error of speed ES is PB then control input as generator torque TE is PB. IF ES is ZE and rate of change in speed RES is PB then TE is PM. The membership function for inputs and output are asymmetrical to provide more sensitivity for a zero offset tracking of turbine speed. These membership functions are illustrated in Figure 4.2 to Figure 4.4. Variables are defined in nominal scale of [-1; 1] then real value of variables is obtained by corresponding scaling factors of each variable. Membership functions are designed more densely distribution around center at values of 0, since most of the time the

error in speed tracking is around zero. More density distribution around zero produces more smoothed changes in control signal. It is an important requirement because a high fluctuation of generator torque is avoided.

4.3. Nonlinear PID

The conventional linear PID is adequate for controlling the nominal processes with Linear Time Invariant (LTI) parameters. The requirements of high-performance control for nonlinear systems which have operating points changing such as wind power system are not obtained by using traditional PID controller. A single fixed-gain PID is not sufficient for controlling wind turbine speed at all working points (as illustrated in Figure 4.5).

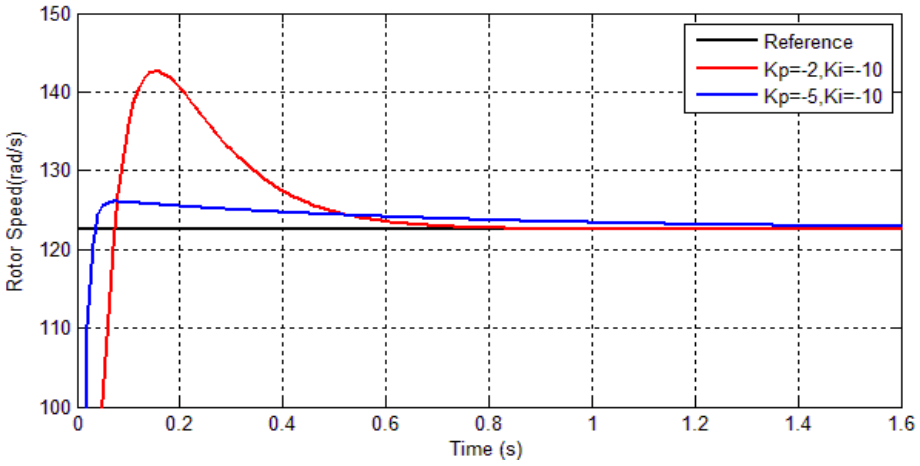

Figure 4.5. Step response of speed loop under fixed-gain PID controllers

A well tuning PID controller for transfer function at optimal operating point of wind power gives large overshot during transient period, and vice versa another PID tuned well for transient period delivers large off-set tracking at steady-state. More specifically, the observation from step responses of linear PID controllers for the corresponding transfer functions shows that the linear model at point O (in Figure 2.12) is a more suitable presentation of a plant at steady state, while the linear model at point A is more suitable for a transient mode (as discussed in Section 2.3.3). These problems can be avoided by employing an extension of linear PID to a nonlinear PID controller. The similar approaches for other industrial processes are

found in [60-63] while a self-tuning PID based on Lyapunov approach for wind energy conversion system is presented in [64]. The combination of fuzzy and PID for a wide range of wind speed is popular and it is found in the [65-67]. In this section, rather than using fuzzy PID controller, polynomial nonlinear PI controller with variable gains accordingly to different operating points of wind power system is presented. The proportional and integral gains are nonlinear functions which adaptively adjust to the change of mechanical angular speed. The effectiveness of the proposed controller is validated by simulation results in comparison with that of linear fixed-gain PID controller and FLC controller.

4.3.1. Design of Nonlinear Proportional Component

The motivation of designing the nonlinear P component based on the natural behaviour of a closed-loop response. When the error is large i.e. the actual output is far from the reference, hence the proportional gain should be lager to produce a fast response. And vice versa, when the tracking error is small, the P gain should be small to reduce tracking offset. In the wind power case study, the gain P should be designed to be large at transient period and convergence to the P gain designed for the linear plant which is obtained at point O (in Figure 2.12). Therefore, the automatic adjustment of the P gain as a continuous function of the tracking error can attain the two contradictory requirements of a fast response and small offset at steady state. This is not able to achieve by a linear fixed gain PI controller. The proposed P gain function is a third order polynomial function of the error as follows.

$$f_p(e) = a_3 e^3 + a_2 e^2 + a_1 e \ + a_0 \tag{4.6}$$

where a_0, a_1, a_2, a_3 are user-defined constants which are attained by tuning process. When error $e = 0$, $f_p(e) = a_0$, hence the value of a_0 can be chosen as P gain designed for the linear plant which is obtained at point O in Figure 2.12 and model (2.38), $a_0 = -5$

4.3.2. Design of Nonlinear Integral Component

The integral action of a PID controller has the effects of settling time and steady state error caused by proportional gain. The natural contribution is that larger integral gain will cause longer settling time and vice versa. In contrast with the effect in steady state error, a large integral term is only required when the error is small in order to get small steady state offset. In order to get the both contradict requirements of short settling time and small steady state error, the integral term should be carefully designed to change from small value at initiation progress to a large value at steady state. To achieve this goal, the similar polynomial function of the proportional gain is introduced

$$f_i(e) = b_3 e^3 + b_2 e^2 + b_1 e + b_0 \tag{4.7}$$

where b_0, b_1, b_2, b_3 are user-defined constants which are attained by tuning process. When error $e = 0$ $f_i(e) = b_0$, hence the value of b_0 can be chosen as I gain designed for the linear plant which is obtained at point O, $b_0 = -5$. Figure 4.6 shows a polynomial curve of $f_p(e), f_i(e)$ as a function of e when $a_1 = 0; a_2 = 0$ and $a_3 = -2/30$; $b_1 = 0; b_2 = 0$ and $b_3 = -2/14.6$.

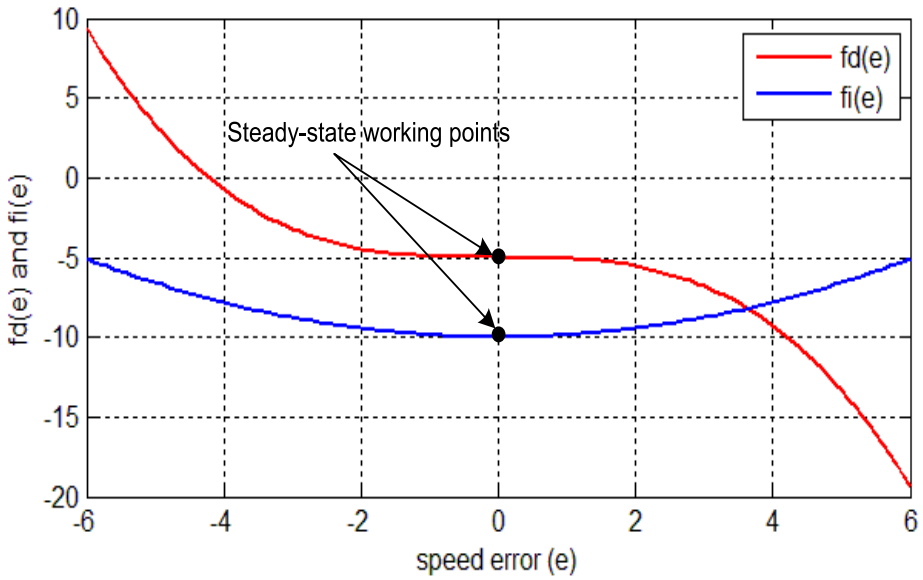

Figure 4.6. Nonlinear curves of PI gains

4.4. Simulation Results of FLC, PID and NPID Controllers

Simulation is done using the Matlab/Simulink environment to test the performance of studied controllers. Nonlinear model of VSWT in (2.34) which has specification in Appendix 3 is used for simulation. PI and predictive controllers were designed based on the linearization models in (2.38) and (2.39) respectively. Simulation results shown in Figure 4.7 as follows.

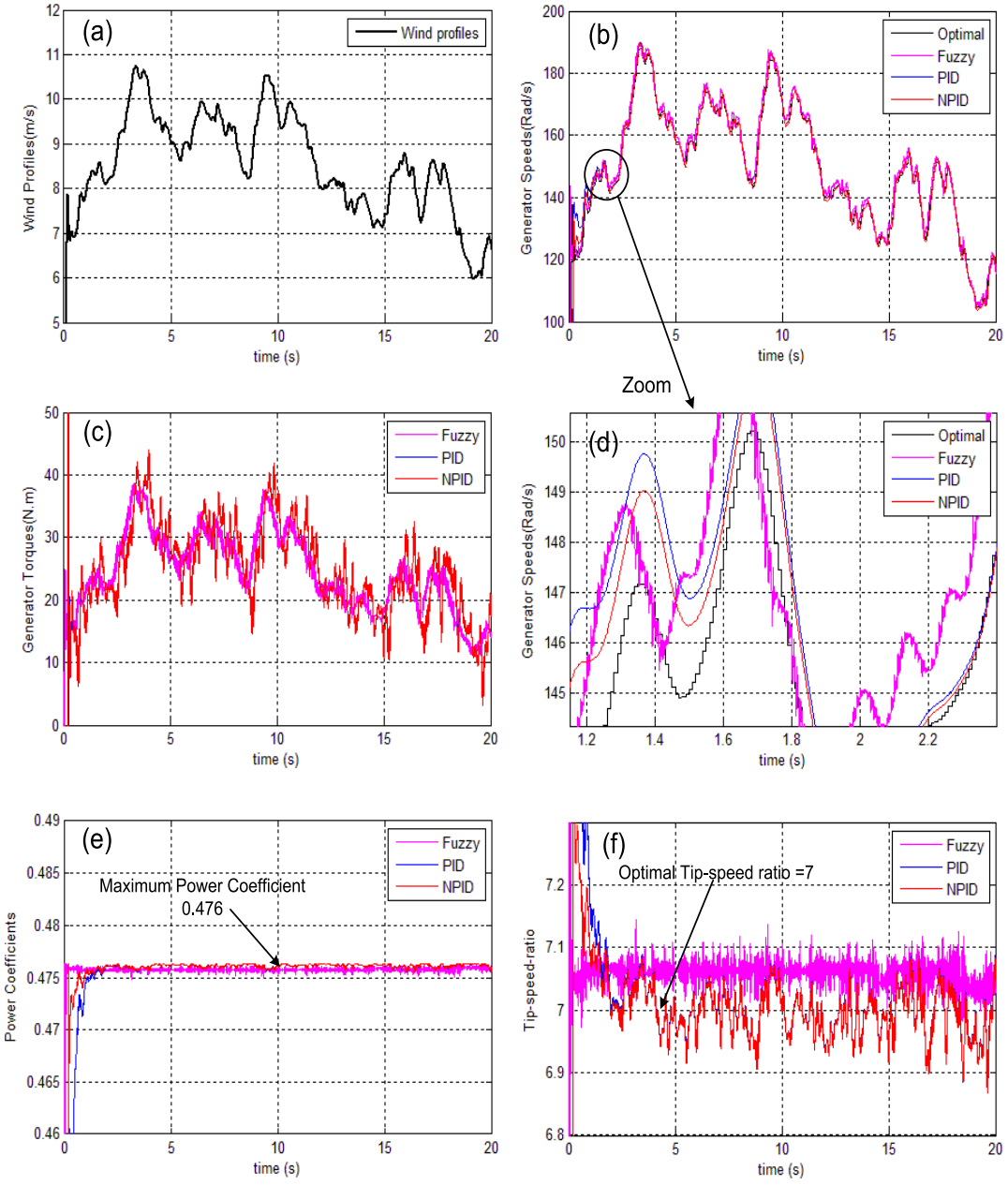

Figure 4.7. Simulation results of FLC, PID and NPID controllers

Generator speed responses of fuzzy logic, classical PID and proposed nonlinear PID controllers are illustrated in Figure 4.7(b) for input wind speed in Figure 4.7(a). The generator speed of fuzzy controller (in magenta colour) presents a fair tracking response. It has a small offset from the reference due to limited number of membership functions was designed. On the other hand, classical PID controller response (in blue) provides good tracking at the steady state (from 3rd second onward) but it is seen an overshot and long settling time during transient period (from 0-3rd second). Lastly, the nonlinear PID controller response (in red colour) presents good result at both transient and steady state regions.

Generator torque as control input of fuzzy logic controller (magenta color) in Figure 4.7(c) has high frequency oscillation which effects to the life cycle of system. The linear and nonlinear PID control inputs (in blue and red color) are seen to be smoother than that of fuzzy controller. In Figure 4.7(e-f), the power coefficient and tip speed ratio of PID and nonlinear PID also stays around the optimal values while there is an offset seen from that of fuzzy controller. From the simulation results, it is obviously concluded that nonlinear PID controller provides best results over the two preceded controllers. Fixed gain PID controller has advantages at steady state region while fuzzy controller gives better response at transient region without over shoot. Nonlinear PID controller inherits stability property of PID at steady state regions while improves the quality at transient period at less overshoot and small convergence time delay.

4.5. DMPC for Entire Working Conditions of VSWT

Most of the current work presents control algorithms for either normal wind speed region or for higher than rated wind speed region separately [17, 19, 29, 33, 37, 81, 82]. The reason is that the current approaches encounter difficulties when both modelling and performance criteria are different between the partial load and full load regions. Firstly, at wind speeds below the rated value, the optimization of power harvested from the wind is the main target of current approaches. Maximum power point tracking (MPPT) and linear quadratic Gaussian (LQG) control are of widespread interest [19, 32, 42, 83, 84]. Among them, MPPT is the simplest control

method but does not produce such good results. Multi-model algorithms using Linear Quadratic Gaussian (LQG) and robust Quantitative Feedback Theory (QFT) are found in [33, 82]. The nonlinear aerodynamics was linearized at different wind velocities to get a class of linear models for which the controller designs were applied. Secondly, for wind speeds above the rated value, wind turbine controllers usually have the objective of keeping the power constant at the rated value. A controlled-pitch angle to limit the energy captured is mostly seen in the current work [17, 29, 45]. The classical PI controller is commonly found for pitch angle mechanism [17, 29]. The linear MPC for levelling of the output power at high wind speeds by optimally changing pitch angle is also found in [45]. Lastly, for a wide range of wind speeds from normal to higher than rated value, the wind power system has different working regions as well as control objectives. A common trend of using two different controllers for each region has been seen in [31, 35].

Turbine speed and pitch angle control loops are designed separately for partial load and full load region by using PI controllers with the transition torque equation introduced for switching between two regions [31]. In [35], an intelligent controller using least square support vector machine is employed to adjust pitch angle at above rated wind speed conditions and an adaptive fuzzy controller at below rated wind speed conditions. A high order sliding mode controller of permanent magnet generator is mentioned in [12]. The control law that covers entirely all operating regions is found in [42]. In this reference, the proposed Linear Parameter Varying (LPV) control structure selects a proper operating trajectory as a function of estimated wind speed. The pitch angle and generator torque are used as control inputs for the corresponding working regions. However, controlled-pitch system is particularly efficient in large-scale wind turbines in which the cost of pitch angle production is less in comparison to the whole system price. In small and medium scale wind turbines, no pitch angle changing devices are widely exploited. Rotor speed is manipulated by changing the electromagnetic torque from the generator, which is generally an induction or permanent magnet machine fed by full-scale power converters.

In this section, DMPC for the aerodynamics loop of a wind turbine are presented by

exploiting the active stall control scheme without using pitch-angle mechanism [54] for both partial and full load conditions. All the problems related to wind power system control such as multiple objectives; linear time-varying parameters due to wind velocity changes, different working regions and mechanical limitations are easily solvable by the proposed controllers. Firstly, the quadratic cost function of errors, between the actual generator speed and the optimal speed reference, and the rate of change in electromagnetic torque is formulated. In order to get speed variation converges with optimal speed variation reference, the least square tracking criterion function is formulated to be minimized in a discrete time domain as

$$Q_1 = \sum_{i=0}^{N_1} [\omega_g(k+i\,|\,k) - \omega_g^*(k+i\,|\,k)]^2 + \alpha \sum_{i=0}^{N_{u1}} [\Delta T_e(k+i\,|\,k)]^2 \tag{4.8}$$

where $\omega_g(k+i\,|\,k)$ is the generator speed predicted at time i.

Secondly, by considering cut-in and full load regions as lower and upper bounds of the partial load region, the lower and upper limitations in turbine speed and generator torque are easily integrated to the criterion function through initiation of output and input constraints. Different working regions are combined into one continuous region with boundaries thus achieving a smoothing transient between different regions.

$$\begin{array}{ccccc} \Delta\omega_g^{\min} & \le & \Delta\omega_g(k) & \le & \Delta\omega_g^{\max} \\ \Delta T_e^{\min} & \le & \Delta T_e(k) & \le & \Delta T_e^{\max} \end{array} \tag{4.9}$$

Finally, due to the stochastic behaviours of winds, the optimal reference is also fluctuating proportionally to the wind speeds. The non-stationary reference in high speed operation is a challenge in designing the controller. Thanks to computational methods in engineering, Quadratic Programming (QP) has been developed recently. The optimization objective function is carried out on every sampling interval to obtain new and updated control input which is the electromagnetic torque. As a result, the predictive controllers are adaptive to changes in wind profile. By defining the cost function (4.8) together with state-space modelling (3.2), the LMPC with constraints for wind turbine control problem is constructed as (4.10)

$$\text{Min} \quad Q_1 = \sum_{i=0}^{N_1} [\omega_g(k+i\,|\,k) - \omega_g^*(k+i\,|\,k)]^2 + \alpha \sum_{i=0}^{N_{u1}} [\Delta T_e(k+i\,|\,k)]^2 \tag{4.10.a}$$

subject to:

$$\dot{\omega}_r = A\omega_r + BT_e \tag{4.10.b}$$

$$\omega_g(k) = \eta\omega_r(k) \tag{4.10.c}$$

$$\omega_g^{\min} \le \omega_g(k) \le \omega_g^{\max} \tag{4.10.d}$$

$$T_e^{\min} \le T_e(k) \le T_e^{\max} \tag{4.10.e}$$

DMPC parameters are obtained during the tuning process of designing the controller. In order to balance between tracking errors and reducing control input variations, here a weighting factor of $\alpha = 0.1$ is chosen ; output prediction and input prediction are set to typical values for predictive controllers, $N_p = 10$, $N_u = 2$. Control input is limited to the range $-50 \le T_e \le 50$ (N.m). Observer gain was tuned to get a stable estimate of control output and unknown noise to be cancelled, $L = 0.7$. A step disturbance $d(k) = 1$ was added to the models.

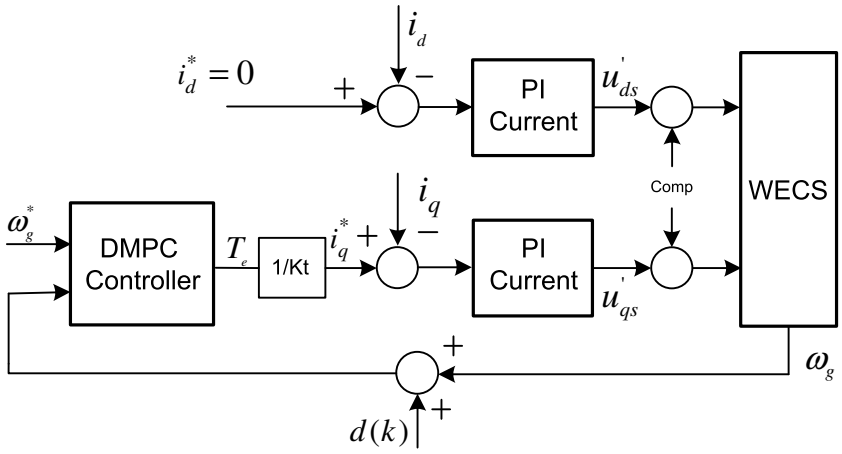

Figure 4.8. Controller structure of DMPC for VSWT

The controller structure of DMPC for VSWT is shown in Figure 4.8, with $d(k)$ being the output disturbance which is also augmented to the DMPC controller. ω_g is the control output while ω_r is the state variable; and the control input is the equivalent generator torque at the low speed shaft T_e.

4.5.1. Under rated wind speed simulation results

Simulation is done using the MATLAB/SIMULINK environment with a DMPC controller which has the parameters as mentioned in above section. The principal objective of the controller for the wind turbine is to harvest the maximum available wind power, despite the variation of wind speed.

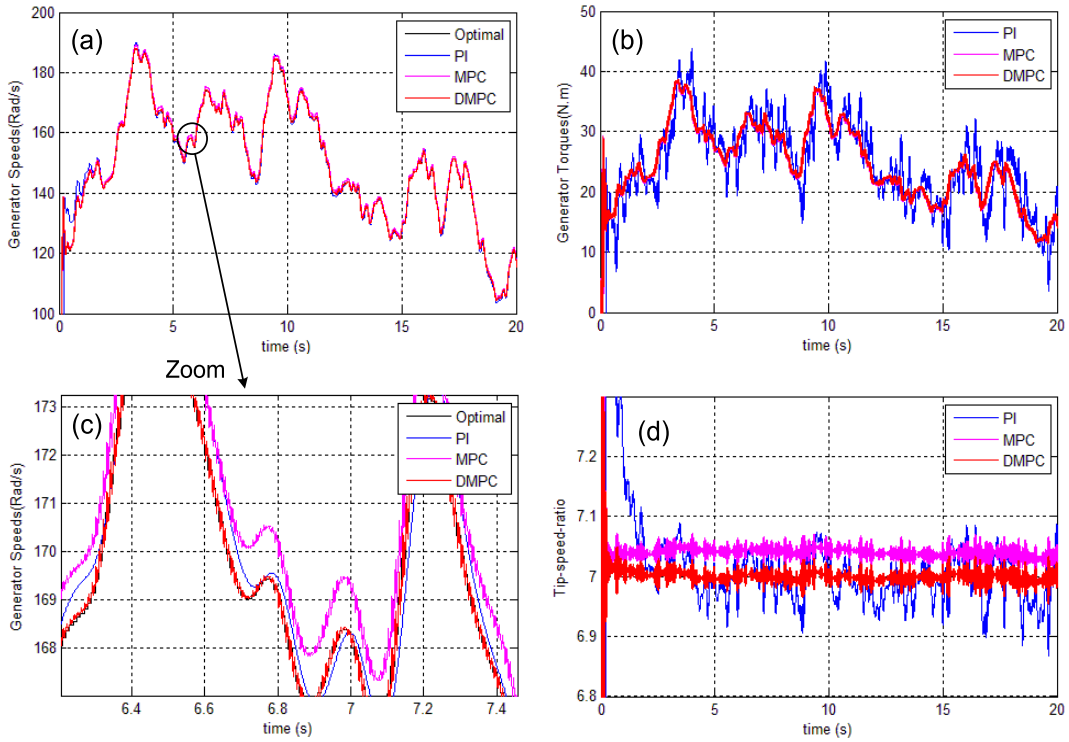

Figure 4.9. Simulation results of PID, MPC and DMPC controllers

Figure 4.9 shows the optimal speed reference, in black color, which is calculated from (2.54). The red curve is the actual speed response of the DMPC closely tracking the reference speed. The results show the effectiveness of the proposed DMPC controller with respect to traditional PID (plotted here in blue) and conventional model predictive control (MPC seen in magenta). The results also show a constant offset in the MPC tracking output, whereas the DMPC provides an offset-free tracking. Small fluctuations in computed generator torque (as control input) are common among the three controllers. This is shown in Figure 4.9 (b). The maximum energy is obtained when the tip speed ratio is maintained at the optimal

value of 7 from Figure 4.9(c) with very minor errors in DMPC controller (red color), in contrast with a constant error in predictive controller (magenta color) and large variations seen from PI controller (in blue). Figure 4.9 reveals the superiority of the proposed controller.

4.5.2. Full load condition with output constraints

Simulation is done using the MATLAB/SIMULINK environment with a DMPC controller which has the parameters as mentioned in above section. The principal objective of the controller for the wind turbine is to harvest the maximum available wind power, despite the variation of wind speed.

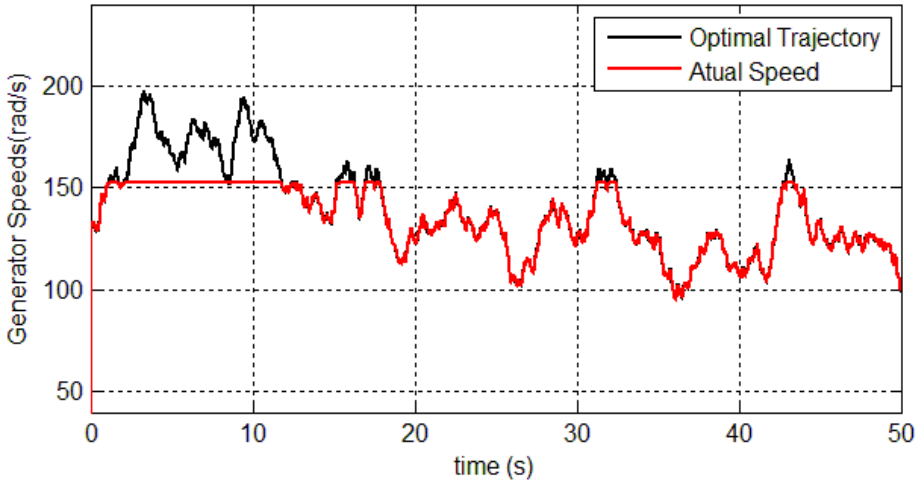

Figure 4.10. DMPC with output constraint: generator speed response

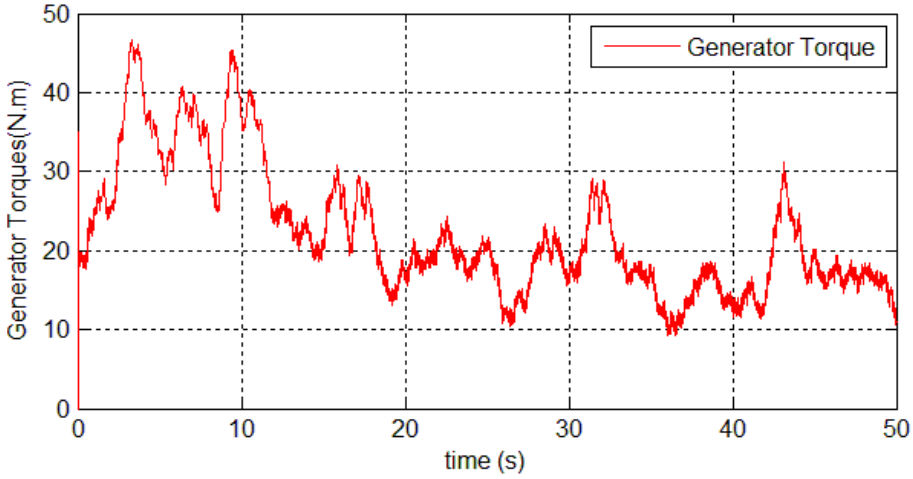

Figure 4.11. DMPC with output constraint: generator torque

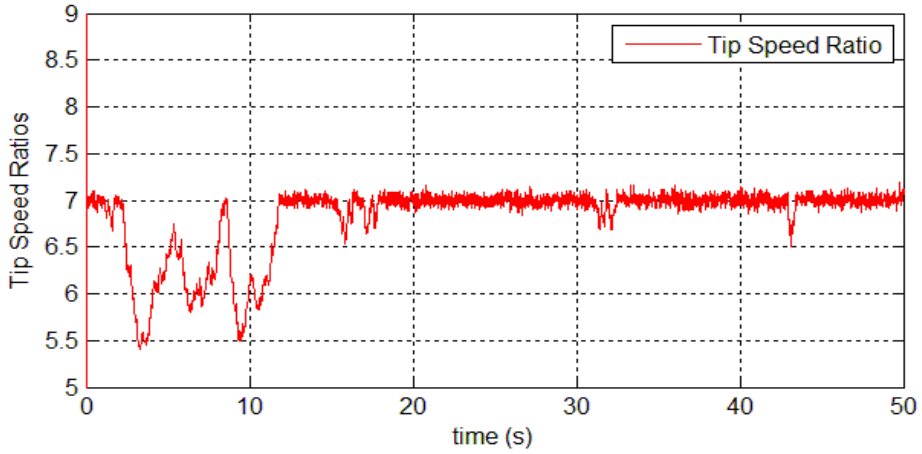

Figure 4.12. DMPC with output constraint: Tip speed ratio

When wind increases to higher speed, the optimal reference is increased proportionally. However, the actual turbine speed is designed to work within a bounded region which is known as the rated value. The turbine speed should be kept under the limitation to protect wind turbine from damage. This capability is integrated in DMPC controller. Control algorithm will generate a higher value of control input, in this case is generator torque, to compensate the increment of aerodynamic torque (Figure 4.11). As the results, the turbine speed, in red color as can be seen from Figure 4.10 with time from 2nd second to 12nd second, is maintained at the rated value although the optimal reference goes higher value. The tip speed ratio (Figure 4.12) is now less than the optimal value, which means the working of the turbine has lower of power efficiency. From the 12nd second onward, wind reduces speed to the normal operating region; the controller resumes the maximum power objective. By exploiting the constraints handling properties for full load condition of wind turbine, the DMPC provides a smooth transient between different working regimes. One controller is sufficiently used to cover entire load conditions (from partial load to full load) of wind turbine.

4.5.3. Full load condition with input constraints

The second scenario of full load condition for variable speed wind turbine is control input (generator torque) reaches its maximum value due to limited power converter capacity.

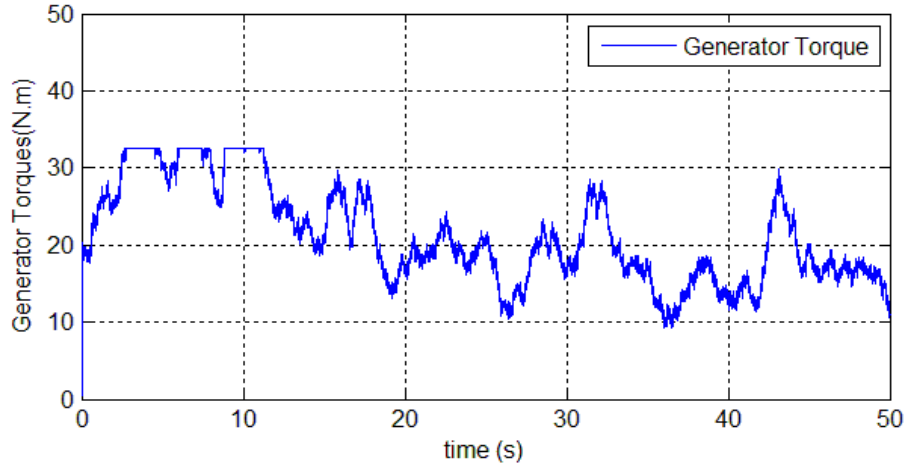

Figure 4.13. DMPC with input constraint: generator torque

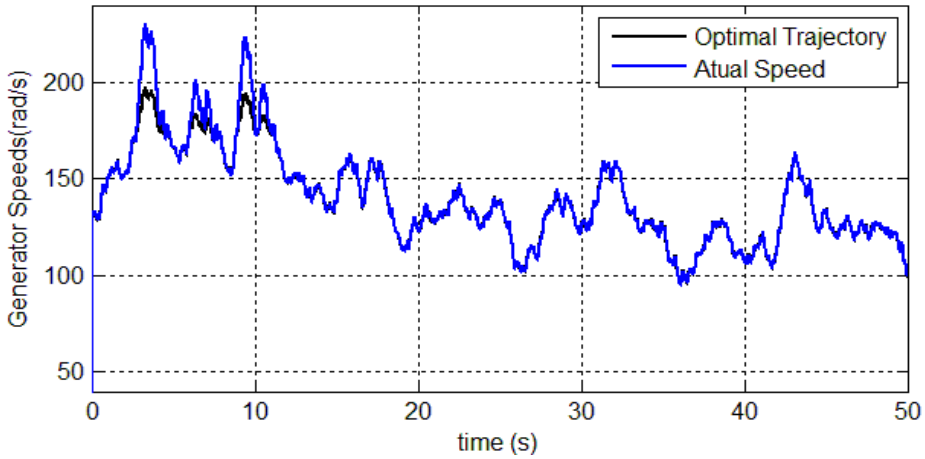

Figure 4.14. DMPC with input constraint: generator speed response

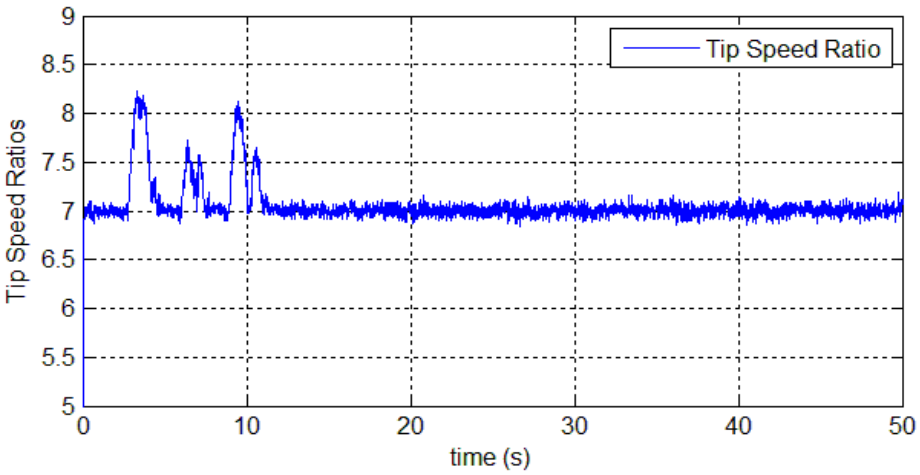

Figure 4.15. DMPC with input constraint: Tip speed ratio

If wind speed increase to a high value than rated value it means that aerodynamic torque is high. Generator torque should be controlled to be increasing to until reaching the rated value (as seen in Figure 4.13). In this case, the actual turbine speed is higher than the optimal value (as in Figure 4.14), wind turbine is working at lower power coefficient with corresponding tip speed ratio higher than the optimal value (e.g. $\lambda_{opt} = 7$) as from Figure 4.15. The third scenario is that both output and input reach their limits. This is known as power limitation scheme, wind turbine is pushed into a shutdown mode to protect from electrical and mechanical damage by activating brake.

4.6. Experiment Results

The further test was carried out with experiment test rig to validate the proposed controller. The linear PID, nonlinear PID and DMPC controllers were run using a laboratory scale test rig system.

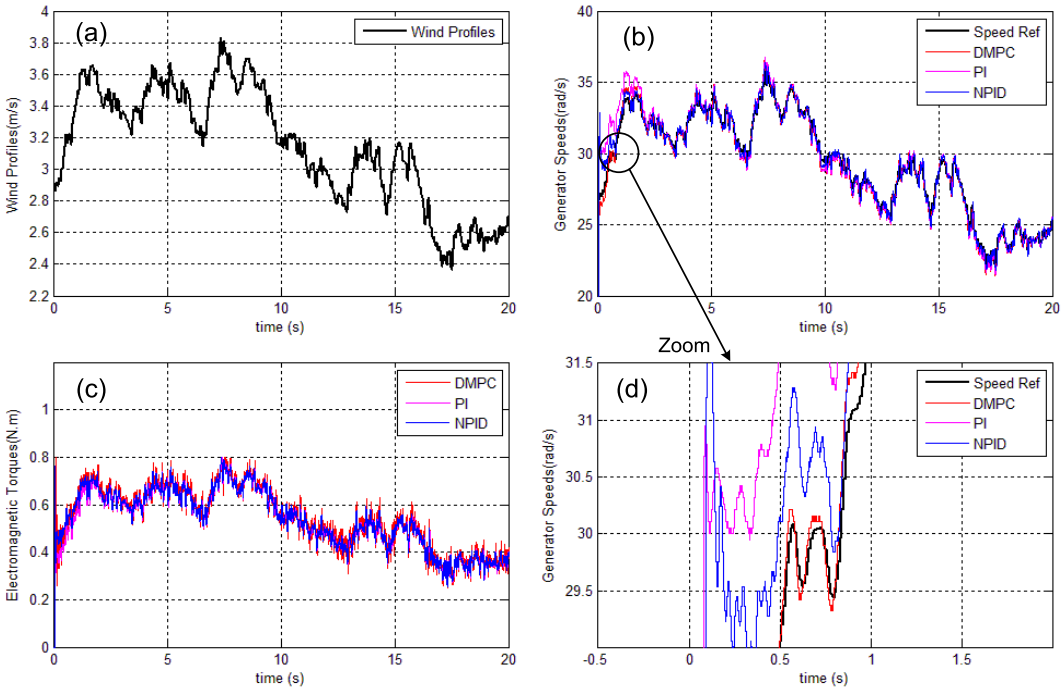

Figure 4.16. Experimental results of PID, NPID and DMPC controllers

Due to limitations of the laboratory scale test bench which is only suitable for low power wind turbines, low speed wind profiles were used for testing the controller

(Figure 4.16(a)). The proposed DMPC and two PID controllers for experimental testing were re-designed based on the new set of parameters (see Appendix 4) which are different from VSWT used for simulation (see Appendix 3). The experimental linear modeling transfer function of VSWT is different from that of (2.38). However, the DMPC controller has almost the same parameters as presented in Section 4.4.

Experiment results agree with the simulation results; the generator speed of the DMPC and nonlinear PID are better than the response of the PID speed controller in the transient period from 0 to 3 seconds, (Figure 4.16(b)). At steady state, all controllers deliver very good tracking results with superiority is seen from DMPC. The generator torque as the computed control command from all controllers is shown in Figure 4.16(c). A little less variation is seen from the DMPC (in red) with respect to that of the PI controller (in magenta) and NPID controller (in blue).

4.7. Conclusions

Simulation and experiment results reveal that the proposed NPID and DMPC controllers ensure the high performance of optimal power tracking of wind power system at both transient and steady state operating conditions. The superior performance is seen from these two controllers over simple classical PID and FLC controllers. The DMPC with capability of handling constraints has been successfully applied to overall working conditions of wind power in a single controller. Experimental result for laboratory scale wind power test-rig also confirms that DMPC is well suitable for industry implementation.

The control approaches in this chapter rely on the linearization of wind power aerodynamic at an operating point representing to nonlinear system. It should be a good progress of development, if a nonlinear control scheme applies directly to wind power system. The Nonlinear Model Predictive Control (NMPC) as well as a real-time iteration scheme of NMPC is presented in the next chapter.

CHAPTER 5

NONLINEAR MODEL PREDICTIVE CONTROL AND REAL-TIME ALGORITHM FOR WIND POWER SYSTEM

This chapter presents the Nonlinear Model Predictive Control (NMPC) designed directly from the highly nonlinear modeling of wind power aerodynamics. All the properties of the DMPC presented in Chapter 4, such as multi-objectives optimization and covering all working conditions, are easily attainable in the nonlinear version. The nonlinear controller provides better results over the linear controller since it cancels the error due to linearization process. Moreover, feasibility of a real-time algorithm applied to a wind energy conversion system (WECS) is also investigated. To speed-up the calculation time of the NMPC algorithm, an advanced process, which employs the multiple-shooting method, partially reduced sequential quadratic programming (PRSQP), and an iteration scheme, is adapted. A practically motivated simulation program running in a real-time Linux operating system is developed to validate the effectiveness of the proposed controller.

5.1. Introduction

Wind power system is obviously high nonlinear process in different operating regimes from partial load and full load conditions. This led to the development of the nonlinear model predictive control (NMPC) in which an accurate nonlinear model of turbine drive-train is exploited for future prediction and optimization. Nonlinear model predictive control has gained strong attention among control theorists as well as practitioners from the 90s primarily for controlling slow processes in the process control [85]. The concept of NMPC is similar to the linear MPC which lies on future evolution outputs and optimization performance. All constraints on inputs and outputs are also integrated into optimization function then naturally be handled. However, NMPC uses nonlinear dynamic model and therefore nonlinear constraints which give raise extra complexity [85]. The solution of

nonlinear problem in NMPC is much more difficult to solve than the convex quadratic problem in the linear controller. Although there is not many applications of NMPC found in the industry [3,36], it is still a promising control algorithm since there are more and more common as new software tools are developed [86] . In wind turbine control, the similar work of NMPC using neuron-network optimization is found in [87] which provides excellent results over traditional controllers of PI and LQG.

Nowadays, due to the recent development of computational methods, the NMPC algorithm is becoming increasingly accepted in other applications that require faster processing time. NMPC is used to track a desired line for a fixed-wing unmanned aerial vehicle (UAV) in [88], a real-world diesel engine controlled by NMPC employed an extension of the online active set strategy in [89], and a high performance tracking for the rotor speed trajectory while maintaining the d-axis component of the armature current at zero of permanent magnet motor is used in [90].

The nonlinear predictive controller relies on computational methods to find control inputs by minimizing the cost function. The feasibility of a real-time algorithm of predictive controller thus depends on the computing time of the used computational method. In the literature, much effort has been made to reduce the processing time of SQP, which is widely used as a primary computational method in NMPC. The most time-consuming part of SQP is the process of updating the Hessian matrix. Reference [91] presented a fully RSQP method to update the Hessian into the next iteration without a re-computed matrix. However, the drawback of fully RSQP that is only applicable to some special structure of system. Two interior-point path-following algorithms that solve the convex optimization problem that arises in a recentred barrier function are found in [92].

In this chapter, NMPC controller which uses standard SQP programming in discrete time domain is firstly designed for wind power system to show the MPPT capability. Further improvement in reducing calculation time of NMPC algorithm which employs the direct multiple-shooting method and the PRSQP framework

proposed in [93] in parallel with the real-time iteration scheme presented in [94] are applied to wind power control. The simulation results in the MATLAB environment of the proposed controller validate the effectiveness in power optimization by tracking the optimal regime closely. Then a practically motivated simulation of NMPC for a wind power system was implemented using the ACADO toolkit [95] in C++. The software program is compiled into an executable program which is able to run in real-time simulation on a Linux workstation computer. Some NMPC configurations for a drive-train loop only, for current loops of PSMG, and whole structures of WECS are investigated to find appropriate conditions for practical implementation of proposed controller in wind power system.

5.2. Controller Design

In a similar way, the cost function for the NMPC controller can be defined as having the same weighting factor as from DMPC which is shown in Chapter 4. The reference tracking trajectory is one step ahead of the predicted optimal shaft speed. However, because of the complexity of high order nonlinear function, the output prediction is limited to a short prediction ($N_2 = 2, N_{u2} = 1$).

$$Q_2 = \sum_{i=1}^{N_2} [\omega_g(k+i\,|\,k) - \omega_g^*(k+i\,|\,k)]^2 + \alpha \sum_{i=1}^{N_{u2}} [T_e(k+i\,|\,k) - T_e(k+i-1\,|\,k)]^2 \tag{5.1}$$

The nonlinear predictive control problem for wind turbine study case is formulated as nonlinear problem which includes cost function subject to nonlinear modelling (re-written in discrete time domain) and all constraints.

$$\text{Min} \quad Q_2 = \sum_{i=1}^{N_2} [\omega_g(k+i\,|\,k) - \omega_g^*(k+i\,|\,k)]^2 + \alpha \sum_{i=1}^{N_{u2}} [T_e(k+i\,|\,k) - T_e(k+i-1\,|\,k)]^2 \tag{5.2.a}$$

$$\text{subject to} \qquad \omega_r(k+1) = \frac{1}{J_t}[T_a(k) - B_t\omega_r(k) - T_e(k)] \tag{5.2.b}$$

$$\omega_g(k) \quad = \quad \eta\omega_r(k) \tag{5.2.c}$$

$$\omega_g^{\min} \quad \le \quad \omega_g(k) \quad \le \quad \omega_g^{\max} \tag{5.2.d}$$

$$T_e^{\min} \quad \le \quad T_e(k) \quad \le \quad T_e^{\max} \tag{5.2.e}$$

Sampling time of NMPC controller is set much smaller than that of the wind speed which is known to be few seconds to minutes. This has meaning that the optimal control of wind power is achieved for every irregular change in wind velocity since the controllers are tuned to get convergence to references in few sampling-times.

5.3. Simulation results

Simulation is done in the MATLAB environment with toolboxes provided for small wind turbine case-study which is introduced in [82] then later described in [19] with specification in the Appendix 3.

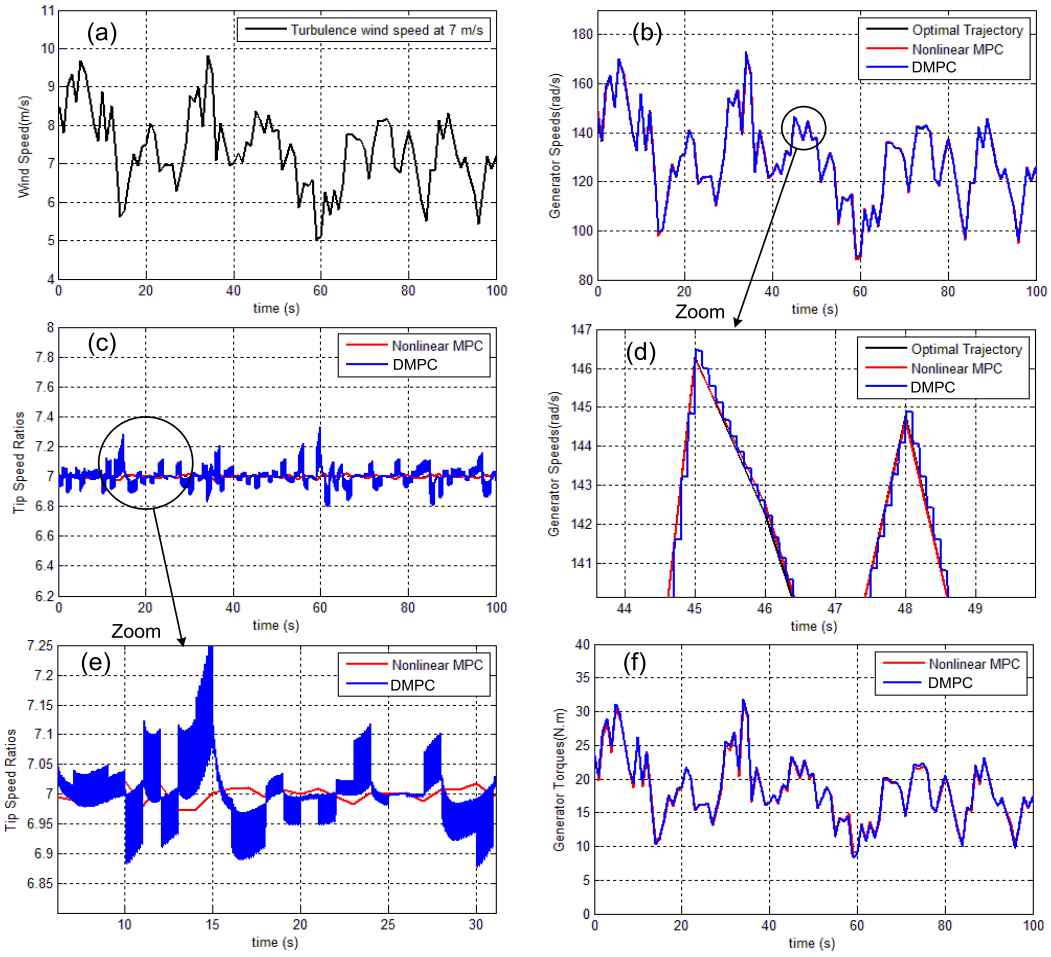

Figure 5.1. Simulation results at normal wind condition

5.3.1 Maximum power captured under rated wind speed.

When the wind speed is not too high, the essential goal of wind turbine control is maximum power capture, regulating generator speed to track the optimal trajectory

in (2.54) by an appropriate control input e.g., generator torque. In the proposed short prediction horizon controller, wind speed is assumed to be constant within a very short time frame. This assumption is reasonable since the changes of wind profiles occur in the interval time of seconds to minutes which is much higher than controller sampling time, which are few milliseconds in the NMPC.

Figure 5.1 shows the simulation results of NMPC controller for wind turbine working at normal condition. The actual generator speed corresponds closely with the optimal trajectory (Figure 5.1(b)) under a turbulence range of wind speeds from 5.5 to 9.8 (ms^{-1} in Figure 5.1(a)). Figure 5.1(c) show the tip-speed-ratio which is maintained at optimal value of 7. The computed generator torque control input applied to the wind turbine plant is shown in Figure 5.1(f). As expected, all controllers are robust at high turbulence wind velocities. Overall, the best results are obtained from NMPC than the DMPC controller.

5.3.2 Active stall control with generator speed and torque constraints

As the wind speed increases beyond design-defined rated values, the maximum power strategy allows the generator speed to rise proportionately until reaching maximum levels for each individual wind turbine i.e., 183.75 (rad/s) which can be seen from Figure 5.2(b) and its zoomed-out Figure 5.2(d) at the 54^{th} to 56^{th} second. In this case, the inequality constraints in (5.2(d)) reaches the limits, with the active set method for the SQP problem (5.2) then implemented. Predictive controllers set generator speed to its maximum value, while maintaining the minimization function (5.2(a)) by increasing generator torque to higher than normal condition of working levels - which is calculated from the below rated wind speed region. Generator speed is now lower than the optimal value and the wind turbine is pushed in to the stall working region (region III from Figure 2.14), with power coefficient and lower tip speed ratio (at 6.5 as in the Figure 5.2(e) from the 54^{th} to 56^{th} second).

If the wind velocity keeps increasing from the level at which generator speed achieves the rated value, the electromagnetic torque also goes higher. The increase in generator torque will stop when it reaches the maximum limit i.e., 39 (N.m) in our case-study which is shown in Figure 5.2(c) at the time from 56^{th} to 58^{th} second.

Wind turbine is now working at the power-limited region and being shut-down for safety purposes (region IV from Figure 2.14). Whenever the wind velocity falls down to below rated level, from the time of 59th second onward, the wind turbine moves back to the optimal regime tracking condition (region II from Figure 2.14).

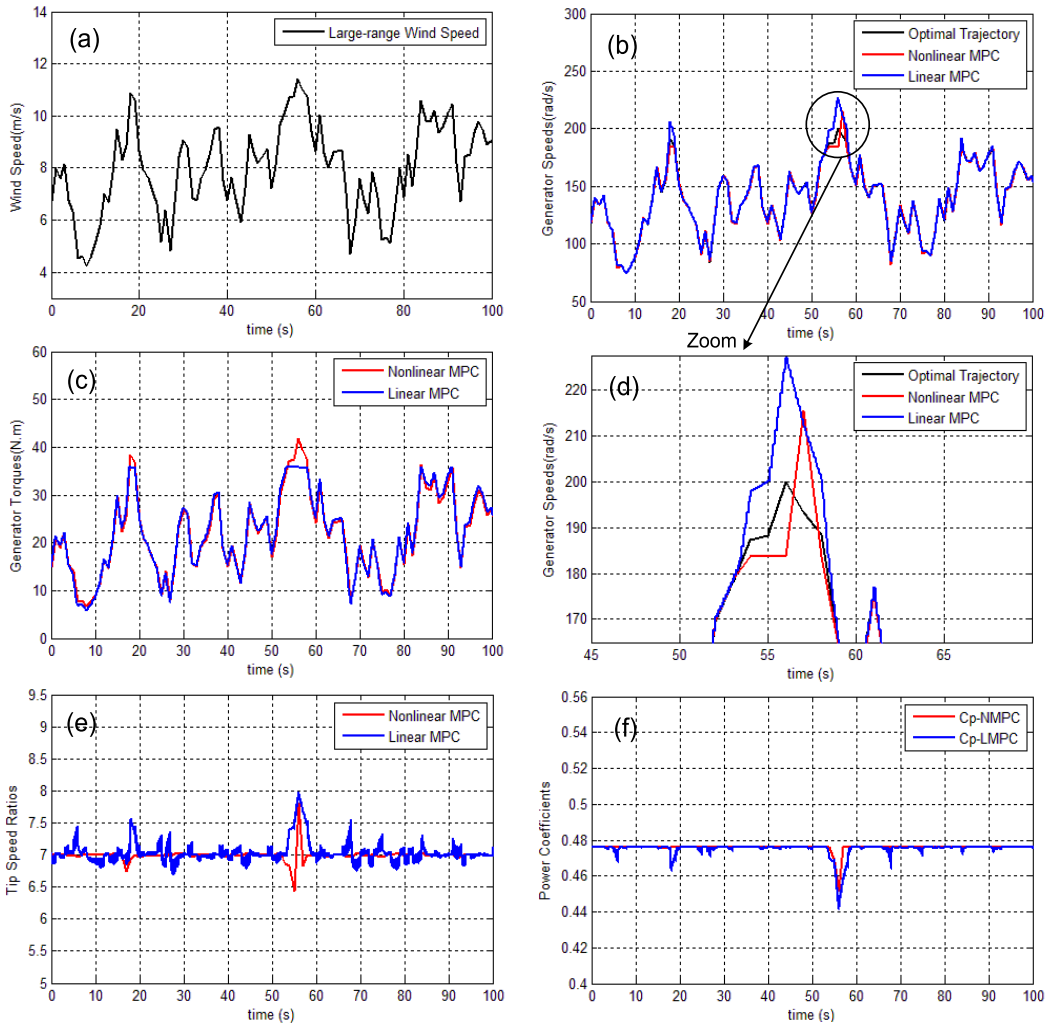

Figure 5.2. Simulation results at speed limitation condition

Now it can be seen that for our proposed controller, which is designed for whole working regions of the wind turbine considering the high wind speed region as an upper bound, a fall in wind speed acts as the lower bound of one continuous working region by exploiting the constraints that are well-handled by the predictive controllers. As a result, there is switching between those regions, obtaining smoothing for all operating regimes under a wide range of wind velocities from 4.2-11.2 ms^{-1} (in the Figure 5.2(a)).

5.4. Real-Time Algorithm of NMPC

NMPC was originally developed for process control where slow updating of the system's parameters is required [85, 96-98]. The feasibility of real-time NMPC is highly dependent on the time-consuming optimization solutions of the nonlinear problem. However, by introduction of a real-time iteration scheme and direct multiple-shooting method, NMPC is now promising to be an advanced control algorithm for other areas of application, such as automotive engineering and robotic control, where system dynamics are much faster, requiring a real-time input trajectory to be updated. In general, NMPC solves the control problem of the form

$$Min \quad Q_{npc} = \int_0^{T_p} L(x(t), u(t), v(t))dt \tag{5.3}$$

subject to an Ordinary Differential Equation (ODE) function and all the terminal as well as contour constraints. T_p is a so-called prediction horizon which may change for a moving horizon optimization problem.

$$\begin{aligned} dx(t)/dt &= f(x(t), u(t), v(t)) \\ x(0) &= x_0 \\ u(0) &= u_0 \\ 0 &= g(x(t), u(t), v(t)) \\ 0 &\le h(x(t), u(t), v(t)) \end{aligned} \tag{5.4}$$

where $x(t)$ is the state variable, $u(t)$ is the control input, and $v(t)$ is the system variable.

5.4.1. Direct multiple-shooting method

The multiple-shooting method is the direct method for solving optimal control optimization problems that combine the advantages of the single shooting and the collocation method [93]. The combination of the two preceding direct methods is used to make piecewise control inputs and states. The parameterization of the above finite optimization problems (5.3-5.4) is carried out in two steps [80, 86, 93, 99]. Firstly, control input is discretized into N subintervals during control horizons $[0, T_p]$

$$0=\tau_0<\tau_0<\tau_1<...<\tau_N=1 \tag{5.5}$$

The subinterval time periods may be equal or unequal in length, but for simplicity we suppose that every interval has the same length. Then, the control horizon $[0,T_p]$ is rescaled into small subintervals $[t_i,t_{i+1}]$ by defining $t_i=\tau_i*T_p$ for $i=0,1,...,N$. For each step, control inputs are discretized constant piecewise values $u(t_i)=u_i$ = constant in $[t_i,t_{i+1}]$ In the second step, the ODE solutions are discretized by using multiple shooting with the same interval time of the control input, by introducing the artificial variable s_i in each time interval $[t_i,t_{i+1}]$

$$\begin{aligned}\dot{x}_i(t)&=f(x_i(t),u_i,v_i(t))\\ x_i(t_i)&=s_i\end{aligned} \tag{5.6}$$

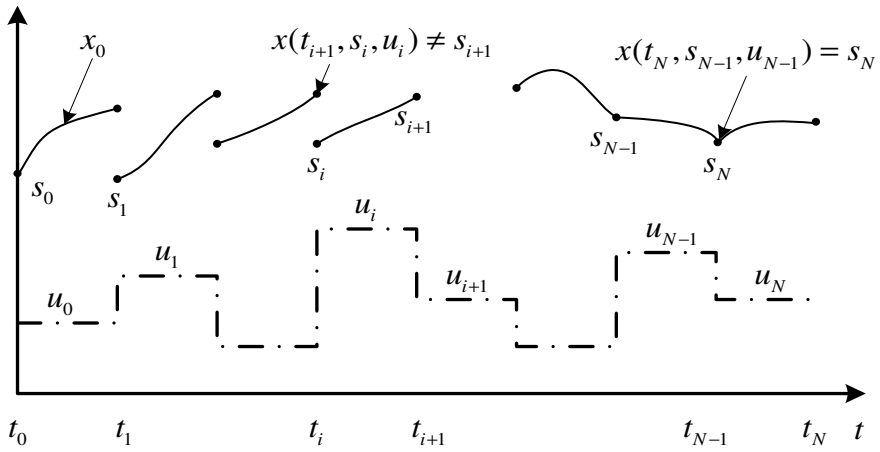

Figure 5.3. Multiple-shooting method

Using a numerical differential equation solver, i.e the ode45 function in the Matlab mathematical toolbox, the trajectory piece of states $x_i(t\ ,s_i,u_i)$ is obtained; and then the integral term in the objective function is also numerically computed in each sub-control horizon $[t_i,t_{i+1}]$

$$l_i(s_i,u_i,v_i)=\int_{t_i}^{t_{i+1}}L(x_i(t_i,s_i,u_i),u_i,v_i)dt \tag{5.7}$$

To find the physical meaning of state signals, the continuous condition must be satisfied

$$s_{i+1} = x_i(t_{i+1}; s_i, u_i) \tag{5.8}$$

Finally, the parameterization of the whole optimal control problem is as following. A more obvious illustration of the multiple shooting methods is shown in Figure 5.3.

$$\text{Min} \quad \sum_{i=0}^{N-1} l_i(s_i, u_i, v_i) \tag{5.9}$$

$$\text{subject to} \quad \begin{aligned} & s_0 - x_0 = 0 \\ & s_{i+1} - x_i(t_{i+1}; s_i, u_i) = 0 \\ & g(s_i, u_i) = 0 \\ & h(s_i, u_i) \geq 0 \end{aligned} \tag{5.10}$$

Between two continuous sample times, the control input is a piecewise constant vector function. The piecewise time instant here is different from the controller sampling time. However, for simplicity, the time length between two states is set equally to the sampling time of controller.

5.4.2. Partial Reduced Sequential Quadratic Programming (PRSQP)

After parameterization of the control and state variables by multiple-shooting method, the nonlinear problem (NLP) in (5.3-5.4) has a piecewise representation in every sampling time in (5.9-5.10). The NLP problems (5.9-5.10) is rearranged in the other forms as

$$\text{Min } F(w) \text{ subject to } \begin{cases} g_1(w) = 0 \\ g_2(w) = 0 \\ h(w) \geq 0 \end{cases} \tag{5.11}$$

where w is a matrix containing all input and state variables

$$w = (s_1, s_2, ..., s_N, u_1, u_2, ..., u_{N-1})$$

$F(w)$ is the objective function, $g_{1,2}(w)$ are the vector valued functions containing all equality constraints, and $h(w)$ is the vector valued function containing all inequality constraints from NLP in (5.9-5.10). This NLP has a special structure which can be solved by KKT, and then PRSQP is applied [80, 86, 93].

To gain a good explanation of the PRSQP method, we start with the full-space RSQP with iterations [100]:

$$w_{k+1} = w_k + \sigma_k \cdot \Delta w_k \tag{5.12}$$

where the increment term Δw_k is the solution of the quadratic program:

$$\min_{\Delta w_k \in \Omega} \nabla F(w_k)\Delta w_k + \frac{1}{2}\Delta w_k^T H_k \Delta w_k \tag{5.13}$$

$$\text{subject to:} \quad \begin{aligned} & g_1(w_k) + \nabla g_1^T(w_k)\Delta w_k = 0 \\ & g_2(w_k) + \nabla g_2^T(w_k)\Delta w_k = 0 \\ & h(w_k) + \nabla h^T(w_k)\Delta w_k \geq 0 \end{aligned} \tag{5.14}$$

With H_k as an approximation to the Hessian of the Lagrange $L(w,\lambda,\mu)$ of (5.15)

$$L(w,\lambda,\mu) = F(w) - \lambda_1^T g_1(w) - \lambda_2^T g_2(w) - \mu^T h(w) \tag{5.15}$$

where λ (short for λ_1 ; λ_2) and μ are the Lagrange multipliers of the constraints $g_{1,2}(w)$ and $h(w)$. The step size $\sigma_k \in (0,1)$ is used as a parameter of the line search method [78].

To obtain the PRSQP method, a kernel basis of linearized equality constraints $g_1(w)$ is defined in [93]. The variable w_1 of the linearization equality constraints $g_1(w)$ has the Jacobean of $\nabla w_1 g_1$, which is regular over the whole variable domain. This linear equality partitions the variables into $w = (w_1^T, w_2^T)^T$. The definition of a coordinate basis which allows exploitation of sparse structures in $\nabla w_1 g_1$ is as follows [93].

$$\Delta w = (\Delta w_{1,k}^T, \Delta w_{2,k}^T)^T = S_{1,k}^R y_k^R + S_{1,k}^N y_k^N \tag{5.16}$$

With the range-space basis $S_{1,k}^{RT} = [\nabla w_1 g_{1,k}^{-1} : 0]$, the null-space basis $S_{1,k}^{NT} = [-\nabla w_2 g_{1,k} \nabla w_1 g_{1,k}^{-1} : I]$. The range-space component $y_k^R = -g_{1,k}$, and the null-space component $y_k^N = \Delta w_{2,k}$ as the solutions of the reduced quadratic program.

$$\min_{y_k^N \in \Omega_k^N} \nabla F_k^T S_{1,k}^N y_k^N + C_k y_k^N + \frac{1}{2} y_k^{NT} S_{1,k}^{NT} H_k S_{1,k}^N y_k^N \tag{5.17}$$

subject to:

$$\begin{aligned} & G_{2,k} + \nabla g_{2,k}^T S_{1,k}^R y_k^R + \nabla g_{2,k}^T S_{1,k}^N y_k^N = 0 \\ & H_k + \nabla h_k^T S_{1,k}^R y_k^R + \nabla h_k^T S_{1,k}^N y_k^N \geq 0 \end{aligned} \tag{5.18}$$

The second term of the quadratic objective function $C_k y_k^N = y_k^{RT} S_{1,k}^{RT} H_{1,k} S_{1,k}^N y_k^N$ is a cross-term involving both the range-space and null-space bases. Then the iterations continue as function (5.12) until an optimum solution similar to full RSQP is obtained.

5.4.3. Real-time iteration scheme

The final process of the real-time algorithm for NMPC is the real-time iteration scheme [80]. In the industrial processes, there are always delay calculation time due to the finite capacity of computers and existence of disturbances. The exact solution calculated from this time may not be the true solution in the next time step. From this observation, an approximation of the control input could be applied rather than trying to find the true solution, which is a time-consuming process. The control feedback approximation is obtained based on a very carefully designed transition between subsequent problems in two consecutive time intervals $[t_k, t_{k+1}]$ [94]. Starting with guessing the initial s_k, NMPC algorithms will compute solutions for ODE to obtain a local small trajectory s_{k+1} piecewise by the ODE solver. Then the optimization solution is implemented by the PRSQP to find the approximated control feedback to the plant after one or two iterations. The real-time iteration scheme is finally applied to reduce calculating time of the PRSQP method. For a simple explanation, it is suggested that the convergence solution of PRSQP is obtained in exactly one time interval. So, after setting up index k to zero, a real-time iteration divides each time interval $\delta = [t_k, t_{k+1}]$ of a PRSQP into two stages, called preparation and feedback. Figure 5.4 illustrates the idea of the scheme.

- Preparation: based on initial guesses (w_k, λ_k, μ_k), compute partially some components of the vector $\nabla_k^2 L(w_k, \lambda_k, \mu_k)$ and the matrix approximation H_k,

noting that H_k is independent of the value w_k and only the first component of the vector $\nabla_k^2 L(w_k, \lambda_k, \mu_k)$ depends on w_k. This component will be necessary in the second step. Thus, we can compute the linear algebra $(H_k)^{-1}\nabla_k^2 L(w_k, \lambda_k, \mu_k)$ as soon as possible without knowing of value w_k

- Feedback response: At the time when w_k is known, finish the computation of the step vector $\Delta w_k = -(H_k)^{-1}\nabla_k^2 L(w_k, \lambda_k, \mu_k)$ to give the control $u_k := u_k + \Delta u_k$ to the system immediately
- Transition: If $k = N-1$ stop, otherwise compute the initial guess w_{k+1}, setting $k = k+1$, and then go to the preparation stage.

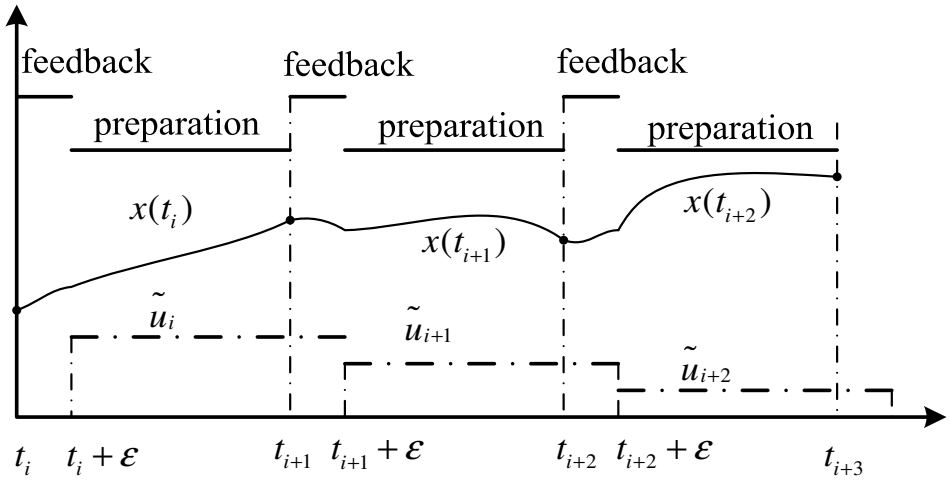

Figure 5.4. Real-time iteration scheme

5.4.4. NMPC formulation for WECS

The modelling details of the wind power system are written in the form of ODE

$$\begin{bmatrix} d\omega_r(t)/dt \\ di_d(t)/dt \\ di_q(t)/dt \end{bmatrix} = \begin{bmatrix} \frac{1}{J_t}(T_a(t) - K_t\omega_r(t) - T_{em}(t)) \\ \frac{1}{L_s}(-R_s i_d(t) - L_s\omega_s(t) i_q(t) + E_d - u_d(t)) \\ \frac{1}{L_s}(-R_s i_q(t) + L_s\omega_s(t) i_d(t) + E_q - u_q(t)) \end{bmatrix} \tag{5.19}$$

$$T_{em} = \eta K_e i_q$$

Due to mechanical and electrical limitations of wind turbines, the constraints of these variables can be initialized

$$\begin{aligned} &0 \le \omega_r \le \omega_{\max} \\ &i_{\min} \le i_d, i_q \le i_{\max} \\ &u_{\min} \le u_d, u_q \le u_{\max} \end{aligned} \tag{5.20}$$

The control goal for the wind power system is discussed in Section 2.2. The power harvested by the wind turbine is maximized when the rotor speed tracks the optimal regimes in (2.54). The least squares function of the tracking reference is then formulated as following

$$\text{Min} \quad Q_{wecs} = \int_0^{T_p} (y(t) - y^*(t))^T Q (y(t) - y^*(t)) dt \tag{5.21}$$

where $x(t) = [\omega_r(t) \quad i_d(t) \quad i_q(t)]'$ are state variables. The control variables are direct and quadrant voltages $u(t) = [u_d(t) \quad u_q(t)]'$ while the outputs are $y(t) = [\omega_r(t) \quad i_d(t) \quad T_e(t)]'$. To minimize the computing time of the optimization problem, a short prediction horizon is exploited. The prediction horizon T_p is set equal to one controller sampling time. This means that NMPC has one step prediction, and the multiple-shooting method has one piecewise time interval; the reference $y^*(t) = [\omega^*_r(t) \quad 0 \quad 0]'$ is obtained from (2.54). Q is a 3 × 3 diagonal matrix determining the weighting factor between output variables. The third element Q(3,3) is chosen much smaller than the two values Q(1,1) and Q(2,2) to ensure a tight tracking of the rotor speed and direct current.

5.5. Feasibility of Experimental Implementation of NMPC

A practically oriented simulation program is created to evaluate the real-time algorithm NMPC for a wind power system. The program is created using the ACADO toolkit [95] in C++ and then compiled to an executable program which can be run in real-time mode on a Linux workstation computer. The wind power plant is

also simulated by using the simulation environment feature of the toolkit. The total simulation time is set to 8 seconds; the total running time from an HP workstation which has an Intel quad-core of 2.66 GHz and 4.00 Gigabytes of RAM was recorded. The controller sampling time is set equal to the piecewise time of multiple-shooting methods. Different sampling times are used in simulation for study and various NMPC schemes are also investigated for the drive train loop, PSMG current loops, and whole WECS including both drive train and currents loops. The sampling time for which total running time equal to simulation setting time and good tracking quality is confirmed to be appropriate time interval.

Firstly, the NMPC algorithm is applied for the only drive train which is modelled in (2.36). Electro-magnetic torque is considered as a control input to regulate rotor speed tracking the optimal reference in the presence of aerodynamic torque fluctuation. The formulated criterion function has the main objective of a tracking feature. The prediction horizon is also set to one controller sampling time. The SQP algorithm has two iterations and different sampling times are tested with the results shown in Table 4. With a sampling time of 0.015 seconds, the actual running time of the machine is 8.556 seconds, which is close to a total simulation time, providing excellent results of tracking. It is concluded that the NMPC algorithm for the drive train loop of the wind power system is effective at a sampling time of 0.015 seconds based on a current computer specification.

Table 4. NMPC running time for drive train loop

Sampling time	Running time	Tracking quality
0.010 s	24.463 s	Excellent
0.015 s	***8.556 s***	***Excellent***
0.020 s	4.312 s	Excellent
0.021 s	3.869 s	Excellent
0.022 s	3.501 s	Good
0.023 s	3.199 s	Good
0.024 s	2.939 s	Good

Table 5. NMPC running time for PSMG current loop

Sampling time	Running time	Tracking quality
0.001	45.317 s	Excellent
0.002	***7.126 s***	***Excellent***
0.003	2.716 s	Excellent
0.004	1.443 s	Excellent
0.005	0.924 s	Excellent

Table 6. NMPC running time for whole WECS (drive train and d-q currents)

Sampling time	Running time	Tracking quality
0.010	31.203 s	Excellent
0.015	13.426 s	Excellent
0.020	***8.455 s***	***Excellent***
0.021	***7.904 s***	***Good***
0.023	***7.005 s***	***Good***
0.025	***6.263 s***	***Good***
0.030	4.928 s	Good
0.035	4.156 s	Fair
0.040	3.693 s	Fair

Secondly, NMPC with all the same setting parameters is designed for only two PSMG current loops which are modelled in (2.45-2.46). The results are provided in Table 5. With a less complex non-linearity structure in comparison with a drive train loop, the NMPC algorithm for the current loops is able to run at 0.002 seconds, which gives a total machine running time of 7.126 seconds. Finally, the NMPC controller for the whole structure of a wind power system including the drive train and PSMG current loops was designed as in Section 4.1. A summary of machine running times is in Table 6. The feasible sampling time of NMPC for WECS

including drive-train and d-q current loops is in the range 0.020 seconds to 0.025 seconds, at which tracking quality is guaranteed.

In this section, a number of wind turbine configurations for the NMPC controller were investigated to find the suitability of applying NMPC to real-time implementations for wind power systems. From our experimental observations in the laboratory, it is concluded that 0.002 seconds of interval time is not suitable for current loops control where much faster control input updating is required. With ability to run at sampling time of 0.020 seconds to 0.025 seconds, NMPC is still progressing towards finding a position in wind energy control. However, the drive train loop of the wind power system always has a slower dynamic than the electrical subsystem. Wind aerodynamic power is only effective when wind profiles are below the frequency of 10 Hz with a time interval of 0.1 seconds. Ability to run at a sampling time of 0.015 seconds, NMPC is suitable for practical implementation for a wind power drive train control loop. This is promising because the aerodynamics of a wind turbine is known to be highly nonlinear and therefore the traditional controller faces a lot of difficulties. This nonlinear property and the constraints of the drive train loop, where a fast dynamic response is not required, are handled well by NMPC. Meanwhile, the PSMG current loops are easily handled by two traditional PI controllers. The cascade structure of NMPC for speed loop plus two PID controllers for generator current loops is highly recommended for a WECS system.

5.6. Conclusions

In this chapter, NMPC controller is proposed for WECS to overcome the nonlinearity and time varying parameters properties. NMPC appears to be a very strong candidate for aerodynamic drive-train control of wind turbines. A very closely tracking of the non-stationary optimal reference was seen during simulation. Maximization of power captured from the available wind power was then achieved. However, NMPC is an advanced controller which relies on the calculation ability of the nonlinear programming method such as SQP and its variant versions RSQP and PRSQP. These computational methods are known to be computing-resource greedy so that NMPC was initially suitable for slow processes in process control.

A practically oriented simulation was done to investigate the feasibility of applying NMPC in real-time control. A real-time algorithm of NMPC was studied with the latest research findings from literature. A multiple-shooting method to discretize the control problem to piecewise nonlinear problem, partially-reduced sequential quadratic programming, and a real-time iteration scheme were applied. NMPC is a good option in wind energy control for a drive train loop in the cascade structure with two traditional PID controllers for the electrical current loops of PSMG.

Chapter 3, 4 and 5 are mainly for aerodynamic drive-train loop and electrical d-q current control loop in the generator. Following by a natural development, the next chapter studies the grid connection of wind turbine system though converter in a wind farm. Controller design must fulfil grid code requirements to assure power quality and stability of large scale wind power system.

CHAPTER 6

CONTROL STRATEGIES OF PMSG WIND FARM

This chapter deals with the strategy and control of wind turbine inter-connected to wind farm using HVDC network transmission. With small capacity, wind turbine is considered as a passive distributed generation which means that the technical requirements to connect generation source are determined by the public electricity system. In contrast, large capacity wind power system at farm level should have active capability to assist the grid system by supplying the ancillary services such as reactive power control and fault ride-through. Robust linear model predictive control, with outstanding properties presented in Chapter 3, 4, is also applied in this chapter for the grid integration controller of wind farm. The performance of control method is assessed by the mean of simulations in MATLAB/SIMULINK and SimPowerSys toolbox.

6.1. Introduction

The rapid increase in wind power contribution to electrical energy production has been evident over the last few decades in many countries. In some European countries, wind power contributes to about 30% of total energy production, and is expected to produce about 50% of generated power. An increased number of medium and large wind farms connected to national transmission systems, especially offshore plants, are being built. Wind power plants now play a more significant role as an active generation source in electrical networks. In other words, wind farms must have the capability to support the electric grid when required. A study of the effect of wind farms on the stability of a weak grid was seen in [101]. The major requirements for a wind farm connected to the grid are active and reactive power control, fault ride-though support for a weak grid [102]. To achieve these grid code requirements, a smart controller needs to be developed to replace the existing software in the traditional wind farms. In literature, there are not many control techniques found for wind farms. Most of the current work focuses on the

traditional PID controller [103-105], while the other nonlinear control approach based on the Lyapunov theory was found in [47]. It is seen that PID controller still keeps a dominated position in wind farm control application.

In this chapter, the most significant control algorithm from control engineering over the last few decades, linear disturbance models of predictive control (DMPC) are proposed for a cluster of few permanent synchronous magnet generators (PMSG) in a wind farm whose individual turbines are interconnected though a 25 kV local AC voltage transmission network. The DMPC algorithm theory and application for maximum power extraction from wind power has been studied in Chapter 3, 4. It is also applied in this chapter to cancel the difficulty in derivation of wind farm models. It is obviously got conclusion that obtaining exact models of farm level wind power system is not possible. There always exist unknown disturbances as well as interconnected effects over transmission system. A large wind farm modelling complexity and fluctuating nature of wind power impose serious challenges to controller design. A smart controller improving high performance which insures stability and reliability for wind farm is a high demand for control specialist.

6.2. System Configuration and Control Strategies of Wind Farm

6.2.1. Wind Farm with HVDC Transmission System

The typical single wind turbine structure is studied in Figure 2.6, Chapter 2. The wind turbine driven permanent magnet synchronous generator is connected to the generator-side full-bridge converter. Wind farm topology which includes 120 units of single PMSG wind turbine is illustrated in Figure 6.1. Three individual wind turbines are selected to form a cluster which has total rated power at 6 MW to fulfil power rating of a common 8 MVA Voltage Source Converter (VSC) interconnected through a local 1.6 kV DC voltage bus. Simple cluster configuration has been selected to demonstrate new type of controller in different working conditions rather than the complexity of wind farm which increases simulation time. The transformer boots up voltage to a 25 kV local AC transmission which connects different clusters in a wind farm. Similar topology of large scale offshore HVDC

wind farms is found in literature [46, 106-111]. Wind farm is connected to the nationwide grid system via HVDC/VSC system which is presented in the following section.

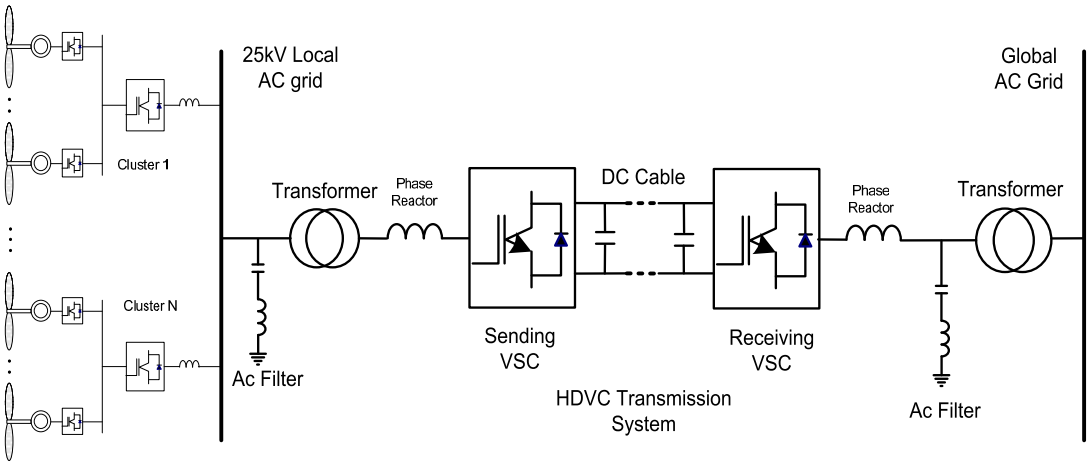

Figure 6.1. Single line diagram of PMSG wind farm using HVDC transmission system

HVDC/VSC Transmission Offshore Wind Farm

A wind farm is generally located far away from global AC grid point of common coupling (PCC). HVDC transmission is therefore more suitable solution for a long distance wind farm and for supporting weak grid [106]. The advantages which are obviously identified of HVDC transmission system over AC connection technology include [46]:

- Power flow is fully defined and control
- Cable charging currents do not affect to transmission distance
- Fewer cables required and lower cable power loss
- It can independently control the active, reactive power as well as voltage and frequency.

The HVDC/VSC transmission system was proposed in [109, 111]. This type of concept developed by ABB is the HVDC Light based on a 6-pulse bipolar VSC with ratings up to 330 MW/±150kV DC. The sending VSC collects energy from wind farm which sums up to 40 clusters of 8 MW VSC through local AC grid and then transmits to the receiving VSC via two XLPE cables.

6.2.2 Control Strategies of a Large Scale Wind Farm

Wind power systems have primarily requirements associated with safety and reliability during operation. These particular problems are fulfilled by protective devices installed in the system. Moreover, large scales wind farm also impose some technical requirements to improve efficiency and economic concern in wind power generation. These strategies were presented extensively in [106, 111, 112] and they are adopted in this study. The common attentions include the following:

- Power control
- Voltage and frequency control
- Dc link voltage control at both wind turbines and transmission system
- Reactive power support to the grid
- Fault ride-through capability

The proposed control strategy divides wind farm control system in to hierarchy levels in which each requirement is defined as in Figure 6.2.

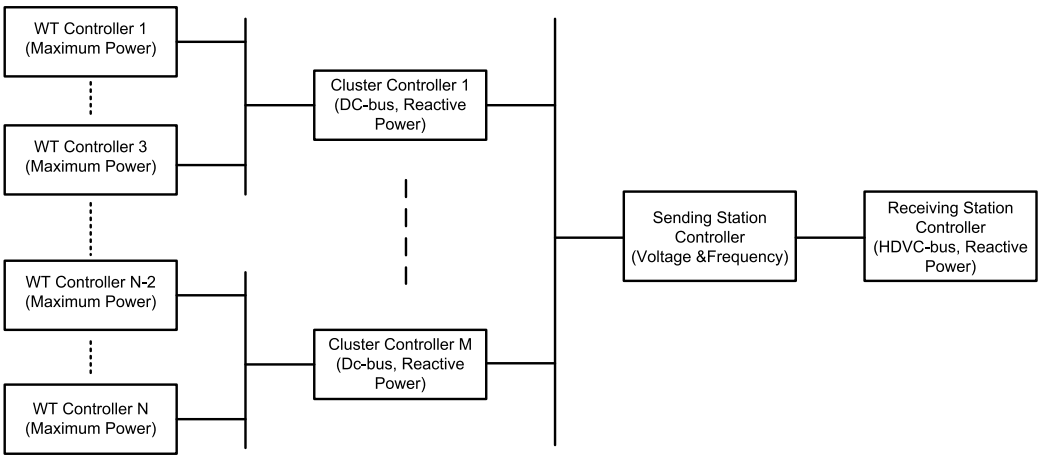

Figure 6.2. Control structure of wind farm and turbine controllers

Power Control

In the case of normal condition, wind turbine operates in maximum power tracking which is studied in Chapter 4 and 5; hence, power control is not applicable to the wind farm in normal operation scheme. This maximum power working condition is also mainly scheme in this chapter. In the other mode, the limited power generation control scheme, individual wind turbine produces a specific power generation

follows energy production scheduling. Power planning scheme is implemented at wind farm management such as supervised and data acquisition control (SCADA) level. Operator sends power command to wind farm control level which ensures the demanded power at the point of common coupling (PCC) by setting the power references in the individual wind turbines. Available power from wind turbine control level is feedback to wind farm level for management and monitoring. As a slave component control network, individual wind turbine controllers then control the requested power reference in the wind turbine connection point. Wind turbine power controllers adjust energy production by changing pitch angle mechanism and/or switch to partial load condition (presented in Section 2.4.1).

Voltage and Frequency Control

Automatic frequency control is necessarily required on the top of the other requirements of power control as stated in the Danish TSO [111]. Frequency is the variable which indicates the balancing condition between production and consumption; hence it is a key aspect in wind farm control [112]. In the Danish TSO, it is specified that the individual wind turbine controllers change the power output in relation with the frequency. The reference [111] proposed a droop and dead band procedure for primary frequency control at wind farm control level. An alternative option of voltage and frequency control in the HVDC/VSC transmission system is that can be fully implemented at the sending VSC from Figure 6.1. This approach provides an independently continuous voltage and frequency [46, 109, 111]. Even though the PMSG wind farm topology decouples generator and turbine from the grid. Wind turbines are not directly subjected to the grid faults. As the results, the frequency fluctuation resulting from wind speed fluctuation does not raise a problem to the power system. It is recommended that the correlation between wind speed and system frequency has to be investigated [112]. Voltage control loop in the cascade structure with current control loop using PID control provides excellent results [109, 111]; hence it is not covered in our controller design.

DC-link Voltage Control

The DC-bus voltages at both wind turbine level as well as HVDC transmission system are on demand to have an automatic controller. The wind turbine level VSC

is shown in Figure 6.1. The first half of converter has the function as a mean for generator side control which was studied in Chapter 4 and 5. To get well performance of generator side control algorithm, the dc-bus voltage of the dc-link is set to be constant value (with acceptable variation of 5% [111]) which can be controlled from the grid side converter. A constant DC-bus voltage is also required to ensure the power from generator being transported to the power grid [110, 113].

Reactive Power Control

Reactive power control is one of the most important issues in wind power plant at the steady-state operating condition. The P-Q-diagram at the PCC is essentially required to take consideration of controller design for wind power plant. The P-Q standard is varied in countries to countries in Europe. It could be a fixed P/Q relationship means constant power factor to varied reactive power for load flow adaption [113]. Reactive power capability is usually defined at the PCC point or sometimes even at the individual wind turbines as the current grid codes. In other words, the grid side VSC at wind turbine cluster and/or the receiving VSC station of the HVDC/VSC are subjected to have reactive control capability.

Fault Ride-through Capability

Since the wind farm is connected to the grid via a full scale converter, it easily accomplishes the capability of fault ride-through to support the grid during the fault [15]. For a well-performed generation of a wind farm, the grid code requirements for wind power integration include [113]: i) Wind turbines have to stay connected to the grid during voltage dips and ii) they have to initiate forced (mandatory) reactive current rejection for supporting the grid voltage. Wind power system must have the capability to remain the connection during the fault at least 300 ms [114].

6.3. Modelling of Grid Side VSC (GRVSC)

It is understood that controller design for all subsystem of wind farm should be studied. However, there are similarities in VSC configuration and d-q current control loops at turbine level and transmission. Once, a controller which is well-

performed for a VSC could be applied for the other VSCs in the wind farm system. The grid side voltage source converter (GRVSC) which connects 3 individual wind turbines to form a cluster is mainly studied in this chapter. The single line diagram of clustering wind turbine is sketched out in Figure 6.3.

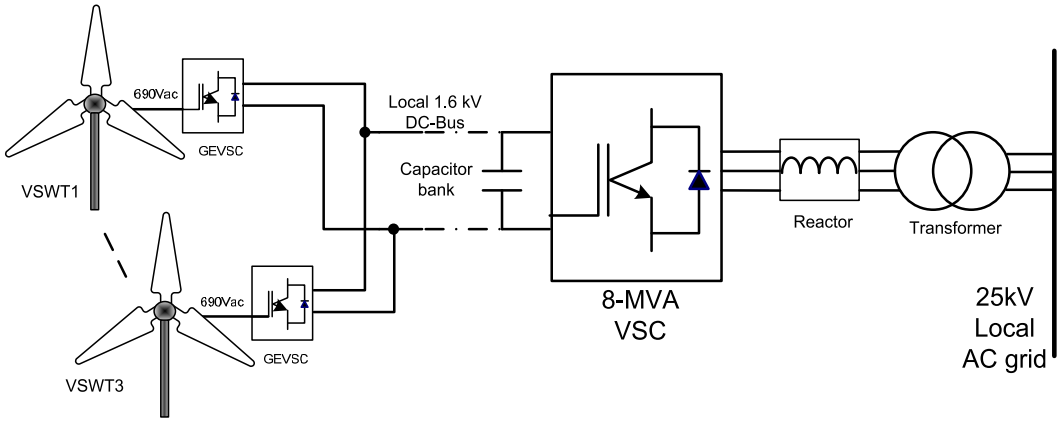

Figure 6.3. A cluster of 3 individual wind turbines

The modelling of GRVSC for controller design is described in this section which includes the grid reactance current modelling and dc-link voltage modelling. More details of models can be found from [15, 109]. Figure 6.4 shows the equivalent circuit of GRVSC. A group of wind turbine generators are connected to the local grid via AC/DC/AC system; only active power is transferred where as reactive power at the grid side can be controlled to support the grid.

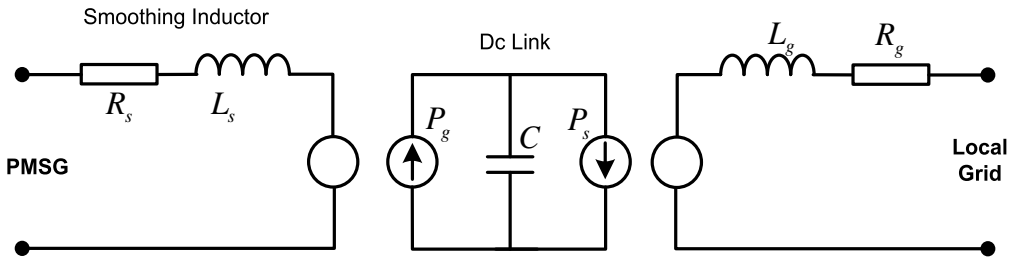

Figure 6.4. Equivalent circuit of GRVSC [15]

Grid reactance

The state equation for the grid-side converter has similarity with generator side as shown in the following [15]

$$L_g di_d^g / dt = E_d^g - R_g i_d^g - L_g \omega_{gr} i_q^g - u_d^g$$
$$L_g di_q^g / dt = E_q^g - R_g i_q^g + L_g \omega_{gr} i_d^g - u_q^g \quad (6.1)$$

If the reference frame is oriented along the supply voltage, the grid voltage vector has the equation:

$$E_d^g + jE_q^g = U_g + j0 \quad (6.2)$$

DC link Voltage

Since the equivalent wind turbine is connected to the grid though a back-to-back converter, only the active power from the generator is transferred to the grid. Assuming that the AC/DC/AC converter works well with no losses and the nonlinearity of the converter can be neglected, the power flow from the generator to the grid via the DC link is depicted in Figure 6.1. In order to inject all the power to the grid, the generator is controlled to run at unity power factor, i.e. the d-axis current is regulated to be zero [15].

The complex power including the active power and reactive power from the grid:

$$S_g = \frac{3}{2}(E_d^g + jE_q^g)(i_d^g + ji_q^g)^* = \frac{3}{2}(E_d^g i_d^g + E_q^g i_q^g) + j\frac{3}{2}(E_q^g i_d^g - E_d^g i_q^g) = P_g + jQ_g \quad (6.3)$$

Substituting (6.2) in (6.3), we have: $P_g = \frac{3}{2}U_g i_d^g \ ; \ Q_g = -\frac{3}{2}U_g i_q^g$. (6.4)

Similarly, total power from the generator side:

$$S = \frac{3}{2}(E_d^s + jE_q^s)(i_d^s + ji_q^s)^* = \frac{3}{2}(E_d^s i_d^s + E_q^s i_q^s) + j\frac{3}{2}(E_q^s i_d^s - E_d^s i_q^s) = P_s + jQ_s \quad (6.3)$$

With the note that when the d-axis current from generator is controlled to be zero $i_d^s = 0$ and generator voltage is aligned to q-axis component, we have

$$P_s = \frac{3}{2}E_q^s i_q^s \ ; \ Q_s = 0 \quad (6.4)$$

Recall the equation (2.47), and voltage from generator $E_q^s = p\omega_g \Psi$; hence, power from generator side can be expressed in the other form:

$$P_s = 3p\Psi i_q^s \omega_g / 2 \quad (6.5)$$

The active power from generator is injected into the DC link, while the power from the other side flows into the grid. With the assumption that losses in generator can be neglected, the model equation for the DC link is as follows [15]

$$U_{dc}\frac{dU_{dc}}{dt}=\frac{1}{C\_link}(P_s-P_g) \tag{6.6}$$

6.4. Disturbance Model Predictive Control Design (DMPC)

The controller structure is shown in Figure 6.5. It is better to equipped with a droop control for variable power in the control scheme [111]. However, for simplified illustration of DMPC for VSC system, the reference value of DC-link voltage and reactive power are set to a constant value. DMPC is designed to control DC-bus voltage loop while d-q current loops are equipped with conventional PI controller.

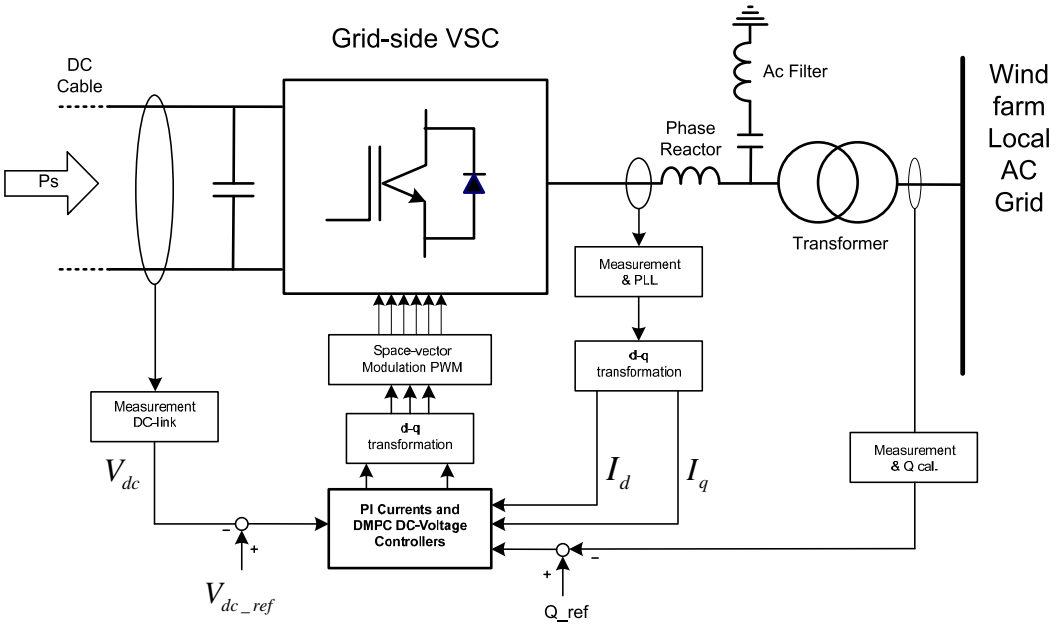

Figure 6.5. Controller structure of DMPC for VSC

DC-link Voltage Controller Design

Control design for a large scale wind farm faces difficulty when a large number of wind turbines are distributed in a large area. With the limitation of communication system, feedback signals such as ω_g, i_q^s from each wind turbines, in (6.5), are not

able to send in real-time to control centre in which centralised cluster converter locates. In other words, total active power from all individual turbines contribute to GRVSC is not available instantly. The component P_s in the control structure is not available for operation of classical PID control algorithm. To avoid this problem, the wind farm can be represented by the collective response of a large wind power system instead of a complete model with all the wind turbines modelled. An equivalent and larger wind turbine represents the group of wind turbines experiencing the average incoming wind of each single wind turbine. The wind speed flowing into a wind turbine depends on its location in the wind farm. Even though wind turbines are placed in rows facing the wind flow, wind speeds are different due to the shadow effect from the turbine blades. Use of the average wind from the different winds incident on the equivalent wind turbine is proposed [115].

$$\upsilon_{eq} = \frac{1}{n}\sum_{j=1}^{n}\upsilon_j \tag{6.7}$$

The total aerodynamic power captured of a wind farm was represented by an aggregated wind turbine.

$$P_{eq} = 0.5\rho\pi R^2 C_p(\lambda,\beta)\upsilon_{eq}^3 \tag{6.8}$$

This equivalent power can be used as a feed forward signal to the DC voltage control loop in similar way of the single wind turbine. This amount of power is not exactly equal to the active power transferred to GRVSC due to power losses from individual generators, transmission system and converters. However, this error can be compensated by using the proposed controller which has advantage properties discussed in Chapter 4.

The DC-link equation in (6.6) can be re-written approximately in (6.9) as follows

$$U_{dc}\frac{dU_{dc}}{dt} = \frac{1}{C\_link}(P_{eq} - P_g) \tag{6.9}$$

The linear predictive controller for the DC link voltage control can be designed on the linear state space model (6.10) obtained from (6.9)

$$\begin{aligned} \dot{x}_{dc} &= A_{dc}x_{dc} + B_{dc}u_{dc} \\ y_{dc} &= C_{dc}x_{dc} \end{aligned} \tag{6.10}$$

where
$$x_{dc} = U_{dc}^2; \quad u_{dc} = P_{eq} - P_g; \quad y_{dc} = U_{dc}^2$$
$$A_{dc} = 0; \quad B_{dc} = 2/C\_link; \quad C_{dc} = 1 \tag{6.11}$$

The cost function which is an essential component in the DMPC control algorithm also is formulated as follows

$$Q_{vsc} = \sum_{j=1}^{N_2} (y_{dc} - y_{dc}^*)^2 + \alpha \sum_{j=0}^{N_1} \Delta u_{dc}^2 \tag{6.12}$$

Control input calculation to be applied to plant follows the standard procedure presented in Chapter 3. Simulation results will be shown in the next section to validate the proposed control scheme.

6.5. Simulations Results

6.5.1. Wind farm under normal conditions

Simulation studies of the proposed controller for a wind farm equipped with 3 single 2MW wind turbines, which has the specifications given in Appendix 5, were performed. Simulation programs were developed in the MATLAB environment using the SimPowerSys and Model Predictive Control toolboxes. The detail structure of simulation program is presented in Appendix 6. Three different wind speeds which have seasonal speed of 5 m/s experienced by individual wind turbines are shown in Figure 6.6 with the corresponding active power shown in Figure 6.7. Each individual wind turbine block (wind turbine 1-3) consists of aerodynamic wind power sub-block which generates wind torque to drive 2MW PMSG connected to a generator-side converter. Variable speed action of individual wind turbine is controlled by DMPC controller (presented in Chapter 4) whereas wind farm level DMPC controller is performed at grid-side VSC. The common point of those wind turbines is DC-link point common coupling (PCC) of 1.6 kV DC transmission. On the other side, grid-side inverter is connected to the 25kV local AC grid transmission system of wind farm. The performance of wind farm level DMPC controller is validated in comparison with traditional PID controller which is most commonly-used control technique in existing power system in the practice.

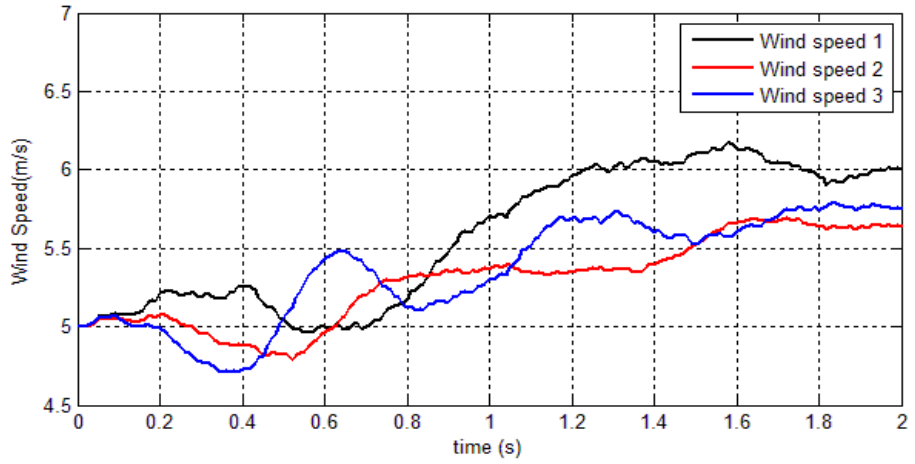

Figure 6.6. Different wind speeds experienced by wind turbine cluster

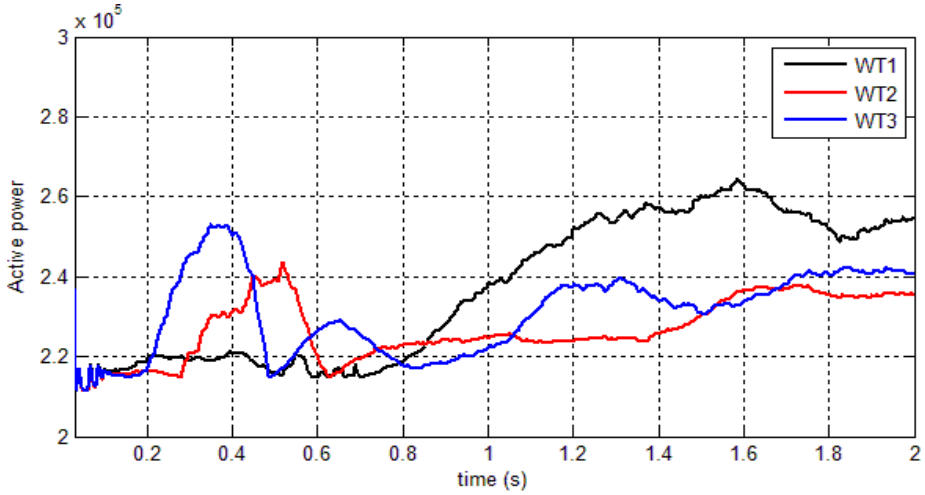

Figure 6.7. Active power injected to grid from wind turbines

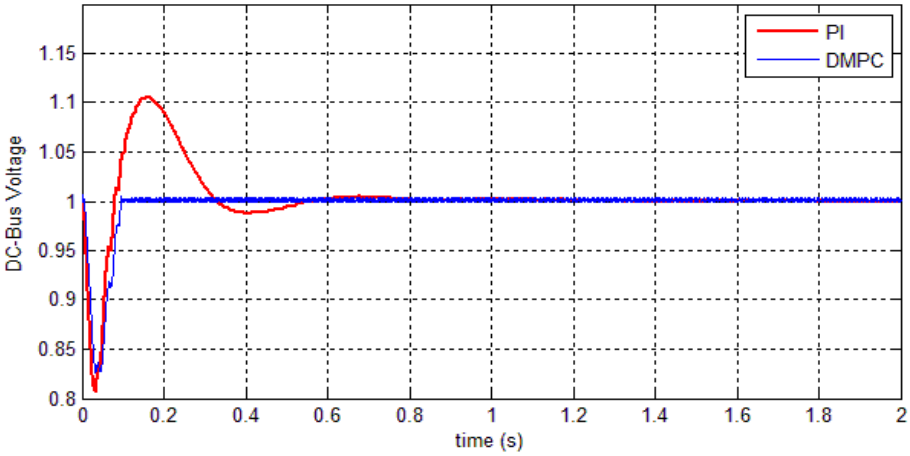

Figure 6.8. DC-bus voltage response of two controllers

The DC link voltage from the proposed controller, in blue, gradually reaches the reference with no overshoot as seen in the PID controller response (red colour) as shown in Figure 6.8. After wind turbines staring period from 0-0.1 second, DMPC delivers a faster recovering time. Both controllers demonstrate very good performance of DC link voltage control in the steady state under presence of high fluctuation in active power injected to DC-link as seen in Figure 6.7.

The reactive power from GRVSC (shown in Figure 6.9) is well maintained at -0.2 (pu) at steady state. The overshoot seen from 0-0.2 second due to three individual wind turbines starting process is acceptable. The objective of grid voltage-supported control strategy is satisfied.

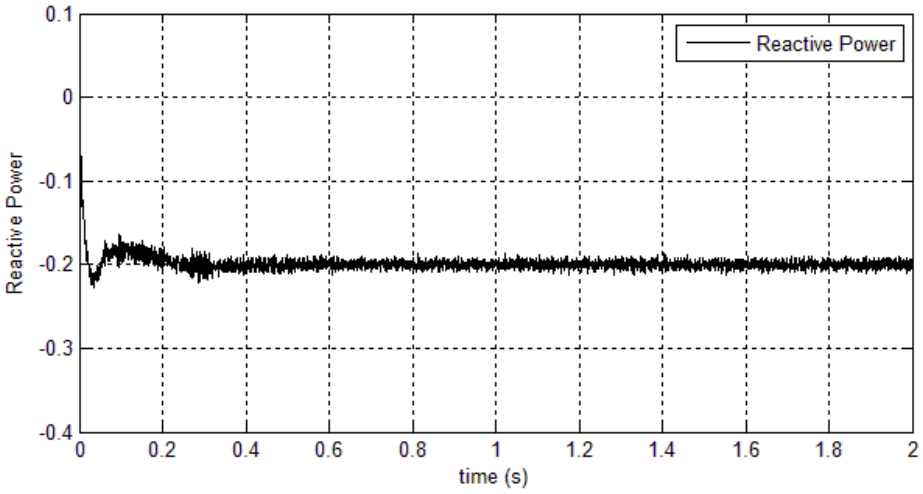

Figure 6.9. Reactive power injected to grid at GSVSC

6.5.2. Fault ride-through capability

The grid codes requirements show that wind turbines must have capability to ride through grid faults by staying connected during the faults occur in at least 300 (ms). With small voltage drops, the wind power system must be able to remain uninterrupted operation while large voltage drops can be followed by a special blocking sequence. These grid codes requirements are directly integrated in the controller design and the permanent magnet synchronous generator itself. A set of simulations in Figure 6.10 to Figure 6.12 illustrate how a PMSG wind farm equipped DMPC controller to overcome the grid faults.

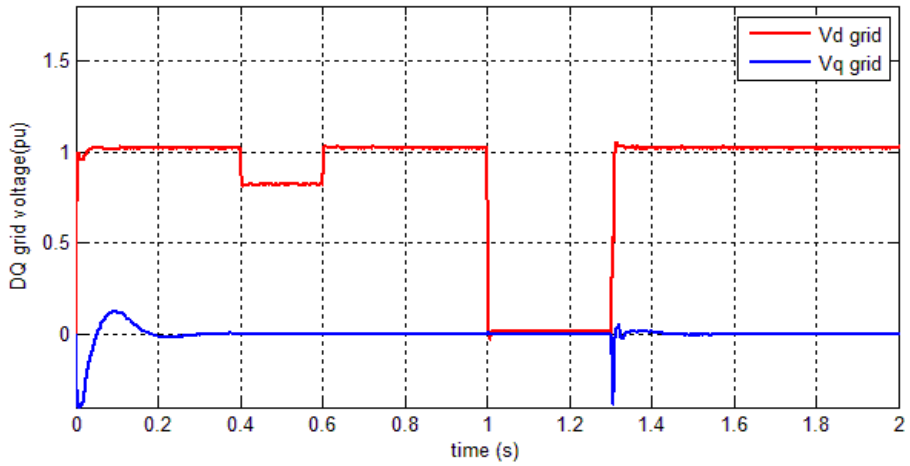

Figure 6.10. Voltage drops to 80% (0.4-0.6s) and 0% (1-1.3s)

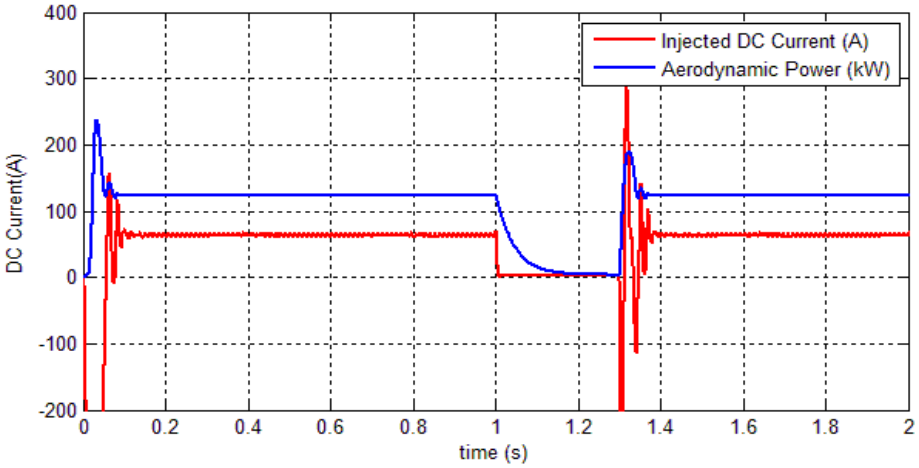

Figure 6.11. Aerodynamic power captured (blue) and DC current via DC-link (red)

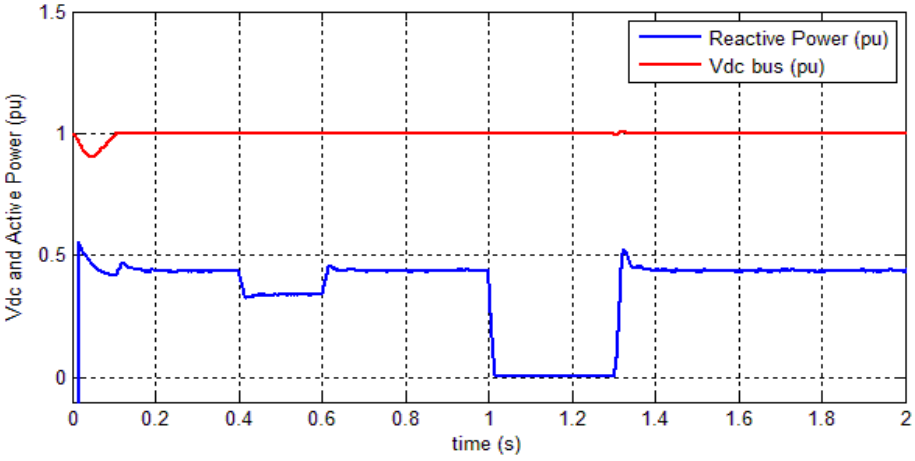

Figure 6.12. Dc-bus voltage (red) and reactive power to grid (blue) in (pu)

From the time 0.4-0.6 second, the grid voltage is dropped to 80% (as in Figure 6.10). The normal condition of wind turbine is still maintained by keeping maximum power tracking with injected DC current and aerodynamic power staying unchanged (as in Figure 6.11). The DC-bus voltage is kept constant at nominal value to ensure power transport from generator to power grid. However, the reactive power of the grid-side converter is controlled to below than normal value to protect from excessive current (Figure 6.12).

Megawatt class multi-pole PMSGs have been introduced and are widely used for offshore wind farms. Their advantages include the use of smaller gearboxes or even gearless turbines, no requirement for an excitation system, and simple fault ride-through by blocking the PWM signals to GEVSC [15]. If the short-circuit fault imposes on the transmission network (from 1-1.3 second in Figure 6.10), the PWM signal is stopped switching and blocked. The generator side converter now works as diode rectifier and grid side converter continues to act as STATCOM. As the results, generator speed increases to push wind turbine working at nearly zero power coefficient, this means that generator is disrupted from the power grid and cannot supply the active power to the grid (Figure 6.11 from 1-1.3 second). During the fault, the DC link voltage is still kept to be constant while reactive power falls down to zero (Figure 6.12). The wind turbine is completely disrupted from the grid with zero active and reactive power. When the short circuit fault is cleared from 1.3 second onward, the generator speed is controlled to track optimal reference then reconnected to supply active power to the grid.

6.6. Conclusions

In this chapter, the robust model predictive control was proposed for controlling a wind farm connected to a power grid. Major requirements of satisfactory operation of wind farm such as DC-link and reactive power are well performed by the reported control schemes. Fault ride-though capability of wind farm subjected to grid faults was also investigated. The simulation results in the MATLAB/SIMULINK using SimPowerSys toolbox demonstrate that the proposed controller gives better performance than the traditional PI controller. DC bus

voltage is well maintained to constant value in steady state while reduced overshoot are observed during transient period. Most important factor is that DMPC is fast, online, real-time control algorithm which is suitable for practical implementation in wind farm.

CHAPTER 7

CONCLUSIONS AND RECOMMENDATIONS

A number of linear and nonlinear controllers have been applied to wind power system in Chapter 4, 5, and Chapter 6. The approaches varying from model-free type controller to complex nonlinear model were investigated. This chapter concludes the effectiveness and feasibility of these controllers and recommends tasks for future research.

7.1. Conclusions

A simple fuzzy logic controller (FLC) was applied to control drive-train loop of variable speed wind turbine under presence of stochastic wind speed. The studied FLC is simple in design and requires model-free algorithm which is similar to the hill-climbed maximum power point tracking (MPPT) method. Based on the knowledge of sensed signals, FLC acts as human behavior to change control input for different wind speed accordingly. This is hence very simple control method. No accurate mathematical algorithm is required. As the results, maximum power regime tracking of wind power system is fairly achieved. The rotor speed stays near the optimal locus.

Another problem of FLC facing in wind power system control is that the wind is randomly fluctuated in high frequency. FLC has rate of change in rotor speed as knowledge source which is very sensitive to fast changes in inputs. This is the reason that FLC is not able to cancel noise produced by wind disturbance component.

The second control method is the extended version of conventional PID (Proportional Integral Derivative) controller; the Nonlinear PID (NPID) controller has variable proportional and integral gains adaptively adjust to different operating point of wind power system. This is stable and simple in design method while a good tracking quality is obtained. Together with the FLC controller, these two

control algorithms are suitable for application in small to medium rating wind power system where simplicity in design has priority than maximum power tracking.

Wind power system is obviously nonlinear system thus linearization at only optimal point is not enough to present the all operating conditions. Unlikely to the NPID which uses variable gains for different operating points, the third control scheme, DMPC considers wind power system is a linear system with uncertainty. The mismatch in linear model and nonlinear plant is always existed. This leads to an offset in tracking reference. The larger mismatch in modeling, the bigger offset is seen in the tracking result. This problem can be avoided by DMPC control scheme by introducing the output disturbance signal and observer design.

DMPC is an advanced controller which well suited for wind power system control at all operating conditions in one single controller. Full load and cut-in conditions are easily integrated into optimal locus by using a well-known property of DMPC, the constraint handling. Moreover, optimization problem is solved in every sampling time; hence, DMPC is adaptively changes to different wind speed. A robust algorithm is used. Finally, QP programming exploited in DMPC is an online, fast and robust. It makes DMPC to be a real-time algorithm which can be implemented in current technology micro-controller or processors. Together with NPID, these two control algorithms are priority choices for wind power control implementation in industry.

The last control scheme NMPC, which is a developed version of the linear MPC, is designed directly to the nonlinear model of wind power system so that the error occurred by linearization is canceled. All the advantage properties of linear MPC applicable for wind power control are maintained in the NMPC with tracking quality improvements.

However, the drawback of NMPC in comparison with linear MPC is that the nonlinear controller requires high calculating capability. The main reason is due to SQP computational method which is executed online to find control input updates. It is an advantage of real-time algorithm, which is a combination of multiple shooting method, partial-reduced SQP and iteration scheme, drastically reduces the

processing time of NMPC. This new research founding brings NMPC to be a promising control method for wind power system. NMPC is suitable for speed control loop in the cascade structure with the generator the d-q axis current PID controllers is highly recommended.

Final conclusion of thesis is on the selection of the best control algorithm for wind power system. Getting results from comparison among different method from linear to nonlinear, from simple to complex algorithm; it is recommended to a widely application of DMPC for wind power system. DMPC has the advantage properties of both linear and nonlinear method. The less computing effort and high tracking capability of optimal regime are observed. DMPC is also well suited to control a large wind farm.

7.2. Recommendations for Future Research

Three improvements are recommended for wind power system control for future research.

Firstly, it is recommended to improve the capability of DMPC controller. In the current research, the cascade structure of DMPC for speed loop and PI controllers for d-q axe current loops are applied. Even there are some advantages of cascade controller configuration such as: canceling the nonlinearity of the coupling term of generator speed and d-q axis currents and a short prediction horizon in DMPC. However, this bulky structure can be replaced by a MIMO (multiple input multiple output) controller. All speed loop and d-q current loops can be integrated into one single DMPC controller.

The second improvement to be made in future research is an implementation of NMPC on embedded controller. Although NMPC is claimed to be a good controller for drive train speed loop of wind turbine though a practically oriented simulation program. It is required to be implemented on a microcontroller. Moreover, NMPC is a generic control algorithm which can be widely applied in other industry.

Without generality, it is suggested a standard toolbox in SIMULINK of NMPC to be developed.

Final recommendation is to have a field testing of wind farm using DMPC controllers together with a management and supervised control system. There has been a lot of control algorithms studied for wind power system awaiting for field testing and practical application. DMPC controller has many advantage properties which got priority for a site testing with real wind profiles. A practical operation of a wind power plant is not limited to speed and d-q axis current controllers; it is required a supervisory system which is so called SCADA system. Monitoring control system of wind power plant is an interesting topic for researchers and engineers. Few more control algorithms and other approaches such as power-based controller design for wind power system would also be meaningful.

AUTHOR'S PUBLICATIONS

D. Q. Dang, Y. Wang, and W. Cai, "Nonlinear Model Predictive control (NMPC) of fixed pitch variable speed wind turbine," in *Sustainable Energy Technologies, 2008. ICSET 2008. IEEE International Conference on*, 2008, pp. 29-33.

D. Q. Dang, Y. Wang, and W. Cai, "Linear and Nonlinear Model Predictive Control of Variable Speed Wind Turbines," *IET Renewable Power Generation* (accepted for publication), April, 2012

D. Q. Dang, Y. Wang, and W. Cai, "Evaluation of Real-Time Nonlinear Predictive Control for Wind Energy Conversion Systems " *IET Renewable Power Generation* (Submitted Paper), 2011

D. Q. Dang, Y. Wang, and W. Cai, "Offset-free Predictive Control for Variables Speed Wind Turbines," *IEEE Transactions on Sustainable Energy,* (accepted for publication), April, 2012. Available online at: http://ieeexplore.ieee.org (DOI: 10.1109/TSTE.2012.2195731)

D. Q. Dang, Y. Wang, and W. Cai, "A Multi-objectives Optimal Nonlinear Control of Variable Speed Wind Turbine," presented at the in the 7th IEEE International Conference on Control & Automation (ICCA'09), in Christchurch, New Zealand, December 9-11, 2009

D. Q. Dang, S. Wu, Y. Wang, and W. Cai, "Model Predictive Control for maximum power capture of variable speed wind turbines," in *IPEC, 2010 Conference Proceedings*, 2010, pp. 274-279

W. Si, W. Youyi, D. Dinhquy, and C. Shijie, "Application of optimal reset control design on PMSG wind generation system," in *IPEC, 2010 Conference Proceedings*, 2010, pp. 1170-1175

BIBLIOGRAPHY

[1] P. Jain, *Wind Energy Engineering*, 1 ed.: McGraw-Hill, Sept, 2010.

[2] *World Wind Energy Association (WWEA)*. Available: http://www.wwindea.org/home/index.php

[3] C. N. Osphey, *Wind Power: Technology, Economics and Policies*, 2009.

[4] WikiPedia. (Accessed date: July 2011). *Wind power in the People's Republic of China*. Available: http://en.wikipedia.org/wiki/Wind_power_in_the_People%27s_Republic_of_China

[5] F. Morel, L.-S. Xuefang, J. M. Retif, and B. Allard, "Comparative study of two Predictive Current Controls for a Permanent Magnet Synchronous Machine drive," in *Power Electronics Specialists Conference, 2008. PESC 2008. IEEE*, 2008, pp. 3068-3073.

[6] S. B. S. Bolognani, L. Peretti, and M. Zigliotto, "Design and Implementation of Model Predictive Control for Electrical Motor Drives," *IEEE Transactions on Industrial Electronics,* vol. 56, No.6, June 2009.

[7] D. Swierczynski, "Direct Torque Control with Space Vector Modulation. (DTC-SVM) of Inverter-Fed Permanent Magnet Synchronous Motor Drive," *PhD Thesis, Warsaw University of Technology, Institute of Control and Industrial Electronics,* 2005.

[8] M. G.-S. Eduardo Torres, "Experimental results of the variable speed, direct drive multipole synchronous wind turbine TWT1650," *Wind Energy,* vol. 7, pp. 109-118, 2004.

[9] L. Arab, A. Belemhedi, M. A. Ahmed, and N. Habani, "Model Predictive Control of the Permanent Magnet Synchronous Motor in State Space with Input Constraints," *AIP Conference Proceedings,* vol. 1019, pp. 203-207, 2008.

[10] I. Schiemenz and M. Stiebler, "Control of a permanent magnet synchronous generator used in a variable speed wind energy system," in *Electric Machines and Drives Conference, 2001. IEMDC 2001. IEEE International*, 2001, pp. 872-877.

[11] M. Chinchilla, S. Arnaltes, and J. C. Burgos, "Control of permanent-magnet generators applied to variable-speed wind-energy systems connected to the grid," *Energy Conversion, IEEE Transactions on,* vol. 21, pp. 130-135, 2006.

[12] F. Valenciaga and P. F. Puleston, "High-Order Sliding Control for a Wind Energy Conversion System Based on a Permanent Magnet Synchronous Generator," *Energy Conversion, IEEE Transactions on,* vol. 23, pp. 860-867, 2008.

[13] K. Amei, Y. Takayasu, T. Ohji, and M. Sakui, "A maximum power control of wind generator system using a permanent magnet synchronous generator and a boost chopper circuit," in *Power Conversion Conference, 2002. PCC Osaka 2002. Proceedings of the*, 2002, pp. 1447-1452 vol.3.

[14] S. Morimoto, H. Nakayama, M. Sanada, and Y. Takeda, "Sensorless output maximization control for variable-speed wind generation system using IPMSG," *Industry Applications, IEEE Transactions on,* vol. 41, pp. 60-67, 2005.

[15] V. Akhmatov, "Modelling and ride-through capability of variable speed wind turbines with permanent magnet generators," *Wind Energy,* vol. 9, pp. 313-326, 2006.

[16] F. D. Bianchi, H. n. De Battista, and R. J. Mantz, *Wind turbine control systems : principles, modelling and gain scheduling design*. London: Springer, 2007.

[17] C. Jauch, S. M. Islam, P. Sørensen, and B. Bak Jensen, "Design of a wind turbine pitch angle controller for power system stabilisation," *Renewable Energy,* vol. 32, pp. 2334-2349, 2007.

[18] P. Sørensen, A. D. Hansen, and P. A. C. Rosas, "Wind models for simulation of power fluctuations from wind farms," *Journal of Wind Engineering and Industrial Aerodynamics,* vol. 90, pp. 1381-1402, 2002.

[19] I. Munteanu, A. I. Bratcu, N. A. Cutululis, and E. Ceanga, *Optimal Control of Wind Energy Systems: Towards a Global Approach*: Spinger Link, 2008.

[20] R. Ortega, A. J. Van Der Schaft, I. Mareels, and B. Maschke, "Putting energy back in control," *Control Systems, IEEE,* vol. 21, pp. 18-33, 2001.

[21] H. H. Song and Y. B. Qu, "Energy-based modelling and control of wind energy conversion system with DFIG," *International Journal of Control,* vol. 84, pp. 281-292, 2011/02/01 2011.

[22] B. Neammanee, K. Krajangpan, S. Sirisumrannukul, and S. Chatrattana, "Maximum Peak Power Tracking-Based Control Algorithms with Stall Regulation for Optimal Wind Energy Capture," in *Power Conversion Conference - Nagoya, 2007. PCC '07*, 2007, pp. 1424-1430.

[23] Y. Jia, Z. Yang, and B. Cao, "A new maximum power point tracking control scheme for wind generation," in *Power System Technology, 2002. Proceedings. PowerCon 2002. International Conference on*, 2002, pp. 144-148 vol.1.

[24] X. He, H. Jing, W. Dinghui, and Y. Wenxu, "Implementation of MPPT for PMSG-based small-scale wind turbine," in *Industrial Electronics and Applications, 2009. ICIEA 2009. 4th IEEE Conference on*, 2009, pp. 1291-1295.

[25] R. Bharanikumar, A. C. Yazhini, and A. N. Kumar, "Novel Maximum Power Point Tracking Controller for Wind Turbine Driven Permanent Magnet Generator," in *Power System Technology and IEEE Power India Conference, 2008. POWERCON 2008. Joint International Conference on*, 2008, pp. 1-6.

[26] M. Abdel-Salam, A. Ahmed, and M. Abdel-Sater, "Maximum power point tracking for variable speed grid connected small wind turbine," in *Energy Conference and Exhibition (EnergyCon), 2010 IEEE International*, 2010, pp. 600-605.

[27] M. Kesraoui, N. Korichi, and A. Belkadi, "Maximum power point tracker of wind energy conversion system," *Renewable Energy,* vol. 36, pp. 2655-2662, 2011.

[28] T. Ahmed, K. Nishida, and M. Nakaoka, "MPPT control algorithm for grid integration of variable speed wind energy conversion system," in *Industrial Electronics, 2009. IECON '09. 35th Annual Conference of IEEE*, 2009, pp. 645-650.

[29] M. H. Hansen, A. D. Hansen, T. J. Larsen, S. Øye, P. Sørensen, and P. Fuglsang, "Control design for a pitch-regulated, variable speed wind turbine," ed. Roskilde, Denmark: Risø National Laboratory, January 2005.

[30] J. Vieira, M. Nunes, and U. H. Bezerra, "Design of optimal PI controllers for doubly fed induction generators in wind turbines using genetic algorithm," in *Power and Energy Society General Meeting - Conversion and Delivery of Electrical Energy in the 21st Century, 2008 IEEE*, 2008, pp. 1-7.

[31] A. D. Wright, L. J. Fingersh, and M. J. Balas, "Testing State-Space Controls for the Controls Advanced Research Turbine," *Journal of Solar Energy Engineering,* vol. 128, pp. 506-515, 2006.

[32] E. Billy Muhando, T. Senjyu, N. Urasaki, A. Yona, H. Kinjo, and T. Funabashi, "Gain scheduling control of variable speed WTG under widely varying turbulence loading," *Renewable Energy,* vol. 32, pp. 2407-2423, 2007.

[33] F. Lescher, J. Zhao, and A. Martinez, "LQG Multiple Model Control of a Variable Speed, Pitch regulated Wind Turbine," *17th IMACS World Congress, Paris, France,* 2005.

[34] I. Munteanu, N. A. Cutululis, A. I. Bratcu, and E. Ceanga, "Optimization of variable speed wind power systems based on a LQG approach," *Control Engineering Practice,* vol. 13, pp. 903-912, 2005.

[35] X. Zhang, D. Xu, and Y. Liu, "Intelligent control for large-scale variable speed variable pitch wind turbines," *Journal of Control Theory and Applications,* vol. 2, pp. 305-311, August, 2004.

[36] J. P. Abreu Vieira, M. V. Alves Nunes, U. Holanda Bezerra, and W. Barra, "New Fuzzy Control Strategies Applied to the DFIG Converter in Wind Generation Systems," *Latin America Transactions, IEEE (Revista IEEE America Latina),* vol. 5, pp. 142-149, 2007.

[37] V. Calderaro, V. Galdi, A. Piccolo, and P. Siano, "A fuzzy controller for maximum energy extraction from variable speed wind power generation systems," *Electric Power Systems Research,* vol. 78, pp. 1109-1118, 2008.

[38] M. El Mokadem, V. Courtecuisse, C. Saudemont, B. Robyns, and J. Deuse, "Fuzzy Logic Supervisor-Based Primary Frequency Control Experiments of a Variable-Speed Wind Generator," *Power Systems, IEEE Transactions on,* vol. 24, pp. 407-417, 2009.

[39] R. M. Hilloowala and A. M. Sharaf, "A rule-based fuzzy logic controller for a PWM inverter in a stand alone wind energy conversion scheme," *Industry Applications, IEEE Transactions on,* vol. 32, pp. 57-65, 1996.

[40] M. G. Simoes, B. K. Bose, and R. J. Spiegel, "Fuzzy logic based intelligent control of a variable speed cage machine wind generation system," *Power Electronics, IEEE Transactions on,* vol. 12, pp. 87-95, 1997.

[41] Q.-N. Trinh and H.-H. Lee, "Fuzzy Logic Controller for Maximum Power Tracking in PMSG-Based Wind Power Systems
Advanced Intelligent Computing Theories and Applications. With Aspects of Artificial Intelligence." vol. 6216, D.-S. Huang, X. Zhang, C. Reyes García, and L. Zhang, Eds., ed: Springer Berlin / Heidelberg, 2010, pp. 543-553.

[42] J. S. P. B. Kasper Zinck Østergaard, "Linear parameter varying control of wind turbines covering both partial load and full load conditions," *International Journal of Robust and Nonlinear Control,* vol. 19, pp. 92-116, 2009.

[43] B. Boukhezzar and H. Siguerdidjane, "Robust multiobjective control of a variable speed wind turbine," in *Eroupean Wind Energy Conference & Exhibition*, London, UK, 22nd-25th November, 2006.

[44] E. Iyasere, M. Salah, D. Dawson, and J. Wagner, "Nonlinear robust control to maximize energy capture in a variable speed wind turbine," in *American Control Conference, 2008*, 2008, pp. 1824-1829.

[45] T. Senjyu, R. Sakamoto, N. Urasaki, H. Higa, K. Uezato, and T. Funabashi, "Output power control of wind turbine generator by pitch angle control using minimum variance control," *Electrical Engineering in Japan,* vol. 154, pp. 10-18, 2006.

[46] X. Lie, Y. Liangzhong, and C. Sasse, "Grid Integration of Large DFIG-Based Wind Farms Using VSC Transmission," *Power Systems, IEEE Transactions on,* vol. 22, pp. 976-984, 2007.

[47] R. D. Fernández, P. E. Battaiotto, and R. J. Mantz, "Wind farm non-linear control for damping electromechanical oscillations of power systems," *Renewable Energy,* vol. 33, pp. 2258-2265, 2008.

[48] C. Nichita, D. Luca, B. Dakyo, and E. Ceanga, "Large band simulation of the wind speed for real time wind turbine simulators," *Energy conversion, ieee transactions on,* vol. 17, pp. 523-529, 2002.

[49] T. Senjyu, T. Kaneko, A. Yona, N. Urasaki, T. Funabashi, and F. Yamada, "Output Power Control for Large Wind Power Penetration in Small Power System," in *Power Engineering Society General Meeting, 2007. IEEE*, 2007, pp. 1-7.

[50] A. G. Abo-Khalil and L. Dong-Choon, "Dynamic Modeling and Control of Wind Turbines for Grid-Connected Wind Generation System," in *Power Electronics Specialists Conference, 2006. PESC '06. 37th IEEE*, 2006, pp. 1-6.

[51] D. S. L. Dolan and P. W. Lehn, "Simulation model of wind turbine 3p torque oscillations due to wind shear and tower shadow," *Energy Conversion, IEEE Transactions on,* vol. 21, pp. 717-724, 2006.

[52] E. Muljadi, C. P. Butterfield, and J. M. L. Buhl, "Effects of Turbulence on Power Generation for Variable-Speed Wind Turbines " *NREL-NWTC,* November 1996

[53] J. A. Baroudi, V. Dinavahi, and A. M. Knight, "A review of power converter topologies for wind generators," *Renewable Energy,* vol. 32, pp. 2369-2385, 2007.

[54] D.-J. Bang, H. Polinder, J. A. Ferreira, and R. P. J. O. M. v. Rooij, "New Active Speed Stall Control compared to Pitch Control for a Direct-Drive Wind Turbine," presented at the EWEC2007, Milan, Italy, 8 May 2007.

[55] B. Neammanee, S. Sirisumrannukul, and S. Chatratana, "Development of a Wind Turbine Simulator for Wind Generator Testing," *International Energy Journal, AIT Thailand,* vol. 8, March 2007.

[56] M. Monfared, H. Madadi Kojabadi, and H. Rastegar, "Static and dynamic wind turbine simulator using a converter controlled dc motor," *Renewable Energy,* vol. 33, pp. 906-913, 2008.

[57] E. Muljadi and C. P. Butterfield, "Pitch-controlled variable-speed wind turbine generation," *Industry Applications, IEEE Transactions on,* vol. 37, pp. 240-246, 2001.

[58] Z. Kovačić and S. Bogdan. (2006). *Fuzzy Controller Design Theory and Applications*.

[59] C. C. Lee, "Fuzzy logic in control systems: fuzzy logic controller. I," *Systems, Man and Cybernetics, IEEE Transactions on,* vol. 20, pp. 404-418, 1990.

[60] W. J. Rugh, "Design of nonlinear PID controllers," *AIChE Journal,* vol. 33, pp. 1738-1742, 1987.

[61] F. Jiang and Z. Gao, "An application of nonlinear PID control to a class of truck ABS problems," in *Decision and Control, 2001. Proceedings of the 40th IEEE Conference on*, 2001, pp. 516-521 vol.1.

[62] D. Koo, J. Lee, D. Lee, C. Han, L. Gyu, J. Jung, and M. Lee, "A tuning of the nonlinear PI controller and its experimental application," *Korean Journal of Chemical Engineering,* vol. 18, pp. 451-455, 2001.

[63] G. P. Liu and S. Daley, "Optimal-tuning nonlinear PID control of hydraulic systems," *Control Engineering Practice,* vol. 8, pp. 1045-1053, 2000.

[64] M. Sedighizadeh, A. Rezazadeh, and M. Khatibi, "A self-tuning PID control for a wind energy conversion system based on the Lyapunov approach," in *Universities Power Engineering Conference, 2008. UPEC 2008. 43rd International*, 2008, pp. 1-4.

[65] C. Fu-qing and Y. Jin-ming, "Fuzzy PID controller used in yaw system of Wind Turbine," in *Power Electronics Systems and Applications, 2009. PESA 2009. 3rd International Conference on*, 2009, pp. 1-4.

[66] S. Liu, K. Zhang, G. Xing, and L. Zhang, "Robust fuzzy PID controller for wind turbines," in *Intelligent Computing and Integrated Systems (ICISS), 2010 International Conference on*, 2010, pp. 261-264.

[67] C. Xiao, L. Zhang, and J. Yan, "Fuzzy PID Controller for Wind Turbines," in *Intelligent Networks and Intelligent Systems, 2009. ICINIS '09. Second International Conference on*, 2009, pp. 74-77.

[68] S. Bolognani, L. Peretti, and M. Zigliotto, "Design and Implementation of Model Predictive Control for Electrical Motor Drives," *Industrial Electronics, IEEE Transactions on,* vol. 56, pp. 1925-1936, 2009.

[69] C. Runzi and L. Kay-Soon, "Repetitive Model Predictive Control of a Precision Linear Motor Drive," in *Industrial Electronics Society, 2007. IECON 2007. 33rd Annual Conference of the IEEE*, 2007, pp. 1132-1137.

[70] P. Cortes, J. Rodriguez, P. Antoniewicz, and M. Kazmierkowski, "Direct Power Control of an AFE Using Predictive Control," *Power Electronics, IEEE Transactions on,* vol. 23, pp. 2516-2523, 2008.

[71] S. Kouro, P. Cortes, R. Vargas, U. Ammann, and J. Rodriguez, "Model Predictive Control --- A Simple and Powerful Method to Control Power Converters," *Industrial Electronics, IEEE Transactions on,* vol. 56, pp. 1826-1838, 2009.

[72] L. C. Henriksen, "Model Predictive Control of a Wind Turbine," *Technical University of Denmark, DTU, IMM-Thesis,* 2007.

[73] M. Soliman, O. P. Malik, and D. T. Westwick, "Multiple model MIMO predictive control for variable speed variable pitch wind turbines," in *American Control Conference (ACC), 2010*, 2010, pp. 2778-2784.

[74] D. Q. Dang, S. Wu, Y. Wang, and W. Cai, "Model Predictive Control for maximum power capture of variable speed wind turbines," in *IPEC, 2010 Conference Proceedings*, 2010, pp. 274-279.

[75] J. M. Maciejowski, *Predictive control : with constraints*. New York: Prentice Hall, 2002.

[76] U. Maeder, F. Borrelli, and M. Morari, "Linear offset-free Model Predictive Control," *Automatica,* vol. 45, pp. 2214-2222, 2009.

[77] G. Pannocchia and A. Bemporad, "Combined Design of Disturbance Model and Observer for Offset-Free Model Predictive Control," *Automatic Control, IEEE Transactions on,* vol. 52, pp. 1048-1053, 2007.

[78] J. Nocedal and S. J. Wright, *Numerical Optimization 2nd Edition*: Springer Science+Business Media, LLC, 2006.

[79] M. Diehl, "Real-Time Optimization of Large-Scale Nonlinear Processes " Ph.D, University of Heidelberg, 2001.

[80] M. Diehl, H. G. Bock, and J. P. Schlöder, " A Real-Time Iteration Scheme for Nonlinear Optimization in Optimal Feedback Control," *SIAM Journal on Control and Optimization,* vol. 43, pp. 1714-1736, 2005.

[81] H. Camblong, "Digital robust control of a variable speed pitch regulated wind turbine for above rated wind speeds," *Control Engineering Practice,* vol. 16, pp. 946-958, 2008.

[82] N. A. Cutululis, E. Ceanga, A. D. Hansen, and P. Sørensen, "Robust multi-model control of an autonomous wind power system," *Wind Energy,* vol. 9, pp. 399-419, 2006.

[83] E. B. Muhando, T. Senjyu, H. Kinjo, and T. Funabashi, "Augmented LQG controller for enhancement of online dynamic performance for WTG system," *Renewable Energy,* vol. 33, pp. 1942-1952, 2008.

[84] T. Ekelund, "Speed control of wind turbines in the stall region," in *Control Applications, 1994., Proceedings of the Third IEEE Conference on*, 1994, pp. 227-232 vol.1.

[85] R. Findeisen and F. Allgower, "An Introduction to Nonlinear Model Predictive Control," *21st Benelux Meeting on Systems and Control, Veldhoven,* pp. 1-23, 2002.

[86] Z. Nagy, B. Mahn, R. Franke, and F. Allgöwer, "Real-Time Implementation of Nonlinear Model Predictive Control of Batch Processes in an Industrial Framework," in *Assessment and Future Directions of Nonlinear Model Predictive Control*. vol. 358, R. Findeisen, F. Allgöwer, and L. Biegler, Eds., ed: Springer Berlin / Heidelberg, 2007, pp. 465-472.

[87] C. L. Bottasso, A. Croce, and B. Savini, "Performance Comparison of Control Schemes for Variable-Speed Wind Turbines," presented at the The Science of Making Torque from Wind, TWIND 2007, The Technical University of Denmark, Lyngby, Denmark, 2007.

[88] K. Yeonsik and J. K. Hedrick, "Linear Tracking for a Fixed-Wing UAV Using Nonlinear Model Predictive Control," *Control Systems Technology, IEEE Transactions on,* vol. 17, pp. 1202-1210, 2009.

[89] H. J. Ferreau, P. Ortner, P. Langthaler, L. d. Re, and M. Diehl, "Predictive control of a real-world Diesel engine using an extended online active set strategy," *Annual Reviews in Control,* vol. 31, pp. 293-301, 2007.

[90] R. Errouissi and M. Ouhrouche, "Nonlinear predictive controller for a permanent magnet synchronous motor drive," *Mathematics and Computers in Simulation,* vol. 81, pp. 394-406, 2010.

[91] L. T. Biegler, J. Nocedal, C. Schmid, and D. Ternet, "Numerical Experience with a Reduced Hessian Methodfor Large Scale Constrained Optimization," *Comput. Optim. Appl.,* vol. 15, pp. 45-67, 2000.

[92] A. Wills and W. Heath, "Interior-Point Algorithms for Nonlinear Model Predictive Control," in *Assessment and Future Directions of Nonlinear Model Predictive Control*. vol. 358, R. Findeisen, F. Allgöwer, and L. Biegler, Eds., ed: Springer Berlin / Heidelberg, 2007, pp. 207-216.

[93] A. Schäfer, P. Kühl, M. Diehl, J. Schlöder, and H. G. Bock, "Fast reduced multiple shooting methods for nonlinear model predictive control," *Chemical Engineering and Processing: Process Intensification,* vol. 46, pp. 1200-1214, 2007.

[94] M. Diehl, H. G. Bock, and J. P. Schloder, "A Real-Time Iteration Scheme for Nonlinear Optimization in Optimal Feedback Control," *SIAM J. Control Optim.,* vol. 43, pp. 1714-1736, 2005.

[95] D. Ariens, B. Houska, H. J. Ferreau, and F. Logist. (2010). *ACADO: Toolkit for Automatic Control and Dynamic Optimization (1.0.2367beta ed.)*. Available: http://www.acadotoolkit.org/

[96] E. Camacho and C. Bordons, "Nonlinear Model Predictive Control: An Introductory Review," in *Assessment and Future Directions of Nonlinear Model Predictive Control*. vol. 358, R. Findeisen, F. Allgöwer, and L. Biegler, Eds., ed: Springer Berlin / Heidelberg, 2007, pp. 1-16.

[97] M. A. Henson, "Nonlinear model predictive control: current status and future directions," *Computers &Chemical Engineering,* vol. 23, pp. 187-202, 1998.

[98] T. Raff, C. Ebenbauer, R. Findeisen, and F. Allgower, "Nonlinear model predictive control and sum of squares techniques," *In Springer Lecture Notes in Control and Information Sciences, Springer Verlag,* 2006.

[99] A. Ilzhöfer, B. Houska, and M. Diehl, "Nonlinear MPC of kites under varying wind conditions for a new class of large-scale wind power generators," *International Journal of Robust and Nonlinear Control,* vol. 17, pp. 1590-1599, 2007.

[100] M. T. Heath, *Scientific Computing: An Introductory Survey*. New York: McGraw-Hill, 1997.

[101] E. Muljadi, C. P. Butterfield, B. Parsons, and A. Ellis, "Effect of Variable Speed Wind Turbine Generator on Stability of a Weak Grid," *Energy Conversion, IEEE Transactions on,* vol. 22, pp. 29-36, 2007.

[102] I. M. de Alegría, J. Andreu, J. L. Martín, P. Ibañez, J. L. Villate, and H. Camblong, "Connection requirements for wind farms: A survey on technical requierements and regulation," *Renewable and Sustainable Energy Reviews,* vol. 11, pp. 1858-1872, 2007.

[103] A. D. Hansen, P. Sørensen, F. Iov, and F. Blaabjerg, "Centralised power control of wind farm with doubly fed induction generators," *Renewable Energy,* vol. 31, pp. 935-951, 2006.

[104] M. El Mokadem, V. Courtecuisse, C. Saudemont, B. Robyns, and J. Deuse, "Experimental study of variable speed wind generator contribution to primary frequency control," *Renewable Energy,* vol. 34, pp. 833-844, 2009.

[105] D. Jovcic and N. Strachan, "Offshore wind farm with centralised power conversion and DC interconnection," *Generation, Transmission & Distribution, IET,* vol. 3, pp. 586-595, 2009.

[106] S. M. Muyeen, R. Takahashi, and J. Tamura, "Operation and Control of HVDC-Connected Offshore Wind Farm," *Sustainable Energy, IEEE Transactions on,* vol. 1, pp. 30-37, 2010.

[107] S. K. Chaudhary, R. Teodorescu, and P. Rodriguez, "Wind Farm Grid Integration Using VSC Based HVDC Transmission - An Overview," in *Energy 2030 Conference, 2008. ENERGY 2008. IEEE*, 2008, pp. 1-7.

[108] N. Flourentzou, V. G. Agelidis, and G. D. Demetriades, "VSC-Based HVDC Power Transmission Systems: An Overview," *Power Electronics, IEEE Transactions on,* vol. 24, pp. 592-602, 2009.

[109] F. Iov, P. Sorensen, A. D. Hansen, and F. Blaabjerg, "Grid connection of active stall wind farms using a VSC based DC transmission system," in *Power Electronics and Applications, 2005 European Conference on*, 2005, pp. 10 pp.-P.10.

[110] Z. Keliang, F. Xiaofan, C. Ming, Z. Xiaodong, W. Wei, and W. Tong, "Topologies and control of VSC-HVDC systems for grid connection of large-scale off-shore wind farms," in *Electrical Machines and Systems, 2008. ICEMS 2008. International Conference on*, 2008, pp. 2357-2361.

[111] P. Sørensen, A. D. Hansen, F. Iov, F. Blaabjerg, and M. H. Donovan, "Wind farm models and control strategies," Risø National Laboratory, Roskilde, Denmark Riso-R-1464 (EN), August 2005.

[112] I. Margaris, A. Hansen, P. Sørensen, N. Cutululis, and N. Hatziargyriou. (2011). *Operation and Control of Wind Farms in Non-Interconnected Power Systems*. Available: http://www.intechopen.com/articles/show/title/operation-and-control-of-wind-farms-in-non-interconnected-power-systems

[113] W. L. Kling, L. Söder, I. Erlich, P. Sørensen, M. Power, H. Holttinen, J. Hidalgo, and B. G. Rawn, "Wind power grid integration: the European experience," presented at the 17th Power Systems Computation Conference PSCC, Stockholm Sweden, 2011.

[114] D. Bary, "Increasing renewable accessibility in ireland," *World Energy Congr,* vol. 1, pp. 1-10, September, 2004.

[115] L. M. Fernández, C. A. García, J. R. Saenz, and F. Jurado, "Equivalent models of wind farms by using aggregated wind turbines and equivalent winds," *Energy Conversion and Management,* vol. 50, pp. 691-704, 2009.

APPENDIX 1. MATLAB COMMAND OF LMPC ALGORITHMS FOR TUTORIAL PROBLEM

```
function [Phi,G]=predictions11(A,B,C,N1,N2,Nu,lambda)
    N=N2-N1;

    temp_phi=[];
    temp_g=[];
    %for MIMO system
    [rb,cb]=size(B);
    [rc,cc]=size(C);
    z=zeros(cb,rc);

    for i=N1: N2
        %calculating each row for Phi
        temp_phi=[temp_phi; C*(A^i)];

        %calculating each row for G
        temp=[];
        j=N1+(i-1)-1;
        while(j>=(i-Nu)&& j>=0)
            temp=[temp C*(A^(j))*B];
            j=j-1;
        end
        for j=i : Nu-1
            temp=[temp z];
        end

        temp_g=[temp_g; temp];
    end
    Phi=temp_phi;
    G=temp_g;
end

%define the plant and set point
az = [1 -0.7]; bz=[2];
w=1;
A=[0.7 2; 0 1]; B=[2;1];C=[1 0];
N1=1;N2=5;Nu=2,N=N2-N1;lambda=0.5;

%function [Omega,Gamma]= form_constraint(A,B,C,N1,N2,Nu)

%N=1, N2=4;Nu=2,N=N2-N1+1
[n,n]=size(A);
[n,m]=size(B);
[p,n]=size(C);

% Initial value
yplant = 0; uplant = 0; xplant=0; ydata=[];
udata=[];wdata=[];tdata=[];

% Calulate Eu
Eu=ones((N+1)*p,Nu*m);
for i=1:Nu
       for j=i+1:Nu
        I1(i,j)=0;
       end
```

```
end

%get G
[Phi,G]=predictions(A,B,C,N1,N2,Nu,lambda);

% form matrix I
I = eye((N+1)*p,Nu*m);
Omega=[-I;-Eu;-G;I;Eu;G]

% calculate matrix Gamma
zeroI= zeros((N+1)*p,n);
gamma = ones((N+1)*p,n);
zeroG=zeros((N+1)*p,n);
Gamma = [zeroI zeroI;zeroG gamma;Phi zeroG;zeroI zeroI;zeroG -
gamma;-Phi zeroG]
[q,f] = size(Omega);

%constraist matrix, is suposed to be less than 1.
%The smaller Beta, the longer time Y reach setpoit
Beta = ones(q,1)*0.2;
zita = [xplant;uplant;xplant;uplant];
omega = Beta+Gamma*zita; % total constraist

%************************************************

for k=1:21
    %measure the current plant output
    yk=yplant;
    uk=uplant;
    xk=xplant;
    %duk=0.1
    %calculate the MPC control, using model 1
    zita_k=[xk;uk];
    F= Phi*zita_k;
    [g,h]=size(G'*G);
    Q=(G'*G+lambda*eye(g,h));
    Hess = ((F-w)'*G);
    [du,J1,flag,intertions]=QUADPROG(Q,Hess,Omega,omega)
    [r c]=size(du);
    I1=zeros(1,r);
    I1(1)=1;
    I2=ones(c,1);
    duk=I1*du*I2;
    uk=uk+duk
    %storage the data for plotting later
    tdata=[tdata;k-1];
    wdata=[wdata;w];
    ydata = [ydata;yk];
    udata =[udata;uk];

    %apply the control law to the plant
    uplant = uk;

    % Simulate the plant
    yp_new = -az(2)*yplant+bz*uplant;
    yplant=yp_new;
    xk_new=yp_new/C(1);
```

```
    xplant=xk_new;
    J= 2*J1 + (F-w)'*(F-w)
end
subplot(211),plot(tdata,wdata,tdata,ydata),ylabel('output'),xlabel(
'Samples')
subplot(212),stairs(tdata,udata),ylabel('Control'),xlabel('Sample')
```

Appendix 2. MATLAB CODES FOR NONLINEAR PROBLEM TUTORIAL

Some MATLAB codes can be written using the ACADO toolbox as:

```
BEGIN_ACADO;                          % Always start with
"BEGIN_ACADO".
   acadoSet('problemname', 'example');      % Set your problem name. If you
   DifferentialState      x;                % The differential states
   Control                u;                %  The controls
   %% Differential Equation
   f = acado.DifferentialEquation();        % Set the differential equation object
   f.add(dot(x) == -x*x + 5*x+ u*u );       % Write down your ODE.
   %% Optimal Control Problem
   ocp = acado.OCP(0.0, 2.0, 20);           % Set up the OCP).
                                            % Start at 0s, 20 intervals, in 2s
   ocp.minimizeMayerTerm((x - 5)^2);        % Minimize a Mayer term
    ocp.subjectTo( f );                     % OCP is always subject to diff. equation
   ocp.subjectTo( 'AT_START', x == 1.0 );   % Initial condition
   ocp.subjectTo(  0.1 <= u <= 1.0 );

   %% Optimization Algorithm
   algo = acado.OptimizationAlgorithm(ocp);      % Set up the optimization
algorithm
```

```
algo.set('INTEGRATOR_TOLERANCE', 1e-5 ); % Set some parameters for the
algorithm

END_ACADO;

   out = example_RUN();                    % Run the test.

   draw;                                   %  Plotting results
```

APPENDIX 3. WIND TURBINE SPECIFICATION FOR SIMULATION STUDIES

Symbol	Quantity	Values
ρ	Air density	1.25 (kg/m^3)
L_w	Wind turbulence length	150
R	Blade length	2.5 (m)
$Cp_{\max}$	Maximum of power coefficient	0.47
$\overline{\lambda}$	Optimal tip-speed-ratio	7
J_r	Rotor inertia	3 (kg.m^2)
J_g	Generator inertia	0.01 (kg.m^2)
η	Gearbox ratio	6.25
$\overline{\upsilon}$	Seasonal wind speed	7 (m/s)

APPENDIX 4. HARDWARE SPECIFICATION FOR EXPERIMENTAL STUDIES

Motor: BLDC motor with rated power 750 (Watts); rated speed 3000 (rpm); controller mode includes torque, speed and position scheme; peak torque of 2.39 (N.m).

Generator: PMSG typed with rated power 600 (Watts); rated speed 3000 (rpm); peak current 12.6 (A); number of pole-pairs p =4; resistance R_s =0.5 (Ohm); inductance L_s =2.1 (mH); torque constant K_t =0.5;

Wind Turbine: Air density ρ=1.25 (kg/m^3); turbine blade length R =0.7 (m); optimal tip speed ratio $\overline{\lambda}=7$; total inertia J_t =2.14e-4 (kg.m^2); viscous friction B_t =1.8e-4 (N/msec^{-1}); gearbox ratio η=1; average wind speed $\overline{\upsilon}$=2.5 (m/s).

Controller Card: dSPACE 1103 PPC controller board; 1 GHz processor; 50 bit-I/O channels, 36 A/D channels, and 8 D/A channels; 6 encoders.

APPENDIX 5. LARGE WIND TURBINE SPECIFICATION FOR WIND FARM STUDIES

Symbol	Quantity	Values
ρ	Air density	1.25
R	Blade length	22 (m)
$Cp_{\max}(\lambda)$	Max. power coefficient	0.47
$\overline{\lambda}$	Optimal tip-speed ratio	7
P_{rated}	Turbine power rated	2 (MW)
J_t	Total equal turbine inertia	536.59 (kg.m^2)
R_s	Generator stator resistance	0.0067 (Ohm)
L_s	Generator stator inductance	0.0075 (mH)
ϕ	Generator magnetic flux	3.83 (Wb)
p	Number of pole pairs	24
R_g	Grid stator resistance	0.00495 (Ohm)
L_g	Grid stator inductance	0.065776 (mH)
U_g	Grid voltage	575 (V)
U_{dc_ref}	DC link voltage	1600 (V)
C_link	Dc-link capacitance	90 (mF)

APPENDIX 6. WIND FARM STRUCTURE AND INDIVIDUAL WIND TURBINE CONTROL

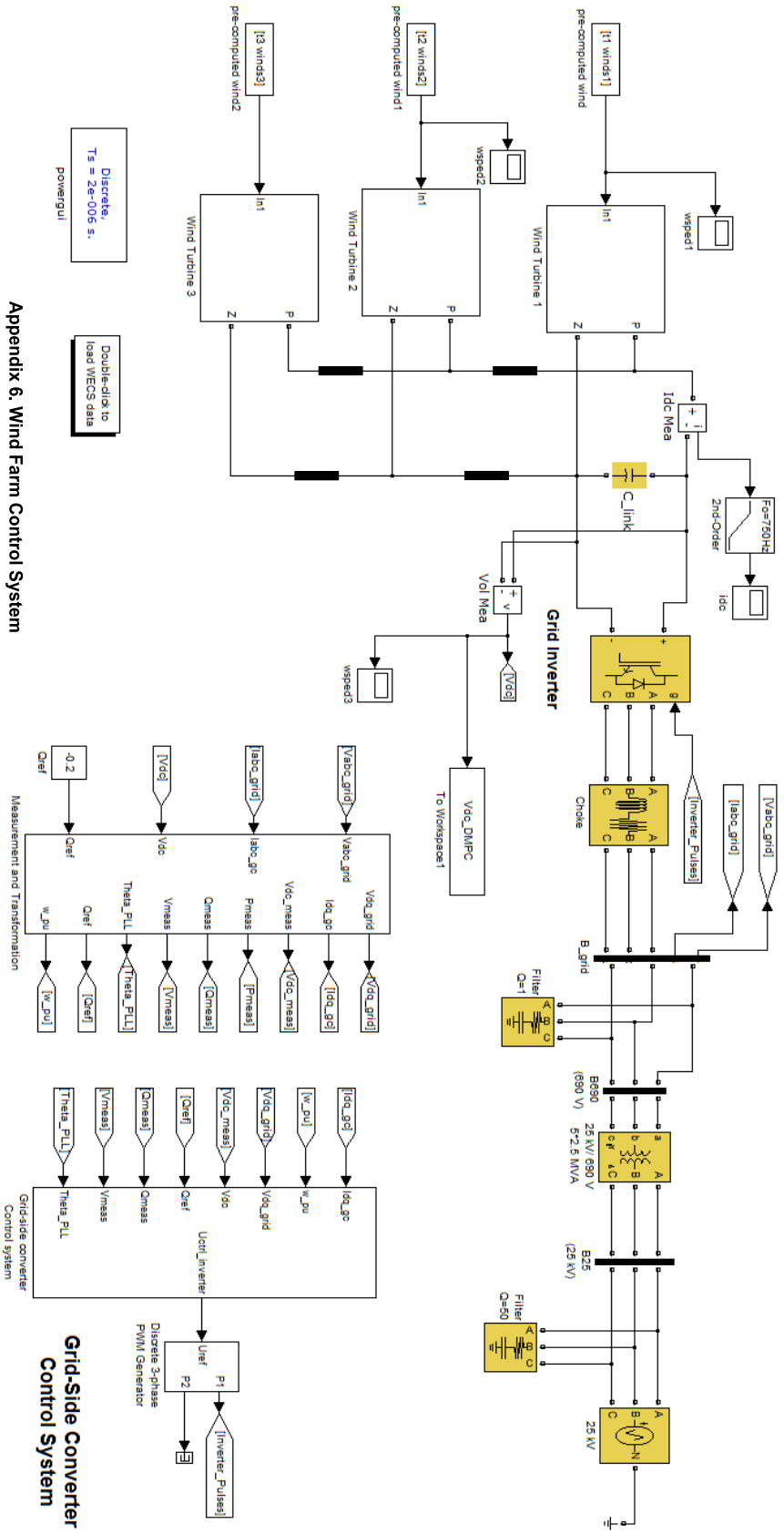

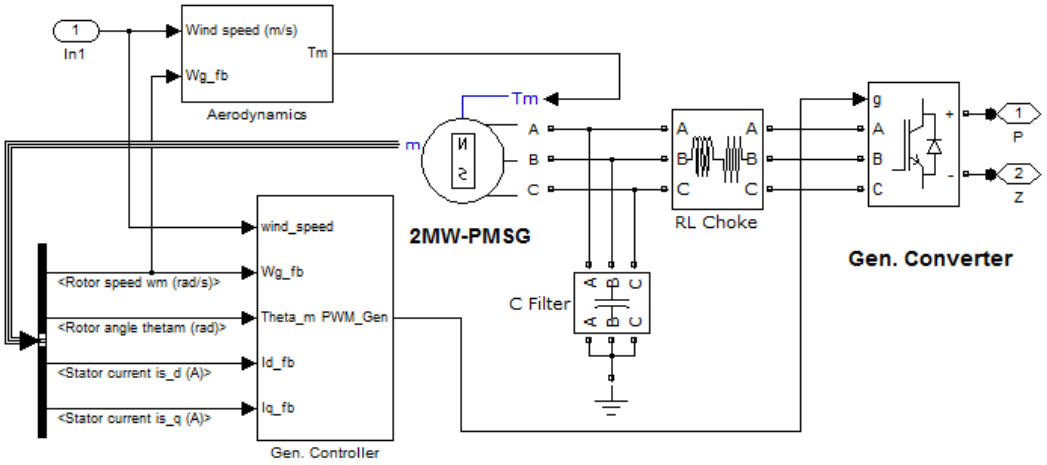

Generator-Side Control System